81/48

NORTHERN TERRITORY GEOLOGICAL SURVEY

GS81/48

TECHNICAL REPORT

FINAL REPORT ON THE MORDOR COMPLEX

CENTRAL AUSTRALIA

BY

D. BARRACLOUGH

Department of Mines and Energy

GS81/48

NORTHERN TERRITORY GEOLOGICAL SURVEY REPORT G.S. 81/48

FINAL REPORT ON THE MORDOR COMPLEX, CENTRAL AUSTRALIA

by D. Barraclough

THE MORDOR COMPLEX : CENTRAL AUSTRALIA

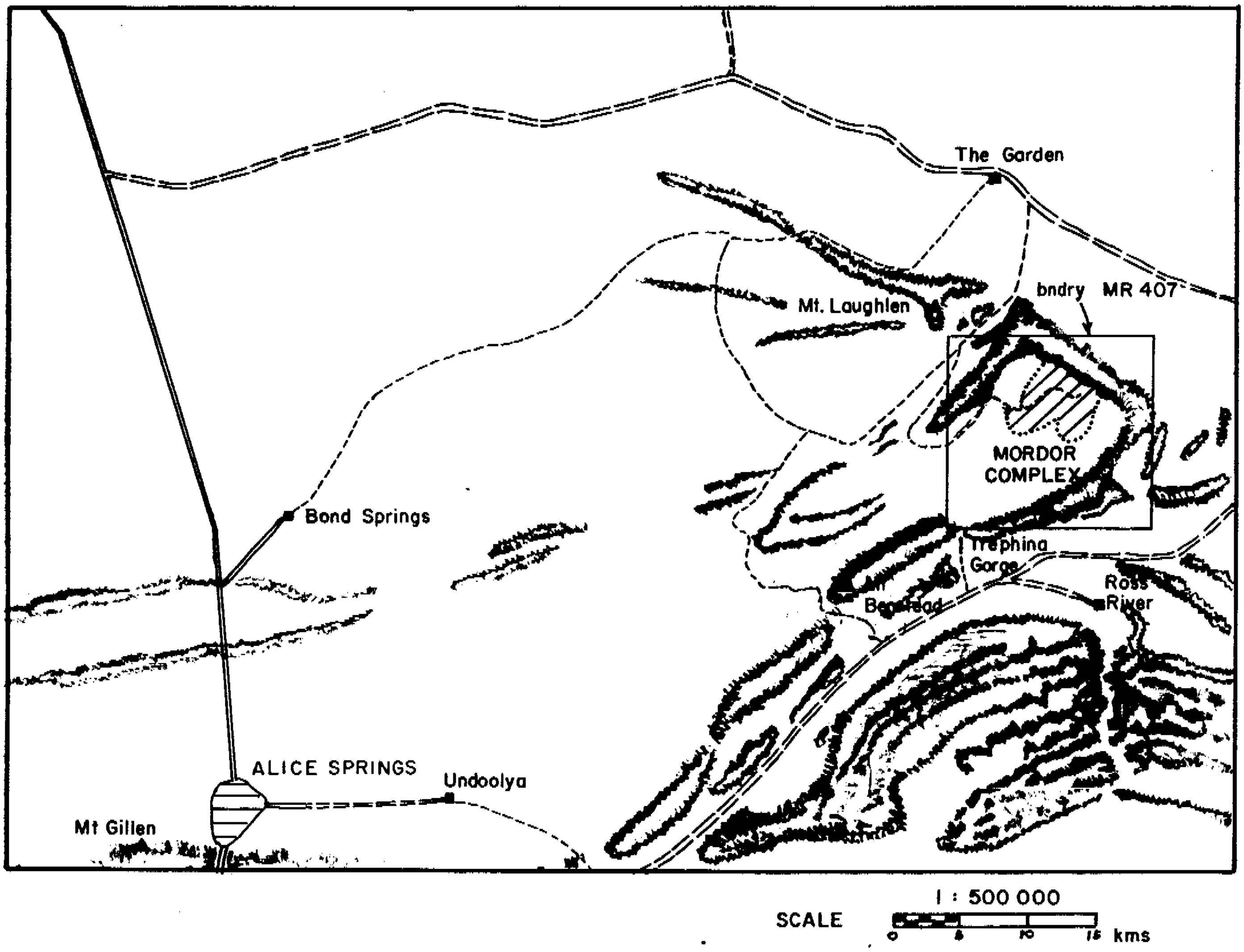

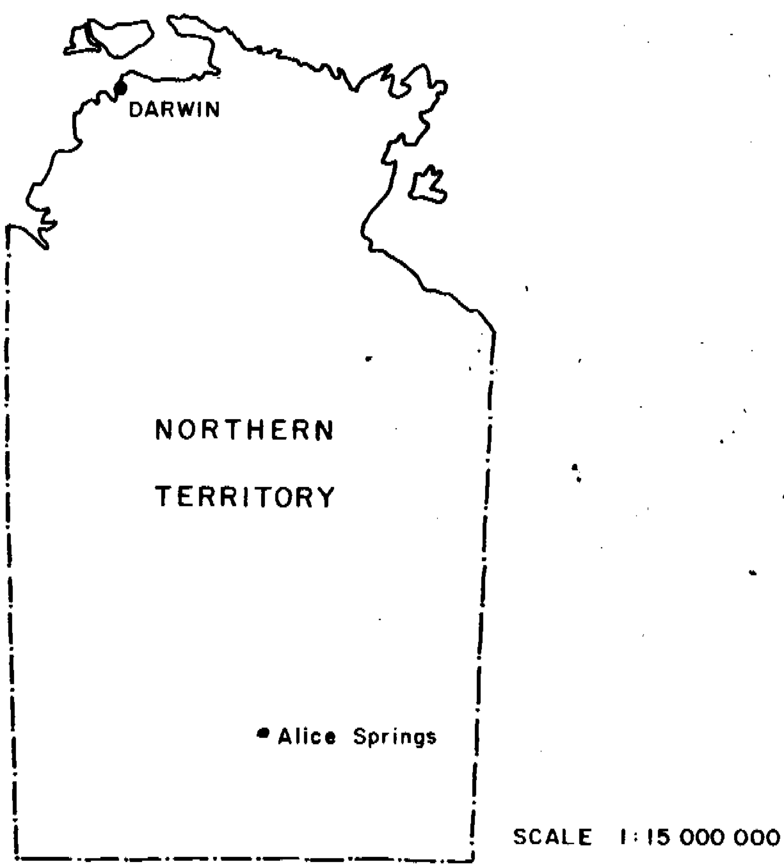

PLAN 1

SUMMARY

The Mordor Complex in Central Australia consists of a consanguineous suite of fractionated rocks ranging in composition from phlogopite dunite to syenite. Variation diagrams and cumulative frequency curves demonstrate the consanguinity of the suite. Soil geochemistry is an aid to mapping and indicates a chemical association between the mafic and ultramafic rocks of the complex. Soil geochemistry shows that a plug of wehrlite, intrusive into shonkinite, is chemically zoned. The chemical zoning continues in the enclosing shonkinite.

Diamond drilling of a fault-bounded block of ultramafic rocks, shows that it is composed of alternating, conformable layers of cumulus olivine and pyroxene. A chemical log demonstrates cryptic layering and indicates at least two cycles of magmatic deposition within the block. The block, made up of basal cumulates (dunite, peridotite, pyroxenite) occurs at the top of a postulated 6 kilometre deep, near-vertical cylinder of ultrabasic rock.

The suite of rocks evolved from a highly alkaline, mafic magma by fractional crystallization. Crystallization proceeded from the base, walls and roof by convective processes until the enclosed low melting-point, volatile-rich residuum escaped from the enclosing ultramafic rocks to form a separate but adjacent intrusive. The roof and walls of the ultramafic body collapsed, blocks were detached and residual mafic intercumulus liquid and pegmatitic liquid from melted country-rock partly mixed and filled the fractures. The separate intrusive, mainly syenite, assimilated some of the pegmatitic liquid.

Post-emplacement faults cutting the complex are filled with calcite and quartz. The calcite is remobilized carbonate, not related to carbonatite. Chemical analyses demonstrate the removal of lime and magnesia from rocks by weathering and the removal of Na, Sr and Ba from syenite by hydrothermal activity. The analyses therefore suggest two methods for the accumulation of superficial barite, calcite and caliche.

CONTENTS

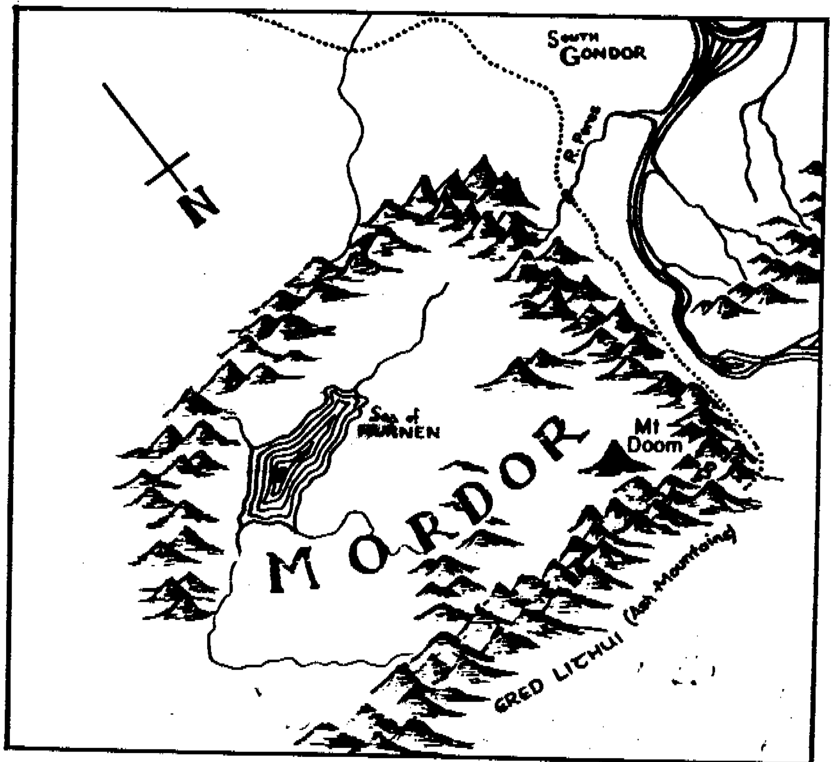

From "The Lord of the Rings" by J.R.R. Tolkien.
Plate 5, page 626.

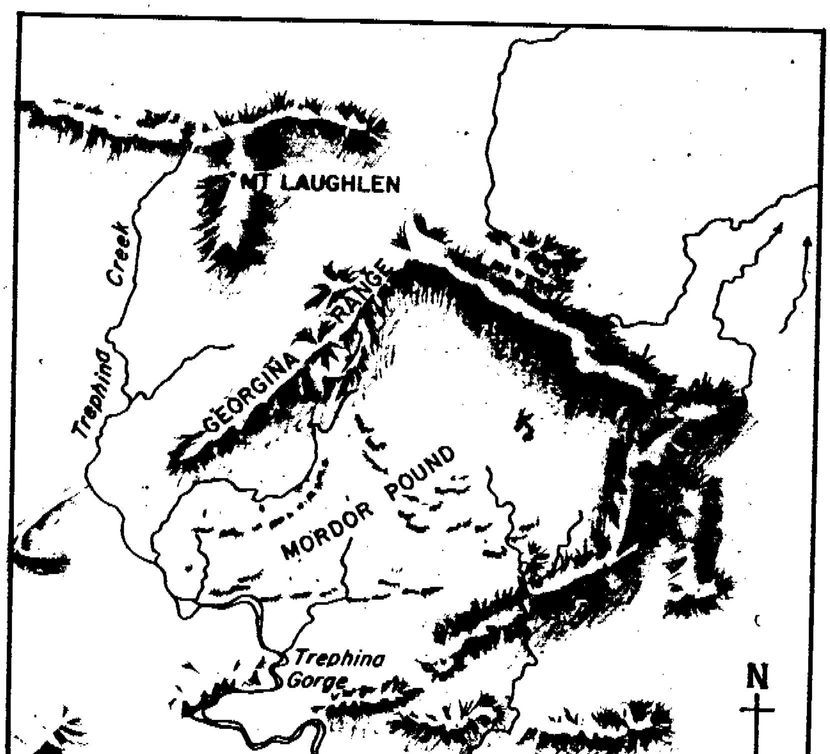

Section of Alice Springs Topographic Map.
1:250 000. SF 53-14.

PLAN 3.

N.T. DEPT OF MINES & ENERGY.

AS79Z24E

INTRODUCTION

The Mordor Complex is a heart-shaped intrusion of potassic igneous rocks located in Mordor Pound, 65 kilometres east-northeast of Alice Springs in Central Australia. (Plans 1 and 2). The Complex intrudes high-grade multiply-deformed metamorphic rocks of the Precambrian Arunta Block, and is partly overlain and partly enclosed by steep-sided walls of Late Proterozoic Heavitree Quartzite.

The very remarkable similarity between the area and the place 'Mordor', conceived by J.R.R. Tolkien in his book 'Lord of the Rings', was first noticed in 1970 by field workers of Conzinc Riotintio of Australia Exploration Pty. Ltd. (CRAE). This similarity (see Plan 3) prompted Alan Langworthy and Lance Black, geologists with the Bureau of Mineral Resources, (BMR), to propose the name 'Mordor' for the Complex and the Pound in which it occurs.

In 1969 CRAE acquired tenure over the area. The company undertook a regional stream sediment survey for base-metals and heavy minerals, and detailed soil-geochemical and geophysical surveys. Kostlin, (CRAE unpubl. rept., 1971) recognised a suite of igneous rocks ranging in composition from pyroxenite to syenite and suggested that the intermediate rocks (shonkinite) could be either basified syenite or a separate magmatic phase. He thought that some rocks appeared to have a metasomatic origin. Scott (Central Mineralogical Services, petrographic report in CRAE unpubl. rept. op. cit.), recognised sovite and suggested an affinity between the ultramafic rocks and kimberlite. Petrographic evidence indicated a genetic association between, and a co-magmatic origin of syenite, shonkinite and pyroxenite.

Magnetic and gravity surveys conducted by CRAE indicate a body of substantial size and magnetization, comprised of a "near-vertical cylinder of ultrabasic rocks of diameter 10,000 feet with its top surface outcropping or very shallow, and its bottom surface about 20,000 feet deep" (Kirton and Doe, CRAE unpubl. rept. 1971). Although barite, brannerite and carbonatite were recorded in outcrop, low base-metal values in soil, stream and chip samples made the area unattractive to CRAE and their tenure was allowed to expire in 1974.

Geologists of the Bureau of Mineral Resources (BMR) investigated the complex during regional mapping of the Laughlen 1:100,000 Sheet area. They saw the complex as a differentiated suite of under-saturated rocks chemically related to kimberlite, and suggested a petrogenesis involving either zone refining of deep mantle partial melt or partial melting of an atypical upper mantle source rock (Langworthy and Black, 1978). They thought that extensive fractional crystallization and gravity settling which began during the evolution of a primary magma continued with magmatic differentiation to syenitic end-products in an intermediate-level chamber. Syenite was considered to have been intruded by basic differentiates which were themselves intruded by numerous plug-like bodies of ultramafic rock, pegmatite and dyke-like bodies of carbonate-rich breccia (Langworthy and Black, op. cit.).

Barraclough (1975) of the Northern Territory Geological Survey (NTGS) suggested a magmatic origin for the ultramafic rocks and a metasomatic origin for shonkinite and syenite. He showed that the ultramafic rocks are enclosed by shonkinite and are not in contact with syenite or country gneiss. Shonkinite, therefore was seen as a metasomatic aureole around the ultramafic cylinder. Barraclough (1975) therefore supported one of Kostlin's ideas — that of basification of syenite — basing his support on the field evidence available.

Additional field, geochemical and petrographic work has shown that there is a continuous chemical association between the rocks of the complex (excluding pegmatite), that there are continuous mineralogical changes from the ultramafic rocks to syenite but that the juxtaposition of the rocks can be attributed to collapse of the roof of the magma chamber (this report). Thus the earlier idea of metasomatism (Barraclough, 1975) is found less compelling. Nevertheless there is field evidence to suggest that some rocks have a metasomatic origin.

The Mordor Complex closely resembles the description of an alkaline ring complex by Wyllie (1967) and the description of a zoned ultra-mafic complex by McTaggart (1971). On the origin and zoning of these complexes, generally two schools of thought are currently accepted: one involving a magmatic hypothesis and the other involving a metasomatic hypothesis. At this time, in the Western world, the magmatic school is in the ascendency. In the U.S.S.R. the metasomatic school has many adherents.

Various mechanisms are proposed for the magmatic emplacement of alkalic ring complexes:

* serial intrusions of ultramafic magmas (Rucknick and Noble, 1959; Smirnov, 1976),
* emplacement of different magmas (Irvine, 1967),

* differentiation in situ and serial intrusion (Langworthy and Black, 1978, for the Mordor Complex)

Some workers attach a greater importance to metasomatic processes. Borodin (1963), for example, believes that the only igneous rocks of these complexes are ultrabasic; the felspathic varieties being formed metasomatically by mineralising solutions. McTaggart (1971) believes that the early formed cumulate masses drop along ring fractures and hydrous fluids from the enclosing metamorphic rocks then metasomatise the still-hot plug.

This report examines the field and geochemical evidence and concludes that magmatic processes can account for all the major rock types and emplacement structures of the complex, but that metasomatism best accounts for some minor features of the complex.

BRIEF GEOLOGICAL HISTORY

High-grade multiply-deformed metamorphic rocks of the Precambrian Arunta Block were intruded by the Mordor Complex about 1200 m.y. ago (Langworthy and Black, op. cit.). Upper Proterozoic Heavitree Quartzite, the basal formation of the Amadeus Basin sequence, was deposited on an eroded Arunta Block about 1000 m.y. ago. The rocks were uplifted and folded to form the Arltunga Nappe Complex during the Alice Springs Orogeny about 360 m.y. ago. The steep sided walls of Heavitree Quartzite partly enclosing the Mordor Complex are eroded remnants of the Arltunga Nappe Complex.

STRUCTURAL SETTING

The Mordor Complex occurs near the intersection of three major faults: the E-W Harry Creek Deformed Zone; the NW-SE Woolanga Lineament; and an E.NE striking fault (Mordor Fault) which truncates the Amadeus Basin sediments of the Georgina Range and displaces the western margin of the Mordor Complex. The latest movement on the Mordor Fault is younger than the Mordor Complex but the fault may be a re-activated extension of the Redbank Thrust Zone, active 1800 m.y. ago (Marjoribanks and Black, 1974). The Woolanga Lineament separates the Papunya Gravity Ridge from the Hale River Gravity Platform and corresponds to a rapid change in Bouguer anomaly values (Shaw and Warren, 1975).

The Mud Tank Carbonatite (Crohn and Gellatly, 1969), 50 kilometres to the north-west of the Mordor Complex, is also adjacent to the Woolanga Lineament and at an intersection with an E.NE striking fault. The emplacement of both intrusives was probably controlled by the Woolanga Lineament, (a deep crustal feature) and by cross-faulting.

GEOLOGY

The Mordor Complex is about 6 kilometres in diameter with an exposed surface area of about 29 square kilometres made up of two overlapping ovals; one to the north west composed largely of syenite, the other to the south east composed largely of shonkinite (Plan 2). The shonkinite is underlain by a large body of ultramafic rock (Kirton and Doe op. cit.). Volumetrically, shonkinite probably contributes only a minor amount to the complex in comparison to an estimated 40 cubic kilometres of ultramafic rock.

The foliation and mineral layering of shonkinite has centripetal dip-steep at the margin of the complex and shallow at the centre. The foliation of the country felspar-quartz-biotite gneiss also has a steep centripetal dip near its contact with the Mordor Complex. The contact is not well exposed but places show weak brecciation, epidotization and chloritic alteration of the country rock. The country felspathic gneiss is strongly porphyroblastic near the contact. Amphibolite alters to spotted hornfels at the contact.

Rafts or xenoliths of gneiss are not uncommon near the margin of the complex but are rare toward the centre. No chilled or mafic margins have been recognised.

The contact between syenite and the country gneiss is regionally gradational in that remnants of gneiss extend up to 500 metres into syenite, becoming smaller and more isolated inwards. Some outcrops of gneiss are underlain by microsyenite. Microsyenite is fairly common in the north-west of the complex (see Plan 4) and is considered to be a chilled syenite.

Within the syenite are small, isolated areas of melanocratic syenite. The contacts between the two rock-types seem to be gradational and so the areas of melanocratic syenite may be either mafic inhomogeneities within a magmatic unit or metasomatic aureoles around a more mafic plug or cognate xenolith. There is no evidence to date that the outcrops of malanocratic syenite contain a mafic core. However in the north of the complex a large body of shonkinite intrudes (or occurs in) syenite. The body is too large to be considered a mafic inhomogeneity, as above. The core of the shonkinite is ultramafic, i.e. mafic shonkinite with less than 20% felspar, and occurs in isolation from the main mafic-ultramafic body. The contacts between the three successive rock-types, syenite-porphyritic shonkinite-mafic shonkinite, are gradational over several metres. It could be argued therefore that the contact between the ultramafic rock and syenite is gradational over several tens of metres. This occurrence of ultramafic rock with an aureole of mafic rock is fairly compelling field evidence for metasomatism or basification of syenite.

In a magmatic scheme of emplacement either the ultramafic rock would have to intrude a prior intrusion of porphyritic shonkinite or two magmas (acid and ultrabasic) intruded the country gneiss more or less simultaneously, mixing to form an intermediate magma.

PETROLOGY

Rocks of the Complex range in composition from phlogopite dunite to pegmatite and gradations have been recognised between each successive member of the suite. Although the rocks form a gradational series, examination of the drill core shows the Complex can be divided into three mineralogical groups:

ultramafic rocks containing greater than 80% mafic minerals

mafic rocks containing 50-80% mafic minerals

felsic rocks containing less than 50% mafic minerals

Table 1 shows the compositions of typical members of the groups.

%	k.spar	diopside	mica	opaques	apatite
Biotite pyroxenite	trace	50-55	15-25	5	up to 8
Mafic shonkinite	10-20	40-50	25-35	10	up to 8
Porphyritic shonkinite	25-35	25-35	25-30	10	5
Melanocratic syenite	45-50	25	15-20	10	5
Syenite	65-70	10-15	10	5	5

The dunite, peridotite and pyroxenite members of the ultramafic rocks are tough with distinctive brown to black-brown weathering surfaces. They occur as steep-sided hills up to 400 metres in diameter, as smaller bouldery masses and as isolated boulders, possible residual lags. These ultramafic rocks are restricted to the south-eastern mafic oval (Plan 2). They are medium-grained holo-crystalline, hypidiomorphic-granular rocks composed of olivine, phlogopite and iron oxides with the amount of diopsidic augite (or hypersthene) varying from trace to major constituent. Mafic shonkinite, ultramafic due to its low felspar content, is friable and weathers fairly readily. With one exception, mentioned earlier, it is restricted to the mafic sector of the complex.

Phlogopite dunite consists of medium to coarse olivine, megacrysts of phlogopite up to 4 cms across, abundant opaque minerals (magnetite, ilmenite, chromite, sulphide), accessory apatite and pyroxene. Most megacrysts of phlogopite are 'Tiger-striped' in thin section, an effect probably caused by the introduction of fine-grained opaque crystals and calcite between the bent and fractured cleavage surfaces.

Interlocking cumulus olivine is fractured and serpentinized to varying degrees. The paucity of intercumulate crystals may be due to the fractionation of olivine by winnowing or by the loss of intercumulous liquid during crystal mush settling. The fracturing of olivine suggests crystal settling or movement.

Peridotite (lherzolite and wehrlite) typically contains fractured olivine and phlogopite with equant anhedral grains of diopsidic augite an anhedral, often poikilitic hypersthene. Accessory apatite (up to 10%) is often enclosed by pyroxene. Larger crystals of apatite are sometimes fractured. Small, well-rounded grains of colourless olivine are enclosed in phlogopite, diopsidic augite and hypersthene. These rounded grains are not fractured or serpentinized and probably are remnants of early-formed olivine.

Peridotite contains microscopic interstitial plagioclase and potash felspar.

Orthopyroxenite contains medium to coarse grained, hypersthene with accessory olivine, diopsidic augite and phlogopite. Most hypersthene grains contain opaque dust and poikilitically enclose phlogopite and small rounded grains of olivine. Orthopyroxenite is not common in the complex.

Phlogopite pyroxenite is the main ultramafic rock of the complex. Typically it contains about 60 to 70% of diopsidic augite and 10-15% of poikilitic megacrysts of phlogopite. Opaque minerals, chief among them magnetite, are ubiquitous ranging between 3 and 15%. Hypersthene is a common accessory and sometimes attains a major role (phlogopite websterite). Olivine is rare and occurs only as small rounded grains enclosed in other minerals. Fractured, serpentine-veined crystals are uncommon and so too is 'Tiger-striped' phlogopite.

Phlogopite pyroxenite grades into mafic shonkinite. Rounded boulders of pyroxenite with a remnant skin of shonkinite are quite common in the complex.

Mafic rocks are typically rich in phlogopite or biotite, most commonly containing 20-30% of the mica. In mafic shonkinite biotite is sometimes the main constituent (up to 35%).

Shonkinite is the main mafic member of the Complex. It is distinguished from the ultramafic rocks by the amount of biotite and potash felspar. However shonkinite may be ultramafic or mafic, depending upon the amount of felspar present. With an increase in the amount of felspar, phenocrysts of orthoclase are developed and mafic shonkinite grades into porphyritic shonkinite.

Mafic shonkinite is a medium-grained, weakly foliated rock containing abundant poikilitic phlogopite, rounded diopsidic augite and fine to medium-grained orthoclase. Olivine is sometimes present as rounded grains in phlogopite. Orthopyroxene is rare, apatite and magnetite are minor constituents. Calcite, ilmenite, sulphide (principally pyrite; rare chalcopyrite and pyrrhotite) and hyalophane are accessory. Hyalophane, a barium orthoclase occurs as small interstitial grains and is distinguished from orthoclase by its low relief and undulose extinction.

Porphyritic shonkinite consists of ubiquitous orthoclase phenocrysts (up to 2 cms long) in a fine grained mafic groundmass. Many of the phenocrysts are intergrown to form vein-like aggregates but most are tabular. They are being replaced by sericite. Some orthoclase is perthitic. Plagioclase felspar is rare, none being identified in several thin sections. The groundmass contains diopside, biotite and accessory apatite, magnetite, ilmenite and sulphide. Calcite is common but much of it seems to be secondary. Rare hematite is present, intergrown with magnetite.

Dykes of micro-shonkinite with a composition similar to porphyritic shonkinite (30% k.spar, 35% diopside, 30% biotite, 5% opaques) cut the mafic rocks. The contacts are normally sharp and intrusive but some wider dykes have rapidly gradational contact with the enclosing mafic rock. Several dykes can be traced over distances up to 1 kilometre however most dykes pinch and swell, and do not persist. Sections of one mafic dyke grade laterally from micro-shonkinite into a felspathic rock and back to micro-shonkinite, the result perhaps of mixing between shonkinite and pegmatite. A dyke of micro-porphyritic shonkinite (sample M7; 22760N, 26700E) has a similar composition to microshonkinite but contains microphenocrysts of kaolinized and sericitized orthoclase. Microshonkinite dykes are common in mafic rocks but rare in syenite and ultramafic rocks. In syenite the microshonkinite dykes are more felspathic, a feature probably reflecting the composition of the host rock.

Within the area of mafic rock, micro-shonkinite dykes trend NE - SW, sub-parallel to pegmatite dykes. Microshonkinite dykes are cut by pegmatite but in a few cases the relationship is ambiguous suggesting that microshonkinite and pegmatite dykes were formed more or less simultaneously.

Felsic rocks include melanocratic syenite, syenite, microsyenite, microgranite, pegmatite and dykes of compositions ranging from pyroxene-felspar through aplite to quartz. Felsic rocks comprise the largest group, in terms of surface area, of the complex.

Melanocratic syenite is gradational between - porphyritic shonkinite and syenite. It is a hypidiomorphic-granular rock containing elongate phenocrysts of orthoclase up to 2 cms. long. The phenocrysts are often intergrown as vein-like aggregates, and are often being replaced by sericite. Orthoclase poikilitically encloses biotite and opaque minerals. Phenocrysts of perthite and perthitic margins to phenocrysts of orthoclase are present but not common.

The fine to medium-grained groundmass consists of anhedral diopside, biotite, orthoclase-hyalophane with accessory apatite, calcite and opaque minerals (magnetite and associated hematite, ilmenite and pyrite) and minor plagioclase and hypersthene. Quartz and barite are rare components.

Syenite is a hypidiomorphic-granular rock containing subhedral phenocrysts of orthoclase up to 3 centimetres long. The medium-grained mafic groundmass consists of diopside, biotite, orthoclase-hyalophane with accessory apatite, calcite and opaque minerals. Plagioclase and microcline are minor constituents; quartz and barite are rare. Apatite occurs as fine euhedra in orthoclase, biotite and pyroxene, and interstitially a fine sub-hedra. The opaque minerals are mainly magnetite (often intergrown with hematite) and pyrite.

Pegmatitic syenite (23000N; 26000E) contains large aggregates of orthoclase (90%), coarse biotite (2-3%), medium-grained diopside (5%) and accessory apatite and opaque minerals. The rock is transitional between pegmatite and syenite. There are several large outcrops of microsyenite within the area of syenite which are considered to be chill phases of syenite. An outcrop of microgranite occurs in shonkinite. The contacts are obscured but the shonkinite is progressively altered over several metres towards the microgranite. The outcrop is considered to be a roof-pendant or xenolith of country rock in shonkinite.

Numerous pegmatite dykes with an arcuate NE - SW trend and northwesterly dips of between 30 and 65°, cut all rock-types of the Complex. Most dykes occur in the mafic section of the Complex although many are present in syenite. Few persist into the enclosing country gneiss. The dykes are up to 6 metres wide in outcrop (more usually 1 metre) but may only occur as narrow veins at depth (see drill logs in appendices). They consist of coarse orthoclase and plagioclase with medium-grained quartz (sometimes myrmekitic in felspar) accessory chlorite, apatite and rare tourmaline. Kostlin (op. cit.) recorded occurrences of apatite-pegmatite and apatitites.

Many dykes have aplitic margins, some grade laterally into mafic rock and many terminate as quartz-rich pegmatite or quartz-blows.

The pegmatite dykes are clearly younger than ultramafic or mafic rocks. Pegmatite often cuts microshonkinite dykes but there are several instances where there may have been mixing of pegmatite and shonkinite and where microshonkinite cuts pegmatite. Field evidence therefore suggests that the pegmatite and microshonkinite dykes are of equivalent age. In a few cases pegmatite grades laterally into syenite a feature suggesting age equivalence for pegmatite and syenite, and hence for pegmatite, microshonkinite and syenite.

Pegmatite and microshonkinite dykes are cut and off-set by carbonate-filled faults, branches of a major east-west fault which truncates late Proterozoic sediments of the Georgina Range. The branch faults are filled with carbonate, quartz and fragments of host rock. The margins of the host rock are brecciated and hydrothermally altered.

CRAE collected numerous samples of fault breccia; <u>sovite</u> was identified in several of them (Scott, op. cit.). Two of the branch faults were diamond drilled by NTGS. Calcite intersected in one (see drillhole Plan 6 MCDDH3) was considered to have been introduced or remobilized during faulting, and not of carbonatite origin (Barraclough, 1975). Carbonate intersected in another fault (see drill hole MCDDH4) was said to contain a high proportion of magnesium and thought therefore to be <u>carbonatite</u>, (Barraclough op. cit.)

Langworthy and Black (op. cit.) said analytical data do not support a carbonatite origin for any carbonate-rich rocks of the Complex and showed that their whole-rock phlogopite age was much lower than whole rock and mineral ages derived for the Complex. They concluded that the carbonate-rich rocks were probably formed by leaching. An oval plug of calcite and <u>barite</u> was also considered to have been formed by leaching.

The plug consists of a narrow (2-3 mms) rim of quartz, an annulus 4 metres wide of coarsely crystalline calcite and a central core of barite (2 metres in diameter). The plug occurs in sheared and hydrothermally altered syenite, at or near an intersection of two shears. The long axis of the plug is parallel to one of them. The shears are associated with faults, branches of the Mordor Fault.

Analyses of hydrothermally altered syenite (see appendix) show depletion of barium by over 60% in syenite adjacent to a fault. It seems likely that the barite plug has been formed hydrothermal alteration of hyalophane (Ba - orthoclase) with subsequent deposition in a cross-fractured fissure.

MINERALOGY

Olivine occurs as colourless to pale green anhedral cumulus grains and as small colourless well-rounded grains poikilitically enclosed in megacrysts of phlogopite, hypersthene and (less commonly) in clinopyroxene. The cumulus grains are invariably fractured and sometimes serpentinized along the fractures. Complete serpentinization is rare. The small rounded grains of olivine are not fractured and not serpentinized. No reaction corona and no zoning have been observed.

Clinopyroxene occurs as very pale green anhedral, cumulus grains up to 4 mms across, and as small rounded grains enclosed by phlogopite and hypersthene in the ultramafic rocks. It occurs as small pale green anhedral to sub-hedral grains in felspathic rocks. In one sample of syenite (MCDDH3 - 38.8) two sizes of clinopyroxene may be present: very fine grains; and fine (0.5 mm) grains which are cored with biotite and possible earlier clinopyroxene.

Clinopyroxene is commonly twinned and rarely zoned (outlined by inclusions of opaque dust). It often encloses opaque minerals, phlogopite and apatite. Widmanstätten figures of opaque minerals are fairly common in the clinopyroxene of felspathic rocks but are rare in ultramafic rocks. Optical measurements on clinopyroxene in lherzolite (MCDDH2 - 49.5) yield γ/c of 45°, in biotite clinopyroxenite (MCDDH2 - 42.5) yield γ/c of 47°, indicating a diopsidic-augite to augite composition and in syenite (MCDDH3 - 32.8) yield γ/c of 42° indicating diopside.

Orthopyroxene occurs as medium to coarse (up to 8mm) anhedral poikilitic and strongly pleochroic (colourless to reddish brown) grains. Most grains enclose phlogopite and opaque minerals, a few enclose well-rounded olivine and (less frequently) clinopyroxene. Orthopyroxene is itself sometimes enclosed in larger clinopyroxene grains (MCDDH2 - 49.5). Fractured grains are common in ultramafic rocks. No zoning has been recognised. In a sample of melanocratic syenite (MCDDH1 - 52.0) orthopyroxene is strongly altered to antigorite.

Phlogopite occurs as anhedral, strongly pleochroic (very pale yellow to pink) poikilitic megacrysts up to 7 cms across (outcrop of mica dunite) enclosing olivine, clinopyroxene and opaque minerals. In ultramafic rocks, most phlogopite grains are bent or fractured, and many display a characteristic 'Tiger-stripe', caused by the introduction of opaque minerals and carbonate grains between the cleaved fragments. 'Tiger-striping' is absent in mafic and felspathic rocks, and pleochroism is less (colourless to deep orange-brown). The megacrysts are unaltered and lack reaction zones.

Orthoclase occurs as partly altered, subhedral phenocrysts (up to 3 cms long in syenite) often in vein-like aggregates in shonkinite and syenite. Twinned orthoclase is rare in shonkinite but fairly common in syenite (sample MCDDH3 - 13.4). Some phenocrysts enclose clinopyroxene and apatite and some phenocryst margins are intergrown with clinopyroxene, opaque minerals, biotite and apatite. Microcline is perthitic and shows replacement of orthoclase, indicating the exsolution of plagioclase with decreasing temperature. Hyalophane, a barium-rich orthoclase has been analysed as $(K_{0.4}\ Na_{0.4}\ Ba_{0.1})(Al_{1.1}\ Si_{2.9})\ O_8$ by Langworthy and Black, (op. cit.). It is recognised in thin section by its low relief and undulose extinction. Hyalophane occurs interstitially in mafic rocks and in fine-grained shonkinite (MCDDH1 - 28.4). It also occurs interstitially in mafic shonkinite (MCDDH1 - 83.0). Hyalophane represents barium-rich residual liquid trapped in a cumulate.

Plagioclase is a very minor constituent in melanocratic syenite (1-2%) and in syenite (1-2% in sample MCDDH3 - 32.0). It occurs in the groundmass as small, multiply twinned grains partly altered or partly replaced by orthoclase. Optical measurements of grains in the groundmass suggest albite-oligoclase but one grain being replaced by orthoclase yielded an extinction angle for andesine.

Quartz is rare. It occurs interstitially (MCDDH3 - 13.4; 1-2%) and as myrmekitic intergrowths (MCDDH3 - 32.0) associated with orthoclase, in syenite.

Opaque minerals are ubiquitous in all rocks except pegmatite. They range up to 15% in some ultramafic rocks but in general are between 5 and 10%. The main opaque mineral is magnetite but chromite occurs up to 1% in some ultramafic rocks. Sulphide is a common but minor constituent (range: trace - 4%) mainly pyrite with rare chalcopyrite and pyrrhotite. Hematite occurs in the later differentiates and in increasing amounts to syenite. It is intergrown with, or is replacing magnetite.

The growth of magnetite and its replacement by hematite suggest a high fO_2 in the magma.

Ilmenite is a very minor constituent of all rocks.

Apatite is present in all rocks including pegmatite. It occurs as interstitial anhedral to euhedral crystals, often poikilitically enclosed by all major minerals except olivine. Its presence (up to 10% in mafic shonkinite) reflects the enrichment of the rocks in phosphorus.

Minute calcite grains occur interstitially in all rocks, and with opaque minerals in 'Tiger-striped' phlogopite of ultramafic rocks.

SOIL GEOCHEMISTRY

In a preliminary soil-geochemical survey conducted by CRAE, 393 samples were analysed for Pb, Zn, Cu, Co, Ni and Cr. In a follow-up survey, 1025 samples were analysed for Cu, Co, Ni and Cr. The correlation between soil-sample and rock type is shown in Table 2.

Table 2

Preliminary survey

Rock-type	Number of samples	%	Cum. %
Colluvium	9	2	not considered
Gneiss	27	7	7.0
Syenite pegmatite	114	29	36.7
Shonkinite	145 (app)	37	74.5
Pyroxenite, Peridotite	98 (app)	25	100
Total	393	100	384 samples

Detailed survey

Pegmatite	6	0.5	0.5
Porph. shonk.	80-90	8.3-8.9	9
Mafic shonk.	250-260	24.4-25.4	34
Pyroxenite	650-660	63.4-64.4	98
Peridotite	20-25	1.9-2.4	100
Total	1025	100	1025 samples

Lead and Zinc

Cumulative frequency plots in Figure 1 indicate log-normal distribution of lead and zinc in the soils over the Complex. The median values are 14 ppm lead and 48 ppm zinc. The median values obtained from drill-core assays (45 ppm lead, 60 ppm zinc) show that there is a slight loss in metal values with the soil-sampling method employed. The log-normal distribution and the low values obtained indicate no lead or zinc anomalies in the Complex. The fairly even distribution of metal values ocross the Complex also indicate a limited use for lead and zinc analyses in any additional soil surveys.

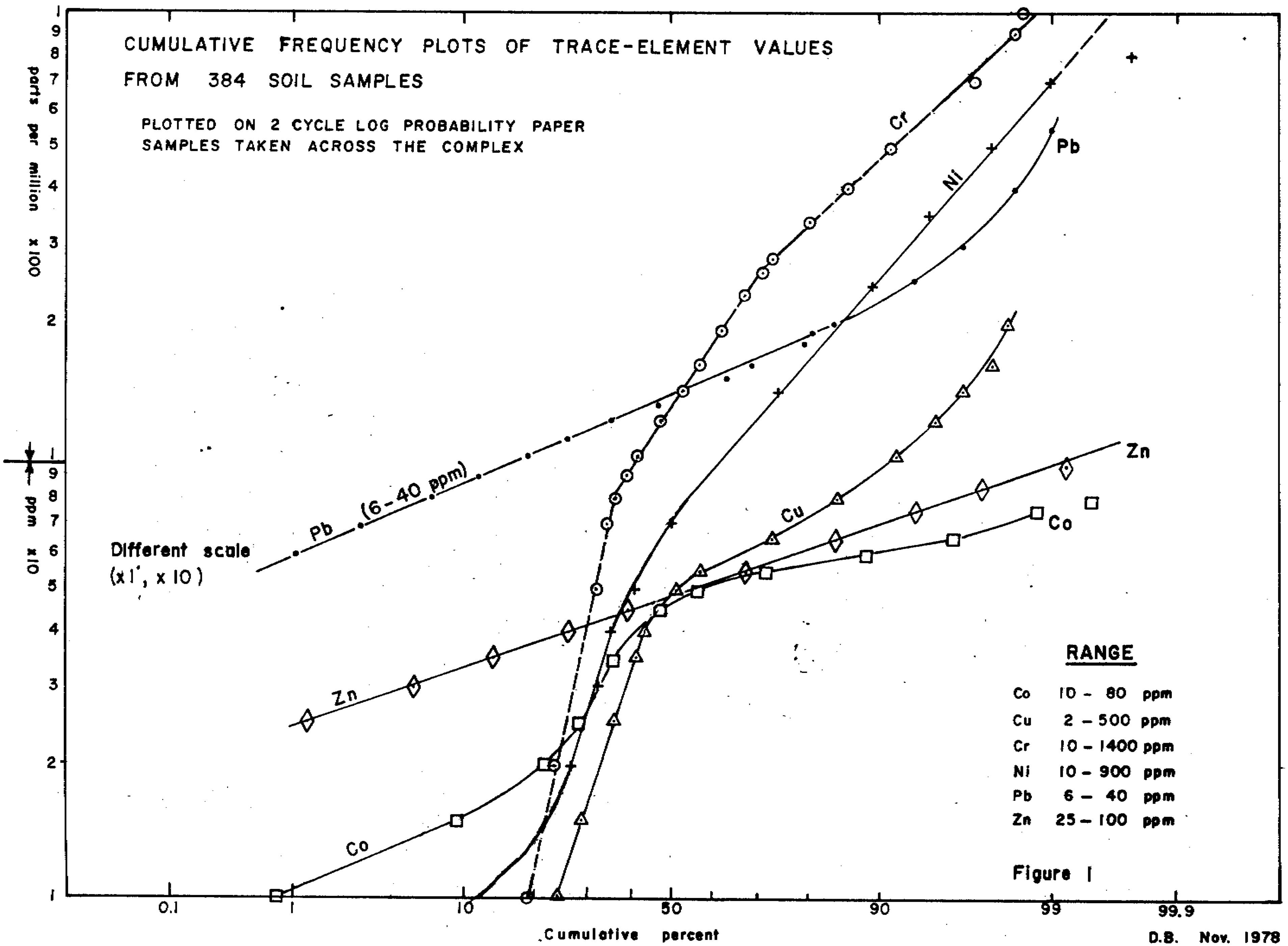

Figure 1

D.B. Nov. 1978

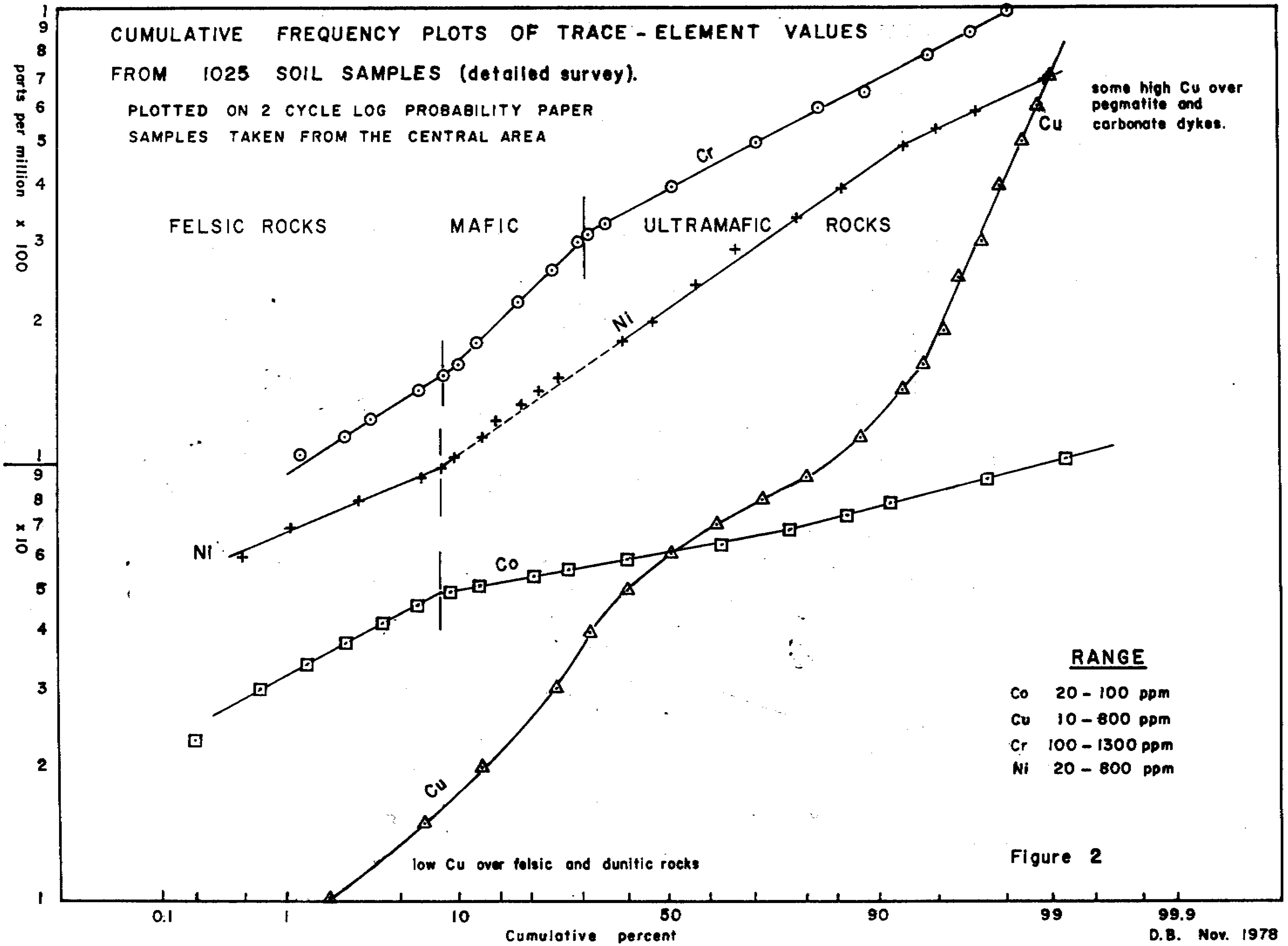
CUMULATIVE FREQUENCY PLOTS OF TRACE - ELEMENT VALUES
FROM 1025 SOIL SAMPLES (detailed survey).
PLOTTED ON 2 CYCLE LOG PROBABILITY PAPER
SAMPLES TAKEN FROM THE CENTRAL AREA
FELSIC ROCKS
MAFIC
ULTRAMAFIC ROCKS
Cr
Ni
Co
Cu
some high Cu over pegmatite and carbonate dykes.
low Cu over felsic and dunitic rocks
parts per million x 100
x 10
Cumulative percent
0.1
1
10
50
90
99
99.9
RANGE
Co 20 - 100 ppm
Cu 10 - 800 ppm
Cr 100 - 1300 ppm
Ni 20 - 800 ppm
D.B. Nov. 1978

Figure 2

Copper

The cumulative frequency plots of log copper values from both soil-geochemical surveys (Figures 1 and 2) show bimodal distribution of copper in the complex. The average copper content obtained from drill core assays (Table 3), of syenite, shonkinite and pyroxenite is 20 ppm, 100 ppm and 130 ppm respectively. The average copper content in peridotite, however, is 25 ppm, copper not being detected in 13 of 31 core samples. Therefore low copper values will be obtained in soils over syenite and peridotite.

Soil samples over the felsic rocks (total 141) and over peridotite and dunite (total 25) constitute the low-copper population in the preliminary soil-survey - 41% of the total population. The inflexion point on the curve (Figure 1) occurs at 42% of the population.

Low copper values in soils of the mafic sector of the Complex may therefore indicate underlying peridotite or dunite.

Cobalt and nickel

The cumulative frequency plots of log cobalt and log nickel values from the orientation survey have inflexion points at between 34 and 39% of the population. Soil samples over felsic rocks (gneiss, syenite and pegmatite) constitute about 36.7% of the population.

The cumulative frequency plots of log cobalt and log nickel values from the detailed survey (Figure 2) show breaks in slope between 8 and 10% of the population, coinciding with the field estimate of 9% for the felsic population (pegmatite and porphyritic shonkinite). The change in slope for cobalt is quite marked but the change for nickel is slight and may be due to sampling or analytical errors. In terms of differentiation (the equivalent of moving from right to left on the cobalt curve in Figure 2), the break in slope indicates either the inclusion of a low-cobalt mineral or the inclusion of a lithologic unit not of the same chemical association. Pegmatite, which may not be of the same chemical association as other rocks of the Complex, constitutes only 0.5% of the population and cannot greatly affect the slope of the graph. Porphyritic shonkinite is of the same chemical association grading into either mafic shonkinite or melanocratic syenite. It constitutes about 8.5% of the rocks over which the samples were collected. The break in slope therefore occurs at the point in differentiation where potash felspar is becoming the dominant mineral at the expense of clinopyroxene. The sulphide content, mainly pyrite, is constant at about 2% and therefore the cumulative frequency plots suggest that cobalt is associated with pyroxene.

The log-normal distribution of cobalt and nickel for the remaining 91% of the population of soil samples suggests a chemical association between the soils over mafic and ultramafic rocks.

Chromium

The cumulative frequency plots of log chromium values from both surveys show two breaks in distribution. In the preliminary survey the breaks correlate with the field estimated populations of 36.7% for felsic rocks and 74.5% for felsic and shonkinitic rocks. In the detailed survey the breaks occur at 8% (for felsic rocks) and 32% (for felsic and shonkinitic rocks).

The nickel, cobalt, copper and chromium assays can be used to identify the underlying rock-type; for example high Ni, Co and Cr and low Cu is an indication of sub-surface peridotite.

Geochemical line-profiles constructed by rolling-averages show changes in metal distribution across the Complex

a) from north to south, along line 30,000E, Figure 3.
b) from west to east, along line 21,200N, Figure 4.

A profile in Figure 3 indicates a steady increase from north to south in the zinc content of the soils. A second zinc profile on line 21,200N shows no progressive change in the zinc content of the soils. Drill core assays (Table 3) show that mafic and ultramafic rocks contain slightly more zinc than do felsic rocks (average 78 ppm vs 45 ppm Zn) and therefore the profile in Figure 3 suggests that the soils (rocks) are becoming more mafic to the south. However the lead profile (Figure 3) and the cobalt profile (not given) show no progressive changes in the N - S direction; no systematic changes in lead or zinc occur in the W - E direction. The N - S change in the zinc content therefore probably has no geological significance.

The coincident peaks in Zn, Pb, Ni and Cr values at 19000N occur where a carbonate-quartz breccia has cut ultramafic rock. The high Cr, Ni and Co values suggest that the rock is peridotite. High Cu, Pb and Zn in the soil sample is probably due to traces of sulphide mineralization in the breccia.

Line-profiles of the sum (Ni + Cr) and of the ratio (Ni + Cr)/Cu can be used to aid mapping. Two examples are given in Figure 5.

In general the profiles show that for:

shonkinite, copper varies directly as (Ni + Cr) so that the ratio (Ni + Cr)/Cu tends to remain constant (at about 4).

pyroxenite, copper remains fairly low and constant so that the sum profile and ratio profile are similar.

peridotite and dunite, copper is very low and varies inversely as the sum (Ni + Cr), so that for dunite which has a high Ni and Cr content, the ratio (Ni + Cr)/Cu tends towards infinity (see Figure 5).

Carbonate-quartz veins carry minor amounts of chalcopyrite so that when a soil sample has been collected over or near these veins, the copper content of the sample is anomalously high. The ratio (Ni + Cr)/Cu is therefore low. The effect of carbonate-quartz veins on the ratio profile is shown in Figure 5. On line 22,200N, the soil samples were collected over pyroxenite and thus the ratio profile should be similar to the sum profile. This is the case except in the area where the pyroxenite is cut by carbonate veins.

Line-profiles of samples from across the main body of pyroxenite suggest that the outcrop is wholly composed of pyroxenite. Random grab samples of rock show that the main rock-type is phlogopite clinopyroxenite but orthopyroxenite, olivine pyroxenite and peridotite are present. The soil sample lines are too widely spaced to define chemical zones in the outcrop.

Line-profiles over a plug of wehrlite intruding porphyritic shonkinite (20,000N; 26,700E) show chemical zoning in the plug. The (Ni + Cr)/Cu ratio increases towards the centre of the plug (Figure 6).

Geochemical Line-profiles : Orientation Survey

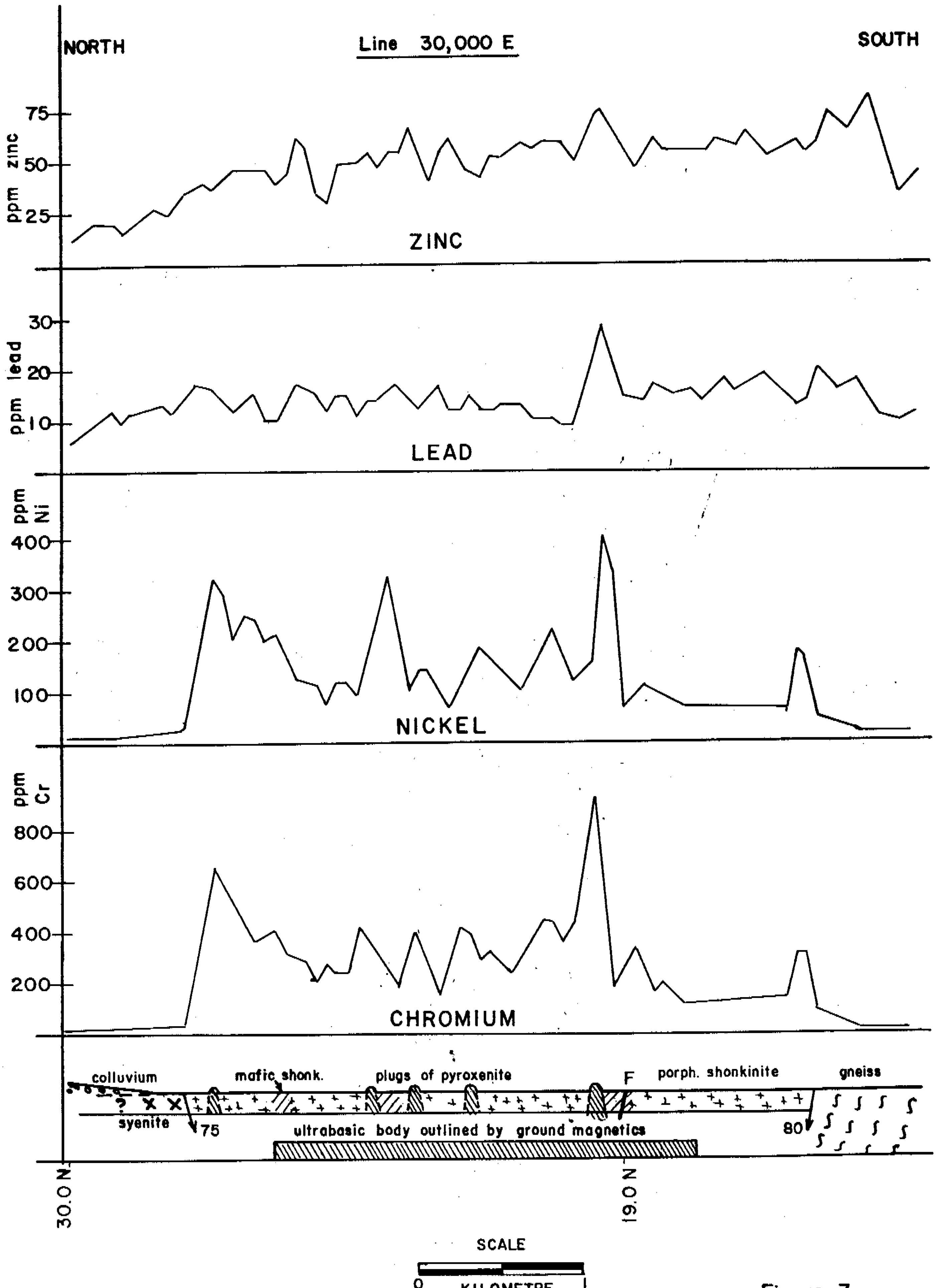

Figure 3

Geochemical Line-profiles : Orientation Survey

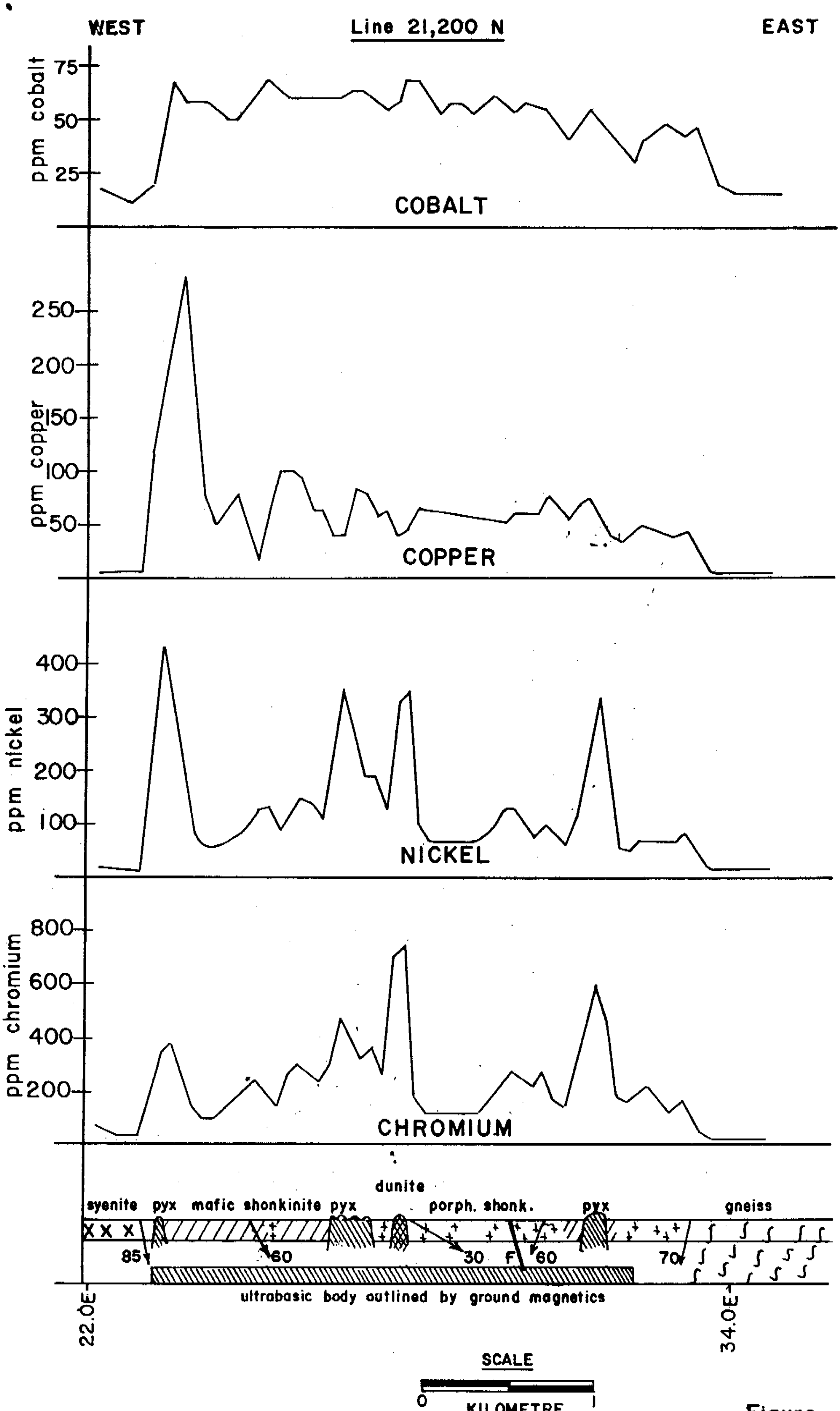

Figure 4

Geochemical Line-profiles : Detailed Survey

Two examples to illustrate the correlation between geochemistry and rock-type

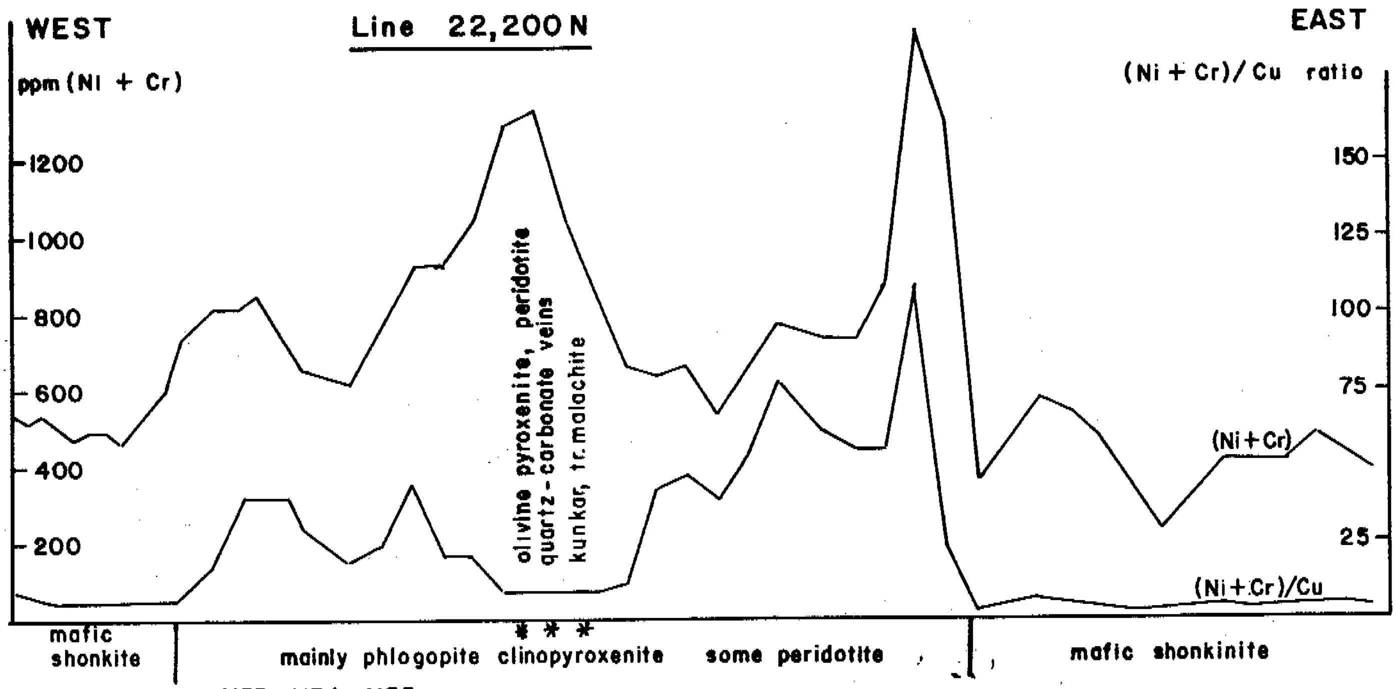

* rock samples M33, M34, M35

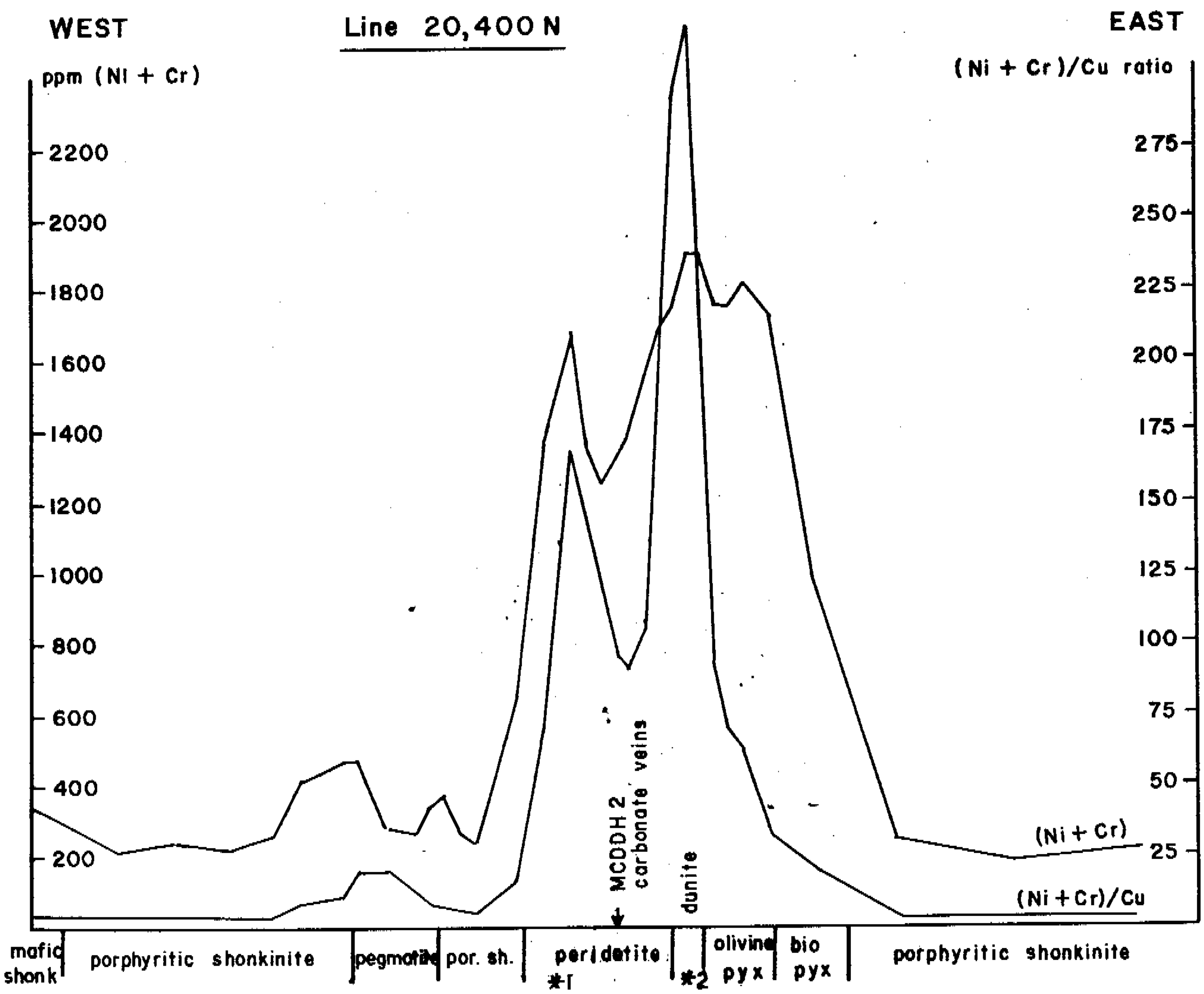

*1 rock samples M45, M46 *2 sample M19, see drill logs

Figure 5

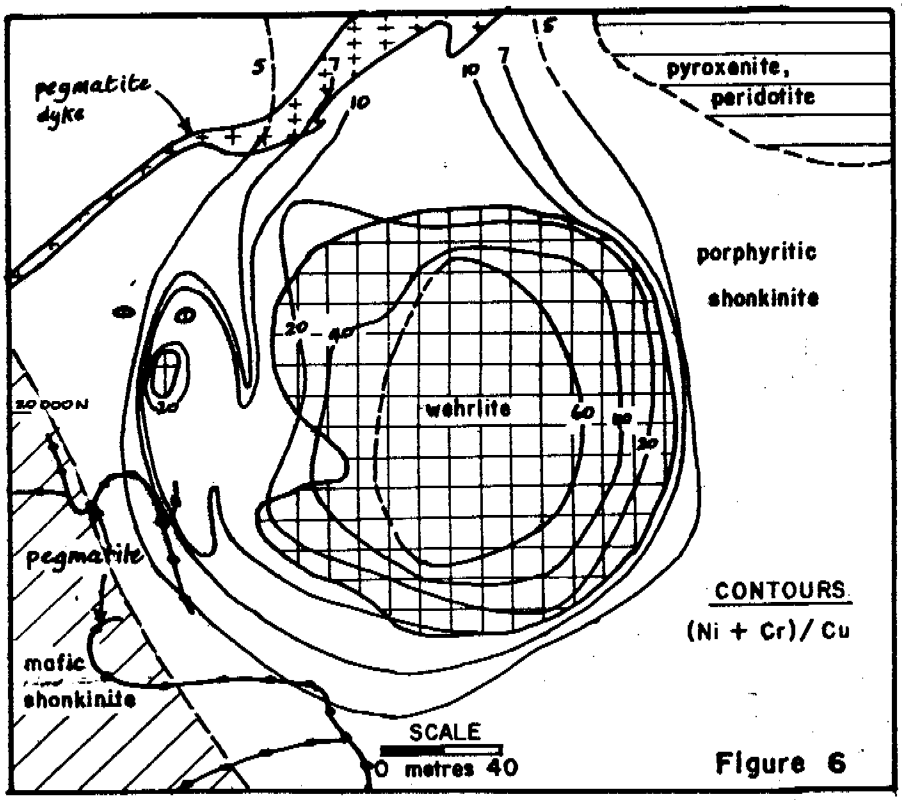

Figure 6

Drill core assays show that copper is low when olivine or orthopyroxene is the main component of the rock. Therefore the chemical zoning may be due to increases in one or both of these minerals towards the centre of the plug.

The concentric chemical zoning implies concentric mineralogical zoning. The zones, perhaps caused by concentric flow-banding, suggest that the outcrop is an intrusive plug, not a cognate xenolith, where banding is unlikely to be concentric. The intrusive nature of the plug is demonstrated by brecciated shonkinite in contact with the tough phlogopite wehrlite.

Chemical zoning, however, extends into the mineralogically homogeneous porphyritic shonkinite to give ratios higher than the usual 4 or 5, for both mafic and porphyritic shonkinite (see Figure 5). The chemical zoning, in this case may be caused by the movement of copper ions from shonkinite to wehrlite.

The loose bouldery nature of the plug precludes definitive petrological and petrochemical work to solve the problem.

AUGER DRILLING

Sixty-nine auger holes were drilled to bedrock in two areas of low topography and no outcrop, to prospect for kimberlite. Examination of the drill chips showed that the holes were drilled in shonkinite and pyroxenite.

DIAMOND DRILLING

Four holes were diamond drilled for a total depth of 322 metres to investigate possible economic occurrences of nickel and chromium in ultramafic rock, and of rare earths in 'carbonatite'.

Summaries are given overleaf and abbreviated diamond drill logs in Appendix 3.

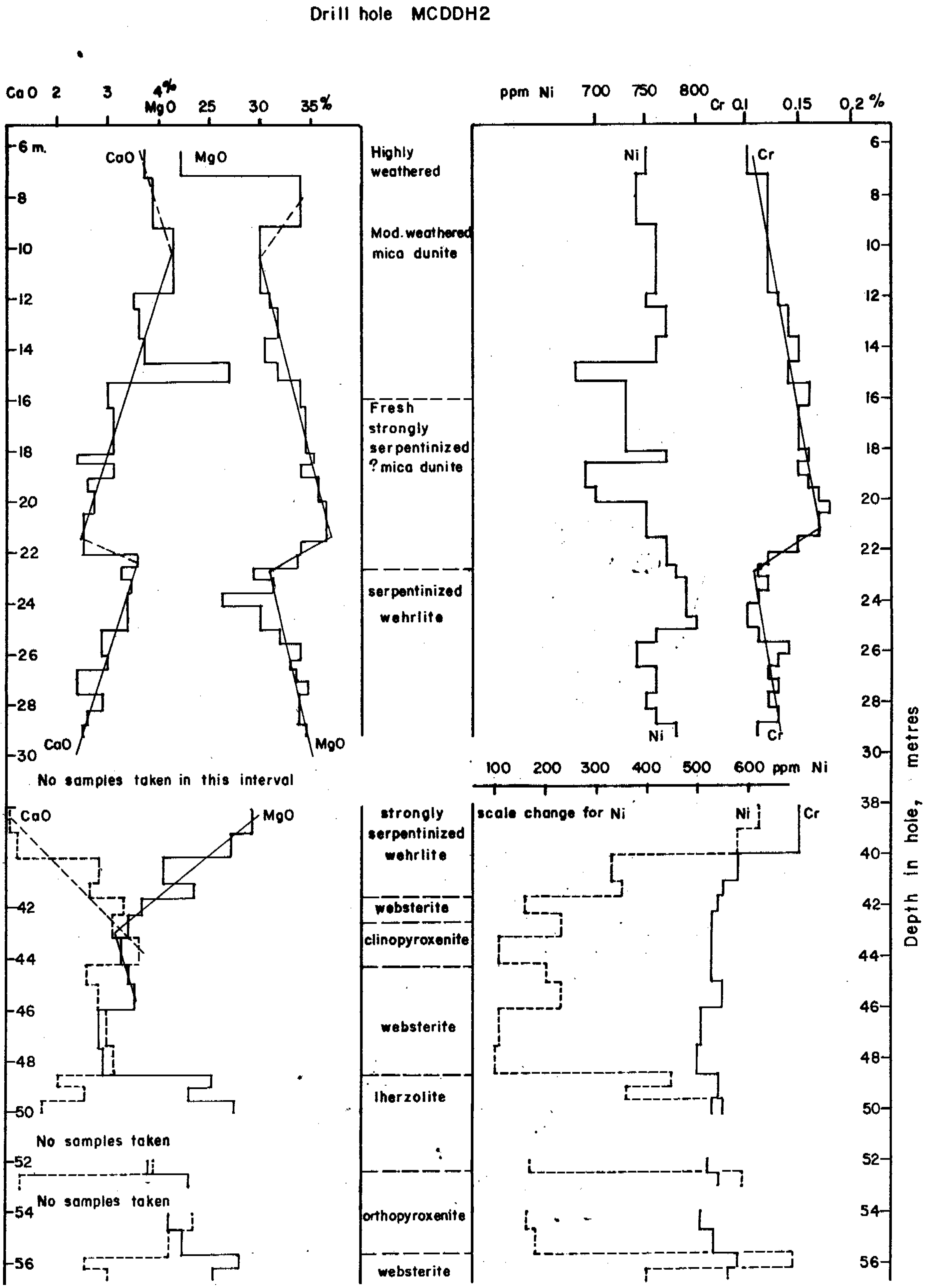

Cyclic units within layers

Figure 7

Drill hole MCDDH1 was collared in porphyritic shonkinite to intersect a dyke-like body of serpentinized dunite at depth in order to test its potential for chromite and nickel mineralization.

The drill intersected porphyritic shonkinite and melanocratic syenite to a depth of 80.6 metres, and foliated mafic shonkinite from 80.6 metres to the end of the hole at 96.6 metres. The dyke-like body of ultramafic rock was not intersected.

Porphyritic shonkinite and melanocratic syenite are intruded by dykes of micro-shonkinite. The contacts are usually quite sharp with only minor hydrothermal alteration present. Contacts between wider bands or dykes are sometimes gradational (over about 10 cms). Both the fine grained and porphyritic rocks are cut by narrow felspar-quartz and by pyroxene-felspar veins.

The mafic shonkinite is also cut by micro-shonkinite dykes and by pyroxene-felspar veins, but the dykes and veins are comparatively rare.

All of the above rocks are cut by carbonate-quartz veins and fractures. Larger veins invariably alter the host rock to form a thin selvage of actinolite, serpentine, epidote and chlorite. The off-set on fractures is usually less than 1 cm.

Many carbonate-quartz veins and fractures are themselves off-set 1 or 2 mms by calcite-filled micro-fractures.

The earlier fractures contain dolomite or dolomitic calcite, minor quartz and rare sulphide (chalcopyrite, pyrite); the later micro-fractures contain only (?) calcite (dilute HCl test).

Drill-hole MCDDH2 was collared in peridotite and drilled on line and towards drill hole MCDDH1 to intersect at depth the dyke-like body of mica dunite. The hole intersected ultramafic rocks to a depth of 59 metres and shonkinite from 59 metres to a final depth of 91 metres. Much of the ultramafic rock is strongly serpentinized and the original minerals and textures are obliterated. However sufficient are preserved to suggest, along with the petrochemistry, that the ultramafic rocks formed part of a layered intrusion. The conformable layers within the fault-bounded block are composed of dunite, lherzolite, orthopyroxenite and websterite. (see Plan 6 and Figure 7). The ultramafic rocks are in fault contact with the underlying shonkinite at about 59 metres.

Orthographic construction indicates the fault plane dips about 70° westwards, similar to a possible southerly extension of the fault (see Plan 5).

No chromite bands were intersected in the layered sequence but chromite reaches a maximum of 0.26% in dunite at 20 metres depth. Nickel reaches 800 ppm in peridotite; sulphide is rare but reaches a maximum of about 2% in websterite at 42 metres. The sulphide is finely disseminated and consists of pyrite, and pyrrhotite exsolving chalcopyrite.

Drill hole MCDDH3 was collared in syenite to intersect a carbonate and hematite-veined fault at depth. Carbonatite had been recorded from the fault by Kostlin (1971). At the surface the fault occurs as a low ridge of brecciated orange-orthoclase syenite with inclusions of carbonated, serpentinized ultramafic rock, pods of siderite, discontinuous carbonate-quartz veins and stringers of specular hematite. Rare chalcopyrite and pyrite occur in the carbonate-quartz veins. At the surface, brecciation and the effects of hydrothermal alteration can be seen over a width of 12 metres.

At depth, unaltered syenite is light grey and consists of large grey phenocrysts of orthoclase in a medium-grained matrix of felspar pyroxene, biotite, carbonate, apatite and opaque minerals.

Narrow bands of orange syenite, containing orange to brick-red phenocrysts of orthoclase, become progressively wider (from 0.2 metres to 0.95 metres) closer to the fault. Adjacent to the fault the groundmass of the syenite becomes fine-grained and within the zone of brecciation the matrix is cryptocrystalline and the rock veined with chalcedony and calcite. The zone of hydrothermal alteration at depth has a true width of about 8 metres (Plan 7). Near the zone of brecciation but within a band of orange syenite is a dyke of pale pink crystalline calcite (HCl test; Langworthy and Black op. cit.), minor quartz and biotite, and rare sulphide. The large crystals of calcite are aligned with their long axes parallel to the dyke walls and show only minor strain. The calcite was clearly emplaced after the intense shearing, brecciation and hydrothermal alteration of the syenite. Later mapping has shown that the fault is part of a fault system which truncates younger Amadeus Basin sediments in the Georgina Range.

Textural and field evidence, trace element and isotope analyses (Langworthy and Black, op. cit.) strongly suggest that the carbonate is not carbonatite.

The inclusions of ultramafic rock in the fault breccia show the possibility of ultramafic rocks at depth in or below the syenite.

Drill hole MCDDH4 was drilled to investigate a second occurrence of carbonatite (sovite - Kostlin, op. cit.) in a carbonate-veined fault. In the vicinity of the drill hole, the fault off-sets pegmatite dykes by about 40 metres (see Plan 7). Later mapping traced the fault 2.6 kms and showed it to be a branch of the fault system mentioned above. Down hole the fault was intersected between 42 and 48 metres, and consists of two shears 2.5 metres apart. The upper shear contains a brecciated and healed quartz vein and a strongly sheared chloritic rock. Green amphibole and hairline veins of sulphide are included in the quartz vein.

Shearing and brecciation is less intense in the lower shear in which occur fragments of felspar-veined shonkinite and narrow carbonate veins.

Carbonate veins are prominent from a depth of 36 metres to the fault zone at 42 metres. Two periods of veining (or fracture-filling) are recognised - the youngest are at 75° to the core axis, sub-parallel to the fault zone. Hydrothermal alteration and carbonation are common, typically forming epidote, actinolite and serpentine in the mafic and ultramafic rocks. Alteration of biotite to chlorite and of pyroxene to amphibole is common throughout.

Conformable, alternating and gradational bands of shonkinite and biotite pyroxenite were intersected throughout the drill-hole. Sulphide is present in all rocks, usually about 2% being mainly pyrite with rare chalcopyrite and pyrrhotite. In some fine-grained pyroxenite the sulphide content reaches 8%.

No carbonatite was intersected in the drill hole. Carbonate veins are almost certainly of post-intrusive age and, like the crystalline calcite from MCDDH3, probably related to the large regional fault which truncates the younger sedimentary sequence.

MAJOR AND TRACE ELEMENT CHEMISTRY

One hundred and thirty eight samples of split core ranging in composition from serpentinized phlogopite dunite to syenite were analysed for CaO, MgO, K_2O, Na_2O and several trace elements. Fifty-four of these samples were also analysed for SiO_2, Al_2O_3, Fe_2O_3 and MnO. Loss on ignition was determined for 24 samples. The samples were analysed by AAS and wet-chemical methods.

Fifty-three of the fifty-four complete major and minor analyses have assay totals well below 100% (see Table 3). A comparison between these assays and assays of similar sections of core by X.R.F. analysis (Table 5) shows the silica assays by wet chemistry to be low and inconsistent. The values obtained for Fe_2O_3, Al_2O_3 and K_2O for the samples of Table 3 are also lower than comparitive assays by X.R.F. Consequently the assay results in Table 3 have been treated statistically, not empirically.

Table 5

	MCDDH1		MCDDH2		MCDDH4	
SAMPLE	8067°	8758*	8108°	8790*	8170°	8782*
INTERVAL	28.4-29.4	28.4-28.6	24.6-25.1	25.0-25.2	43.0-43.5	43.0-43.2
ROCK TYPE	Fine grained shonkinite		Peridotite		Biotite pyroxenite	
SiO_2	34.0	46.34	33.0	39.97	44.1	48.56
Al_2O_3	8.3	11.20	1.0	2.27	6.0	5.92
Fe_2O_3	8.5	11.49	9.0	14.67	10.5	13.02
MnO	< 0.1	0.16	< 0.1	0.17	0.2	0.17
MgO	11.9	11.54	30.0	36.66	14.4	16.16
CaO	10.0	9.37	3.4	3.50	11.7	12.63
Na_2O	1.1	0.58	0.1	0.19	0.3	0.43
K_2O	3.5	5.97	0.6	1.04	0.7	1.22
TiO_2	1.9	1.38	0.4	0.43	0.9	1.09
P_2O_5	1.21	0.86	0.84	0.39	0.95	0.74
BaO	1.4	0.55	< 0.2	0.15	< 0.2	0.27
SrO	0.3	0.15	< 0.1	0.02	< 0.1	0.03
TOTAL	82.11	99.59	78.34	99.46	89.75	100.24
LOI	2.6	2.07	3.8	Av 2.93	3.4	3.88

o Water Resources Branch, Dept. of N.T., Darwin

* Adelaide University; analysts D. Barraclough, J. Stanley.
Na_2O, FeO determined volumetrically. BaO by X.R.F. using prepared standards. Samples and standards checked by A.A.S.

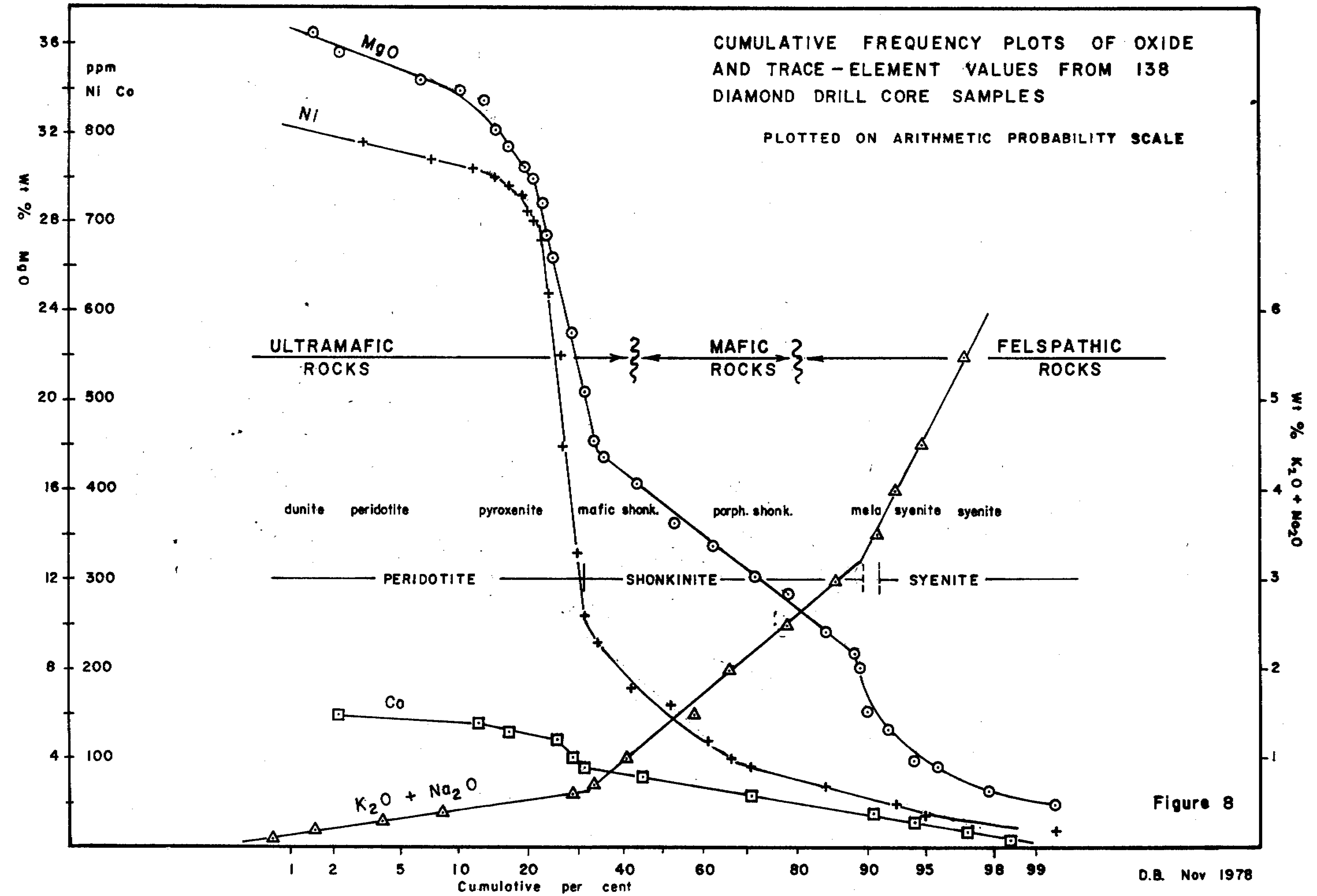

Figure 8

D.B. Nov 1978

Four cumulative frequency plots (Figure 8) show a break in distribution at about 30 percentile. In the case of MgO, Ni and Co the cumulative distribution lines show two breaks, first to a steeper slope and then to a shallow slope. Such graphs are the expressions of dual distribution, suggesting the existence of two distinct populations (Lepeltier, 1969). The two elementary populations are one of high MgO, Ni and Co represented by dunite, peridotite and pyroxenite, and one of low MgO, Ni and Co represented by shonkinite and syenite.

The arithmetic distribution of alkalies (Na_2O+K_2O) shows two breaks to steeper slopes, one at 32 percentile the other at 89 percentile, indicating two increases in alkalic mineralization. The first increase in mineralization at about 0.6% alkalies coincides with the apparent rapid decrease in MgO, Ni and Co mineralization. The decline in MgO abundance is largely balanced by increases in CaO and Fe_2O_3 abundance (see Table 3 and Figure 9). In terms of fractionation the change in element distribution at this point is due to a change in crystallization from largely olivine to pyroxene.

In terms of metasomatism or basification of syenite by the ultramafic rocks, the graphs suggest a major exchange of magnesium for iron and calcium. Clearly neither the country rock (mainly felsic gneiss) nor the syenite contain sufficient iron or calcium to produce such a change. The ideas of metasomatism (Barraclough, Kostlin, ops. cit.) are untenable.

Geochemical logs of the layered sequence intersected in drill hole MCDDH2 show two regular changes in composition between drill depths 6 and 30 metres (see Figure 7). The decrease in MgO and Cr, and the increase in CaO upwards indicates the cumulate sequence is in an upright position. The two changes in composition, separated by a short reversal, show that at least two cycles of magmatic deposition occurred. The rates of change in MgO, CaO and Cr are identical in each cycle but the upper cycle is slightly more calcic, possibly reflecting small changes in differentiation and crystal deposition. The slightly more calcic trend of the upper cycle is another indication that the sequence is in an upright position.

Cycles in the concentration of Ni are features commonly associated with ultramafic rocks of layered intrusions. Within the Muskox intrusion for example, Ni decreases upward within each cycle, increases sharply and gradually declines in the following cycle (Irvine and Smith, 1969). The Ni is essentially contained in solid solution in olivine and the decline in abundance is interpreted as the result of fractional crystallization of olivine from a finite amount of magmatic liquid. During fractional crystallization of each cycle, there is also a gradual decline in the abundance of MgO as more and more olivine becomes progressively more fayalitic. The decline in Ni follows the decline in MgO.

An unusual feature of the Mordor Complex is that although two cycles of MgO and Cr are indicated in Figure 7, there are no corresponding cycles of Ni. Indeed Ni shows very little correlation with MgO in the ultramafic rocks of MCDDH2. However Figures 8 and 10 suggest a general correlation between Ni and MgO but with a wide scatter of points. The ultramafic rocks in MCDDH2 have bands of serpentine running through them and it is possible that there has been some redistribution of either Ni or MgO in the serpentine.

Variation Diagrams

Since the silica assays cannot be used to calculate CIPW Norms or Differentiation Indices, differentiation is illustrated by plotting element and oxide values against magnesia, and illustrated by a ternary diagram.

1. Lime

The CaO:MgO ratio increases from a low value of 0.07 in dunite to a maximum and fairly constant value of about 1.25 in clinopyroxenite, shonkinite and syenite (carbonated and carbonate-veined rocks excluded). CaO increases in abundance to about 15% and declines equally with MgO to low values in syenite. These changes reflect first the increasing, and then the decreasing importance of clinopyroxene in fractional crystallization, as first olivine is displaced by pyroxene and then pyroxene becomes subordinate to orthoclase.

2. Alumina

The Al_2O_3:MgO ratio is initially low due to the small amount of interstitial felspar (hyalophane, orthoclase). The ratio increases slowly at first with the progressive change from diopside to diopsidic augite and the slight increase in abundance of interstitial felspar. The ratio increases more rapidly as felspar becomes a major constituent.

3. Alkalies

The $(Na_2O + K_2O)$:MgO ratio is low and constant throughout the early stages of fractionation. A change in slope occurs at about 18% MgO, when the residual magmatic liquid has become rich in alkalies. The change in slope corresponds to the breaks in slope on the cumulative frequency curves in Figure 8 for MgO and alkalies.

Variation of wt % CaO, Al_2O_3 and alkalies with MgO in drill core samples

Closed symbol represents a sample of a fine-grained dyke

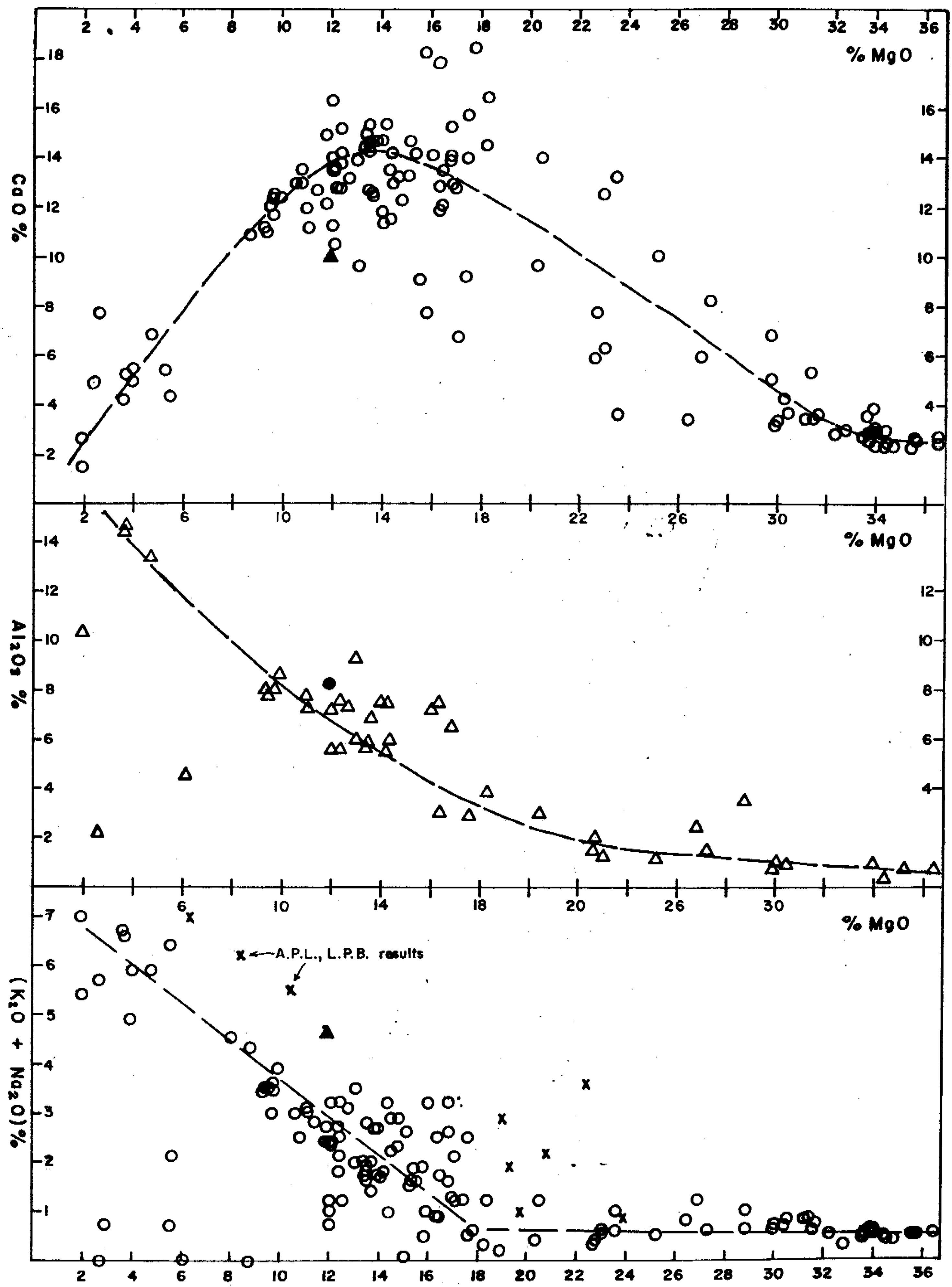

Figure 9

DB Nov 1978

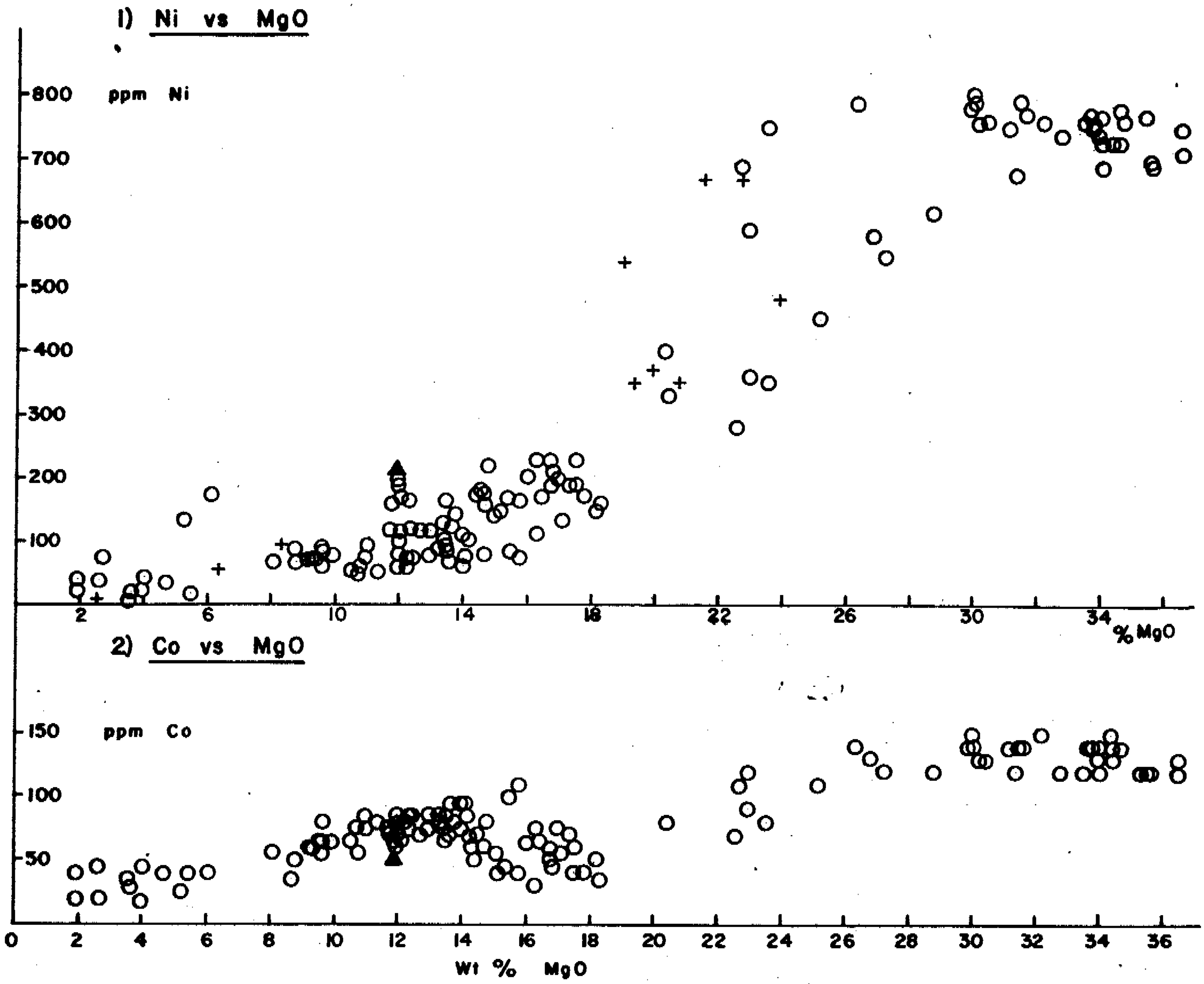

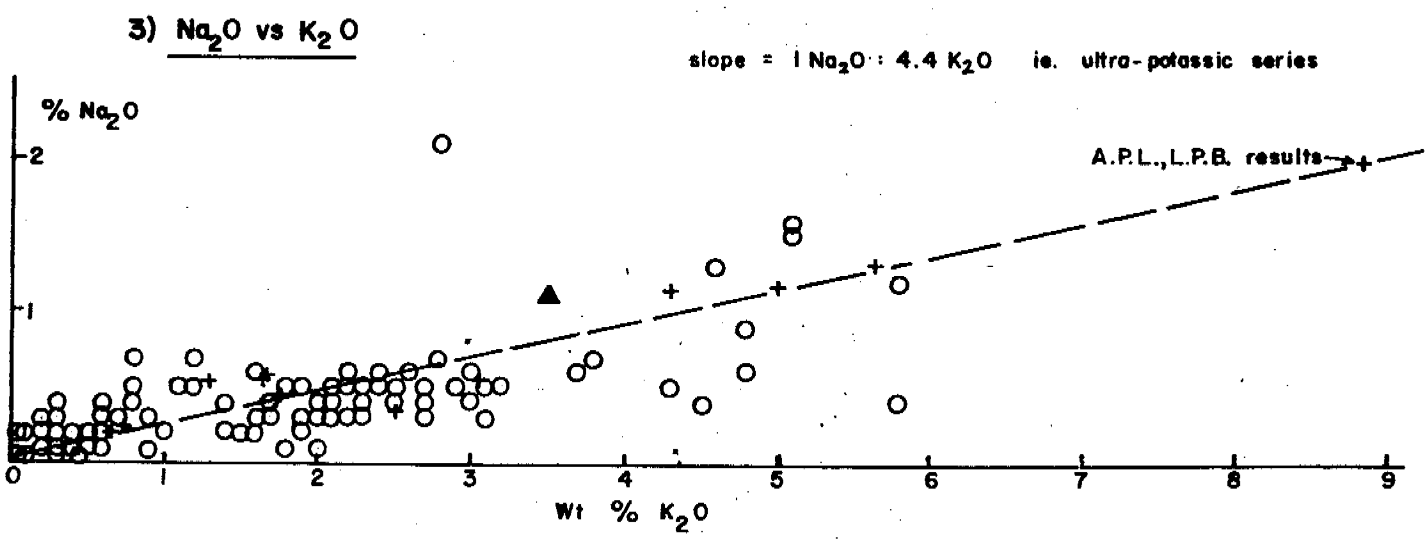

Variation Diagrams : assays of drill core samples

Note — the closed symbol represents a sample of fine-grained shonkinite from a dyke

Figure 10

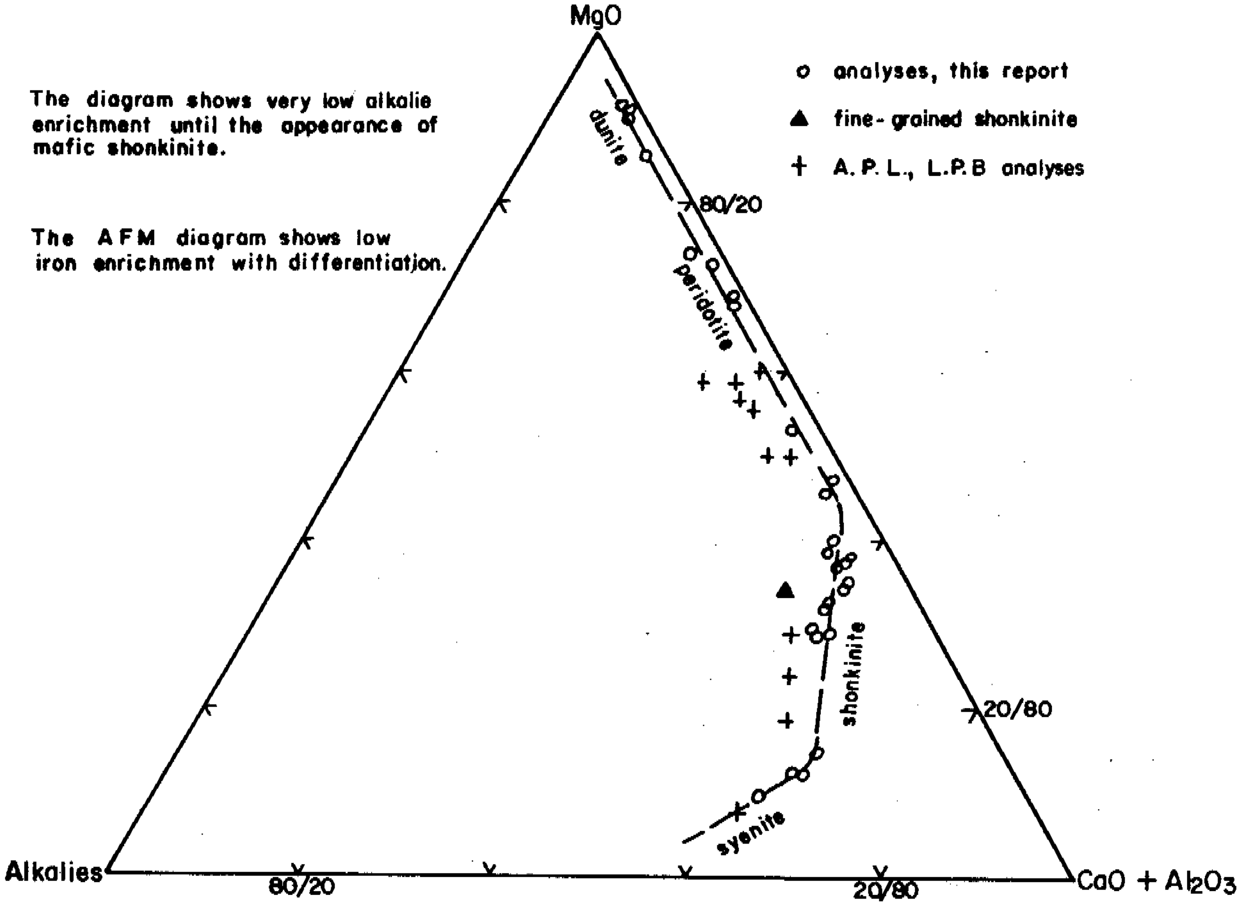

Differentiation Diagram of the Mordor Complex Figure II.

Throughout the crystallization of the magma the $K_2O:Na_2O$ ratio remains constant at about 4.5:1 (see Figure 10; the analyses of Langworthy and Black (op. cit.) have been added to provide a more reliable figure). The high $K_2O:Na_2O$ ratio places the rocks in the 'ultrapotassic series' of Carmichael, Turner and Verhoogen (1974) and suggests that the magma (primary or derived) was enriched in alkalies.

There is a scatter of points in each of the above curves and there is similar scattering when Ni, Co, CaO, Al_2O_3 and alkalies are plotted against each other, suggesting some independant variations. Carbonate veining and hydrothermal alteration may explain some of the scatter but mineral segregation during crystal accumulation is also an important factor.

The ACM diagram in Figure 11 shows a very low alkalic enrichment until the appearence of shonkinite in the later stages of differentiation. An ACF diagram (not shown) indicates low iron enrichment with differentiation.

Effect of Weathering

Table 6 shows some of the changes in the abundance of some oxides with severity of weathering.

Table 6

Analyses of porphyritic shonkinite, drill hole MCDDH1.

Sample	Depth (m)	Weathering	MgO	CaO	K_2O	Na_2O	BaO
8063	2.2-5.1	Moderate	8.1	10.5	3.8	0.7	3.4
8064	5.1-6.1	Mod-sl.	9.7	11.7	2.9	0.5	2.4
8065	6.1-7.1	Slight	9.3	11.2	3.1	0.5	2.6
8066	7.1-8.1	Sl-fresh	9.4	11.0	3.2	0.5	2.6

The analyses indicate that MgO and CaO are partially removed from the rocks by weathering so that samples collected from outcrop may be deficient in MgO and CaO. Sample 8063 seems to have been enriched in BaO a factor of 1.3 by weathering. The assays therefore point to one possible method by which barite may accumulate superficially.

Hydrothermal alteration

A fault intersected in drill hole MCDDH3 is sandwiched between alternating bands of grey and brick-red syenite. The bands of brick-red syenite become narrower and more widely spaced with distance from the centre of the fault and disappear entirely about 5 metres away (see Plan 7). The unaltered host rock is a grey syenite with large light grey phenocrysts of orthoclase. The following analyses in Table 7 suggest that the bands of brick-red syenite are depleted in Na, Sr and Ba with respect to the host rock.

Table 7

Sample	K_2O	Na_2O	SrO	BaO	CaO	MgO	TiO_2
	Brick-red syenite						
8153	5.8	0.4	0.1	1.2	4.4	5.5	1.7
8158	4.5	0.4	0.2	1.8	5.7	4.0	1.7
8160	4.8	0.9	0.4	2.1	7.8	2.6	1.8
Average	5.03	0.57	0.23	1.70	5.97	4.03	1.73
	Grey syenite						
8152	5.1	1.5	0.6	2.7	5.3	3.7	1.4
8154	5.1	1.6	0.5	2.8	4.2	3.6	1.3
8161	4.6	1.3	0.6	2.4	6.9	4.7	1.8
Average	4.93	1.46	0.56	2.63	5.47	4.0	1.5

With depletion, the ratio Na_2O:SrO remains constant at about 2.5, suggesting that the two elements (Na and Sr) occur together in one mineral, in this case probably orthoclase or hyalophane.

Barium is strongly depleted in the brick-red syenite. It is present in hyalophane and occurs as barite. The amount of barite however, in the unaltered syenite is very small. Therefore the depletion of barium is probably due to the alteration of hyalophane (K,Na,Ba,?Sr)($[Al,Si]_4 O_8$) possibly to orthoclase. The analyses therefore suggest a second method whereby barite may accumulate.

DISCUSSION

Langworthy and Black (op. cit.) show by means of chemical analyses that the rocks of the Mordor Complex have an affinity to the ultrapotassic series which include kimberlite and carbonatite. They point to the spatial relationship of the Mordor Complex with Mud Tank Carbonatite and show that the same Sr isotopic relationship exists between them as exists between other spatially related alkalic rocks and carbonatites. They conclude that the Mordor Complex is a highly differentiated suite of crystalline rocks, texturally related to normal ultrapotassic, ultramafic rocks, spatially related to carbonatite and chemically related to kimberlite.

Alkaline intrusives usually take the form of complexes containing a wide variety of alkaline rock types. They are conspicuously round or oval and are almost exclusively associated with continental cratonogenic areas. Many alkaline intrusives are concentrically zoned composite plutons often with a core of dunite. The recurrence of a concentric zoned pattern in cylindrical or funnel-shaped intrusions is similar to that of zoned complexes in orogenic regions. The core of dunite or peridotite shows typical magmatic features.

Alkaline intrusives occur in the same tectonic environment as kimberlite and there are close associations between alkaline intrusives and carbonatite, and between carbonatite and kimberlite. There are therefore, many indirect links between alkaline intrusives, carbonatite and kimberlite in shield areas and zoned ultramafic complexes in orogenic regions.

Repeatedly, geophysics provides evidence of large cylindrical plugs of ultramafic rock intrusive into mafic 'differentiates' for both alkaline complexes in cratonogenic areas, and zoned complexes in orogenic areas (Noble and Taylor, 1960; Irvine, 1967). The magmatic approach is to view the complexes as being formed by either serial intrusion (Ruckmick and Noble, 1959); emplacement of different magmas (Irvine, 1967) or by differentiation in situ (Langworthy and Black, op. cit.).

The lack of a chill phase in alkaline ultramafic intrusions and a general lack of thermal effects on the country rock has led to the suggestion that the alkaline peridotite magma must be at a low temperature, if it exists at all. Some workers (for example Borodin, 1963) believe only the ultramafic rocks have a magmatic origin and that all the other rocks (the so-called differentiates) have a metamorphic or metasomatic origin. McTaggart (1971) sees the annular arrangement of rock-types being caused by downdropping of a central core of high S.G. ultramafic cumulates which then collapses the magma chamber and ring-fractures the enclosing country rock. He suggests that water from the enclosing country rock, guided by the ring-fractures, diffuses and homogenizes the minerals and rocks, and removes plagioclase at temperatures above the formation of serpentine. Any chill margins, he notes, would be removed.

The cumulate nature, layering and chemical cyclicity of the ultramafic rocks of the Mordor Complex confirm their magmatic origin. These rocks are not in direct contact with syenite or the country gneiss. The "intervening" rocks (shonkinite and melasyenite) have shear contact with the country gneiss. No chill margin has been recognised. The foliation of the "intervening" rocks and of the country gneiss has a centripetal dip, steep at the margin, shallow toward the centre of the mafic part of the complex. The inwardly shallowing dip of the foliation, the macroscopic zoning and local banding, together suggest a saucer-like distribution of mafic rocks. These rocks have been intruded by peridotite and pyroxenite. This arrangement is not unlike the one idealized by McTaggart (op. cit.).

The syenitic part of the complex has macrogradational contact with the enclosing gneiss and contains many outcrops of microsyenite, possibly a chilled syenite. Small xenoliths of country gneiss are included in syenite but probably do not persist at depth (see Plan 7). The field evidence suggests that the syenite crystallized at or near its present site.

The contact between syenite and the rocks of the mafic sector is sharp but not, in most observable cases, faulted. The arrangement of the syenite and mafic rocks (Plan 2) is best explained by a separate intrusion of syenite.

To explain these rather complex arrangements of contacts, the centripetal dip of the foliation, the apparent separate intrusions of felsic, mafic and ultramafic rocks and the occurrence of pegmatite, a scheme of intrusion and crystallization is proposed below.

A large body of ultrapotassic ultrabasic magma, <u>at least</u> 40 cubic kilometres (calculated from data supplied by Kirton and Doe, op. cit.), intruded felsic gneiss of the Arunta Complex. Crystallization of the magma proceeded from the base, walls and to a much lesser extent, the roof -- much like the freezing of large ingots of molten metal. Unlike the freezing of ingots, deposition of crystals on the floor of the chamber probably took place by convection -- crystals forming in the upper, cooler part of the chamber being deposited in the manner of alluvial sediments. Gravity settling of olivine and pyroxene may have occurred but the magma viscosity was probably far too high for this type of deposition to be effective. Upwelling liquid would probably overcome any downward movement of crystals.

Crystallization continued until a 6 kilometre deep cylinder of ultramafic rock had formed (geophysical evidence, Kirton and Doe, op. cit.). By now some 40 cubic kilometres of magma had crystallized. The remaining liquid, enclosed by olivine and pyroxene cumulates (probably a thick base with comparatively thin walls and roof) is rich in alkalies and volatiles. At this point, orthoclase crystallized and shonkinite was formed (see Figures 8,9 and 11). Later as fractional crystallization continued orthoclase crystallized at the expense of biotite, and melanocratic syenite was formed.

mafic shonkinite	15 k-spar	45 pyx	30 bio	10 Fe.ox.
porphyritic shonkinite	30 k-spar	30 pyx	30 bio	10 Fe.ox.
mela-syenite	50 k-spar	30 pyx	10 bio	5-10 Fe.ox.

The fugacity of oxygen increased and hematite appeared, intergrown with magnetite. About now the remaining magmatic liquid injected into the country rocks and the roof of the chamber collapsed into the void left by the liquid. Mafic differentiates, the enclosing early ultramafic cumulates and country gneiss dropped onto a crystal mush of mafic and felsic differentiates — themselves underlain by early ultramafic cumulates. Blocks of early formed cumulates of various shapes and sizes broke off the roof arch and assumed various attitudes in the mush of mafic and felsic differentiates. Fractures within the collapsed roof were filled with melted country rock (felspar - quartz pegmatite) and intercumulus liquid (microshonkinite). Some of the fracture-filling liquids mixed to give hybrid liquids. Some pegmatitic and intercumulus liquids intruded the adjacent crystallizing magmatic liquid. Some pegmatite mixed with the syenitic liquid and crystallized as a hybrid pegmatitic syenite. A small amount of intercumulus liquid intruded the syenitic crystal mush of the adjacent intrusive. Volatiles were probably vented during the intrusion of the syenitic magma.

Later, probably during the Alice Springs Orogeny, a fault cut the Complex and displaced the western margin about 1 kilometre. The fault horsetailed through the centre of the Complex, displacing and hydrothermally altering adjacent rock.

Supportive evidence

Petrographic studies show that the ultramafic rocks are composed of cumulate olivine and pyroxene, and are probably layered. Whole-rock geochemistry supports the notion of layering by revealing chemical cycles within the cumulates. Field work and diamond-drill core show that gradations exist between all rock-types of the Complex, from dunite through shonkinite to pegmatite. The early-formed cumulates (dunite, peridotite and pyroxenite) crop out only within the mafic sector of the Complex. Nowhere are they in contact with syenite; there is always some mafic differentiate between the two rock-types. This field evidence may have led Kostlin (op. cit.) to propose a hypothesis of basification of syenite. However whole-rock geochemistry shows this idea to be untenable.

The geophysical evidence of Kirton and Doe (op. cit.), suggests that the Mordor Complex is essentially a cylinder of dense, magnetic and ultrabasic rock, 6 kilometres deep, underlying at shallow depth shonkinitic rocks in the mafic sector. The cylinder is away from the felsic sector of the Complex, therefore the felsic rocks form a separate but adjacent intrusion to the ultramafic and mafic differentiates.

Clearly the Mordor Complex is unlike a lopolithic layered intrusion in which ultramafic cumulates are conformably overlain by basic and acid differentiates, in a funnel-like arrangement.

In the petrogenetic scheme proposed by Langworthy and Black (op. cit.), (extreme megmatic differentiation followed by serial intrusion) syenite is intruded by mafic differentiates which are intruded in turn by plug-like ultramafic bodies. However it is difficult to explain why the plug-like bodies do not intrude the felsic sector and it is also difficult to visualize increasingly higher S.G. rocks progressively intruding syenite, like negative salt domes. It could be argued that each successive intrusion provides a channelway for the next heavier, higher melting point intrusion, and so the complex would be zoned, thereby no ultramafic rock would be in contact with syenite.

This may occur if the ultramafic rock was molten but the field evidence suggests that it was not; mapping shows a plug of phlogopite wehrlite in contact with sheared and brecciated shonkinite. It is probable that by the time the felsic differentiates are formed, the earlier ultramafic cumulates will be solid, but intrusion by heavy, solid early-formed cumulates defies isostacy.

The situation may have been the reverse of serial intrusion as proposed by Langworthy and Black (op. cit.) — the later differentiates may have collapsed on to the ultramafic cumulates. There is much field evidence to support this view.

1. the foliation of the gneiss around the margin of the mafic sector dips steeply inwards.

2. the foliation of the mafic rocks dips centripetally, steep at the margin and shallow at the centre of the mafic sector.

3. the few exposed contacts between ultramafic and felspathic rocks are brecciated.

4. the attitude of the pegmatite and mafic dykes suggest an alignment of fractures somewhat in the manner of a sunken fruit cake (see later discussion).

5. the syenite appears to have passively intruded the country gneiss in a molten state, chilled syenite being present.

The field evidence suggests that the syenite crystallized in situ but that the relationship between the mafic sector and the country gneiss (and by extension, the syenite) is one of downward movement of the mafic sector.

The differentiates of the Mordor Complex have been tightly contained within the enclosing gneiss. The confining pressure has not allowed the magma to spread lopolithically at the upper levels. This confinement may have kept intact the early-formed cumulates of the roof and upper walls unlike the layered sequences of funnel-shaped lopoliths. During cooling of the Complex layers of ultramafic rock built up from the base until the volatiles and low-melting point fraction (syenite) were confined by early differentiates to a relatively small space near the roof of the chamber.

If the roof or walls are fractured during these last stages of cooling, the volatiles will escape, perhaps explosively blowing with them blocks of early-formed cumulates from the roof or walls. Inevitably roof collapse must follow. The heavy cumulates will drop on to and either sink in or push out of the fracture the residual magma. This may have been the case for the Mordor Complex, the residual syenitic magma forming a separate, adjacent intrusive. If fractionation continues to pegmatitic end-products (probably an unlikely event), these final-stage differentiates should be associated almost exclusively with the syenite intrusion. In the Mordor Complex they are not; pegmatite dykes are very largely confined to the mafic sector of the complex.

The pegmatite dykes trend mainly ENE—WSW and dip between 35 and 65° north-westerly. They are largely confined to the mafic sector of the complex where they tend to occur in an arcuate arrangement, parallel to the long axis of the oval sector. To the north of the mafic sector, the dykes have a sub-concentric arrangement. Pegmatite crops out to a lesser extent in syenite but rarely do any dykes extend into the country gneiss. In outcrop they are up to 6 metres wide but at depth in all drill holes the dykes do not exceed a few centimetres. They intrude all rock-types of the complex including micro-shonkinite dykes. However some mafic dykes cut pegmatite and some dykes, both shonkinite and pegmatite, pass laterally into and out of possible hybrid rocks.

The strong alignment of the pegmatite and micro-shonkinite dykes suggests that there was structural control over their emplacement. They may be expansional features in response to NE - SW compression on the mafic - ultramafic body or are tensional features caused by upper-level slumping.

In either case, pegmatitic liquid was available to fill the fractures. This pegmatitic liquid could have been generated from partially melted country rock or by extreme magmatic differentiation of the adjacent syenitic liquid. In the second case, pegmatitic fluids would have to migrate to the mafic sector, but field work shows that most dykes terminate near the contact with syenite and do not originate in syenite. With extreme magmatic differentiation most pegmatite dykes should be intimately associated with the syenitic rocks, and clearly they are not.

The preferred explanation is that pegmatite originated from partially melted country rock. The hot intrusive would almost certainly chill against the intruded gneiss to prevent the mixing of magma and melted gneiss. Fractionation would proceed as outlined earlier but the pegmatitic liquid would remain behind the chill margin until the chamber roof collapsed. The heavier blocks of chill margin and early-formed roof cumulates would drop into or on the remaining liquid. The melted country rock would then fill the fractures but not unduly alter the ultramafic rocks.

The country-rock melt would be centred over and around the chill envelope. There would be very little melt away from the intrusive so that when (or if) the late differentiates extrude from the magma chamber, the amount of melt (pegmatite) would be small and would be almost non-existant towards the outer limits of the syenite intrusion. This is precisely the case.

Mixing of the syenitic magma with country melt would be a distinct possibility but the effect should be most noticeable adjacent to the mafic - ultramafic intrusive. Again, this is the case.

In conclusion, there is sufficient field and chemical evidence to show that the Mordor Complex is a product of fractional crystallization of an ultra-potassic, ultramafic magma. There is no evidence, field or otherwise to support large scale metasomatism or basification of either the country rocks or of any magmatic differentiate. Metasomatism or hydrothermal alteration plays only a small part in the formation of the Complex.

REFERENCES

Barraclough, D. Interim report on the Mordor alkalic ring complex. North. Terr. Geol. Surv. Rec. 75/26 (unpubl.) (1976).

Borodin, L.S. Carbonatites and Nepheline Syenites. Izv. AN SSR ser. geol. 8 (1963).

Carmichael, I.S.E., Turner, F.J., and Verhoogen, J. Igneous Petrology 739p. McGraw Hill New York. 1974.

Crohn, P.W., and Gellatly, D.C. Probable carbonatites in the Strangways Range area, central Australia. Aust. J. Sci. 31, 335-336. (1969).

Irvine, T.N. The Duke Island ultramafic complex, southeastern Alaska: in ultramafic and related rocks (P.J. Wyllie, ed.), John Wiley and Sons Inc., New York p.84-97. 1967.

Irvine, T.N., and Smith, C.H. The ultramafic rocks of the Muskox intrusion, Northwest Territories, Canada: in Ultramafic and related rocks (P.J. Wyllie, ed.), John Wiley and Sons Inc., New York p.38-49. 1967.

Kostlin, E.C. A. to P. 2373, Georgina Range, N.T. Conzinc Rio Tinto of Australia Exploration Pty., Ltd., unbubl. company rept. (1971).

Langworthy, A.P., and Black, L.P. The Mordor Complex: a highly differentiated potassic intrusion with kimberlitic affinities in central Australia. Contrib. Mineral. Petrol. 67, p.51-62 (1978).

Lepeltier, C. A simplified statistical treatment of geochemical data by graphical representation. Econ. Geol. 64 p.538-550. (1969).

Marjoribanks, R.W., and Black, L.P. Geology and geochronology of the Arunta Complex, north of Ormiston Gorge, Central Australia. J. Geol. Soc. Aust., 21 pt 3, p.291-300 (1974).

McTaggart, K.C. On the origin of ultramafic rocks. Geol. Soc. Amer. Bull., 82 p.23-91 (1971).

Noble, J.A., and H.P. Taylor Jr. Correlation of the ultramafic complexes of southeastern Alaska with those of other parts of North America and the world. 21st Intern. Geol. Congr. Copenhagen. Repts 13 p.188-197 (1960).

Ruckmick, J.C., and Noble, J.A. Origin of the ultramafic complex at Union Bay, southeastern Alaska. Geol. Soc. Amer. Bull., 70 p.981-1018 (1959).

Scott, I.F. Central Mineralogical Services rept. in A. to P. 2373 Georgina Range. CRAE Pty., Ltd., unpubl. company rept. (1971).

Shaw, R.D., and Warren, R.G. Alcoota, N.T. 1:250,000 Geological Series. Bur. Miner. Resour. Aust. Explan. Notes. SF/53-10 1975.

Smirnov, V.E., Editor. Geology of mineral deposits. 520p. MIR Publishers, Moscow. 1976.

Wyllie, P.J., Editor. Ultramafic and related rocks. 464p. John Wiley and Sons Inc., New York. 1967.

APPENDIX 1

CRAE Pty Ltd Chip Sample Numbers and Descriptions

APPENDIX 1

CRAE Pty Ltd Chip Sample numbers and descriptions.

Locations of samples shown in Plan 4.

Thin section and polished section descriptions by I.F. Scott, Central Mineralogical Service (various CMS Reports) and by AMDEL. For details, refer to Kostlin (op. cit.) and, for CRAE locations, Plan NT 836.

Number on Plan 4	CRAE sample number	Thin, polished section description
1	192363	Hornblende-hypersthene-plagioclase granulite
2	192362	Altered contact rock
3	192365	Apatite rock, replaced by potash felspar
4	192630	Apatitite
5	W378	Barite
6	145833	Diorite with secondary uranium silicate and thorium silicate
7	145938	Vein quartz with syenite fragments
8	145933	Graphic granite
9	145937	Calcite carbonatite (sovite) with syenite fragments
10	145934	Syenite
11	145936	Plagioclase-diopside-hypersthene-biotite-opaques granulite
12	145935	Andesine-pyroxene-opaques-biotite metamorphic rock
13	52	Mica pyroxenite with shonkinitic affinities
14	192358	Metasomatized ?ultrabasic
15	192357	Actinolite rock with apatite
16	192356	Biotite rock with apatite and rutile
17	192361	Partially serpentinized biotite peridotite
18	145967	Metasomatized microdiorite
19	W373	Tremolite-phlogopite rock with calcite alteration

20	W375	Diorite-gabbro (alkaline), biotite-bearing
21	64	Carbonatite
22	W374	Plagioclase-biotite-pyroxene-epidote-opaques, high-grade metamorphic rock
23,24	197740 192371 197730 197733 197739	Silicified and brecciated biotite-apatite rock plus potash felspar areas; altered ultrabasic rock
25	197727 192377	Silicified biotite-apatite-opaques rock
26	197731 192369	Altered and silicified apatite-biotite igneous rock (ultrabasic intrusive)
27	197729 197741 192375	Extremely altered biotite-olivine and apatite-bearing ultrabasic
28	42	Mica pyroxenite with shonkinitic affinities. Minor marcasite within magnetite; sulphides including pyrrhotite, chalcopyrite and pentlandite, the latter partly altered to violarite.
29	145941 145942 147737	Carbonatite (sovite) Syenite
30	197732 197735 192730	Brecciated and intensely silicified biotite-apatite-rutile-opaques rock of intrusive ultrabasic origin
31	W376	Biotite pyroxenite
32	192376 197724	Silicified and brecciated coarse grained shonkinite. Coarse-grained chalcopyrite altering to neodigenite. Traces of chalcocite, covellite
33	192374 197726	Altered coarse-grained biotite-apatite ultrabasic.
34	192378 197723 197734 197742	Silicified biotite (now chlorite)-?pyroxene-apatite-opaques rock. Chalcopyrite with rims of covellite enclosed in goethite. Minor magnetite replaced by hematite.
35	145832 50	Carbonatite
36	7/52150	Mica peridotite
37	192373 197725 197736 197738	Quartz-tourmaline rock; altered ultrabasic rock

38	197728 192372	Biotite-pyroxene-apatite-potash felspar rock, intensely silicified
39	W351 W352 W353	Quartz-felspar pegmatite, with zircon and allanite
40	192354	Metasomatized and altered pyroxene granulite
41	43	Biotite pyroxenite. Magnetite with traces of sulphide inclusions. Minor ilmenite, magnetite, ?exsolution in silicates. Sulphides occurring as individual composites of pyrrhotite. Chalcopyrite and pentlandite
42	192359	Granulite
43	145965	Syenite-gneiss
44	49	Metagranite
45	145964	Syenite-gneiss
46	44	Biotite shonkinite with syenite affinities. Magnetite partly martized. Important ilmenite with exsolution magnetite. Traces of goethite. Trace sulphide inclusions in silicates. Ilmenite with minor hematite.
47	192044 192045 192379	"Gossan" over shonkinite
48	192228 34	Syenite-shonkinite contact
49	192352	Biotite pyroxenite with alkaline affinities
50	192353	Altered granulite
51	192351	Biotite pyroxenite with alkaline affinities
52	W380	Scapolite-actinolite rock
53	W379 555075	Brannerite in phlogopite-plagioclase
54	145966	Altered diorite
55	46	Monzonite. Ilmenite with hematite exsolution; magnetite partly martized. Traces of pyrite with goethite alteration. Traces of chalcopyrite, pyrrhotite and covellite.

APPENDIX 2

Thin Section Descriptions of Drill-Core Samples

SAMPLE: MCDDH1 - 23.2

Hand Specimen:

A dark grey, weakly foliated porphyritic rock consisting of ubiquitous orthoclase phenocrysts (up to 2 cms long, often in clusters) in a fine grained groundmass.

Thin Section:

A visual estimate of the minerals is as follows:

Potash felspar:	phenocrysts	25%	
:	matrix	8 - 10%	
Diopside		30%	
Biotite		20%	
Opaques		10%	(8 iron oxides, 2 sulphide)

Accessory: mica (2%), carbonate (2%), apatite (2.5%)

This is a hypidiomorphic-granular rock containing some tabular or elongate potash felspar phenocrysts up to 1 cm long, and many of these are intergrown to form aggregates. These phenocrysts are veined with calcite and mica and are being replaced by mica at the crystal boundaries. Some phenocrysts have inclusions of opaque dust, parallel to cleavage, and inclusions of (?) phlogopite and randomly orientated apatite. Apatite is most common in smaller phenocrysts. Euhedral apatite is also present in the groundmass.

The groundmass is fine-grained (< 0.5mm) and contains colourless to very pale green diopside with included opaques, biotite and probable potash felspar. Included opaque dust parallel to cleavage in one crystal suggests zoning. Most augite crystals are veined by calcite and antigorite.

Biotite is strongly pleochroic, commonly with inclusions of opaques. Some very fine (?) felspar may be included, and some biotite crystals may contain earlier, possibly less pleochroic, (?) phlogopite. The opaques are mainly magnetite and pyrite with minor hematite; rare chalcopyrite has been recognised in hand specimen, and chemical analyses suggest ilmenite.

Carbonate is present mainly in veins through the groundmass but it also occurs as fine, discrete crystals and aggregates of crystals, in the groundmass. In hand specimen, carbonate in some larger veins has been identified as calcite.

No plagioclase or quartz has been recognised.

Conclusions:

Megacrysts of orthoclase crystalized early, however some opaque minerals, (?) phlogopite and apatite were present during crystallisation.

Some intercumulus biotite seems to have crystallised around early (?) phlogopite.

After crystallisation, the rock was veined by calcite and antigorite. Antigorite probably formed by hydrothermal alteration of pyroxene.

The rock is a porphyritic shonkinite (≡ melanocratic syenite)

SAMPLE: MCDDH1 - 28.4

Hand Specimen:

A dark grey, homogeneous fine grained mafic rock containing about equal proportions of biotite, pyroxene and felsic minerals.

Thin Section:

A visual estimate of the minerals is as follows:

Potash felspar	25-30%	
Clinopyroxene	30%	
Biotite	30-35%	
Opaques	5%	(4 iron oxides, 1 sulphide)

Accessory: apatite (1-2%), carbonate (1-2%)

This is a hypidiomorphic-granular rock with biotite as the main component. Biotite is strongly pleochroic (pale yellow to dark brown) with minor inclusions of cloudy pyroxene, fine grained opaques and fine needles of apatite. Clinopyroxene (? diopside) is colourless but often cloudy and commonly encloses opaques, some forming Widmanstatten figures. Potash felspar has inclusions of opaques, pyroxene and apatite. Some crystals may be zoned, and most show replacement by mica. The opaque minerals are finely disseminated but a considerable amount is enclosed by other minerals, especially pyroxene where the opaque minerals often form a core.

No plagioclase or quartz was identified.

Conclusion:

The rock is a fine-grained mafic dyke intruding porphyritic shonkinite (sample MCDDH1 - 23.2). The similarity of composition to the host rock, the lack of felspar phenocrysts and a slightly lower potash felspar content suggests that the fine-grained rock represents intercumulus liquid perhaps squeezed out during solidification, to intrude at a higher level.

The rock is a fine-grained mafic shonkinite.

SAMPLE: MCDDH1 - 52.0

Hand Specimen:

A grey porphyritic rock consisting of coarse (up to 2 cm) orthoclase phenocrysts in a dark coloured, fine grained groundmass. Some phenocrysts form veinlike aggregates. The rock is partly epidotized.

Thin Section:

A visual estimate of the minerals is as follows:

Potash felspar	45-50%
Plagioclase felspar	1-2%
Clinopyroxene	25%
Orthopyroxene (hypersthene)	5-7%
Biotite	5%
Opaques	7% (5% iron oxide, 2% sulphide)

Accessory: apatite (5), mica (2), epidote (1-2), chlorite (1-2) %.

This is a hypidiomorphic granular rock containing elongate orthoclase phenocrysts up to 2 cms long, many of which are intergrown to form aggregates. The phenocrysts are invariably being replaced by mica and often enclose opaque minerals. The margins of some phenocrysts are perthitic and are being replaced by epidote, mica and calcite.

The phenocrysts are not zoned.

Plagioclase occurs in the groundmass and is being replaced by epidote and calcite.

All clinopyroxene crystals are anhedral or rounded and most contain opaque dust along cleavage planes. Some enclose apatite. Many crystals are being replaced by chlorite. Pleochroic orthopyroxene is strongly altered to antigorite, chlorite and (?) talc, and only corroded remnants are present.

The rock is veined by carbonate often associated with sericite and vein-like epidote and chlorite.

Magnetite and lesser hematite are often intergrown and associated with pyrite to form blebs.

No quartz has been recognised.

Conclusion:

The rock is similar to sample MCDDH1 - 23.2 but it contains more orthoclase and less biotite.

The rock is a melanocratic syenite.

SAMPLE: MCDDH1 - 83.0

Hand Specimen:

A dark grey, medium grained, weakly foliated rock cut by an altered pyroxene-felspar vein and by an asbestiform serpentine vein.

Thin Section:

A visual estimate of the minerals is as follows:

Host rock		
Potash felspar	10%	
Clinopyroxene	45%	
Biotite	25-30%	
Opaques	10%	(9% iron oxides, 1% sulphide)
Accessory: apatite	(2-3%	(Note: apatite in hand specimen 10%)

Vein

Asbestiform actinolite and calcite

The rock is medium-grained, hypidiomorphic-equigranular containing medium to fine orthoclase crystals, some with undulose extinction. Cloudy, anhedral clinopyroxene encloses biotite, opaques and apatite.

Two varieties of biotite may be present: an(?) earlier pleochroic form, strained and bent; and a brown, unstrained variety poikilitically enclosing opaque minerals and apatite crystals and possibly enclosing the pale coloured, pleochroic type.

Iron oxides occur more frequently near vein walls and occur as dust in pyroxene crystals.

Pale green to green tremolite has grown normally to the vein walls, and encloses fragments of biotite, felspar and altered pyroxene.

No plagioclase or quartz was recognised.

Hyalophane (Ba-orthoclase) is present and recognised by low relief and undulose extinction.

Conclusion:

The rock is more mafic than the preceeding samples but has approximately the same composition and texture as the groundmass in sample MCDDH1 - 23.2. Early biotite, opaques, and apatite were the first to crystallize. They were followed by later biotite, felspar and then by pyroxene. The rock was slightly stressed and veined by calcite and actinolite.

The rock is a mafic shonkinite.

SAMPLE: MCDDH2 - 12.2

Hand Specimen:

A dark green, fine to medium grained serpentinized ultramafic rock with megacrysts of phlogopite 2 cms across.

Thin Section:

A visual estimate of the minerals is as follows:

Olivine	65%	
Orthopyroxene (hypersthene)	5%	
Phlogopite	10%	
Serpentine	10%	
Opaques	10%	(10% iron oxides, ≮1% sulphide)

(The opaques are principally magnetite)

This is a medium-grained, holocrystalline xenomorphic-granular rock consisting of interlocking colourless to pale green cumulate olivine crystals, megacrysts of phlogopite poikilitically enclosing small rounded colourless crystals of olivine, and minor hypersthene.

The interlocking cumulate olivine is invariably fractured and veined with serpentine, however enclosed rounded crystals are not fractured or veined.

Phlogopite has a distinct pink to very pale yellow pleochroism and encloses olivine and opaque minerals. Many crystals of phlogopite are bent.

Orthopyroxene is distinctly pleochroic, it is fractured and veined with serpentine.

The opaque minerals are finely disseminated but also occur in vein-like aggregates. Some are associated with serpentine.

Conclusion:

The lack of zoning and reaction corona in olivine indicate the cumulate crystals are fairly late stage, probably co-precipitating with phlogopite and orthopyroxene. Crystal settling fractured olivine and orthopyroxene, and bent the megacrysts of phlogopite. Intercumulus liquid was squeezed out and probably penetrated and serpentinized the fractured crystals.

The small rounded crystals enclosed by phlogopite may represent earlier formed olivine, and perhaps are relic grains rounded by later crystal movement.

The rock is essentially a serpentinized phlogopite-magnetite dunite. There is insufficient orthopyroxene to be classified as a harzburgite.

SAMPLE: MCDDH2 - 42.5

Hand Specimen:

A dark brown medium grained ultramafic rock with bands and veins of grey green serpentine. Ammonium molybdate - nitric acid indicate high P_2O_5.

Thin Section:

A visual estimate of the minerals is as follows:

Clinopyroxene	50-55%	
Phlogopite	25%	
Opaques	2-3%	(2 iron oxides, 1 sulphide)
Serpentine	1-2%	
Apatite	5-8%	
Carbonate	5%	
Felspar, olivine	2-3%	Not positively identified

This is a medium grained, hypidiomorphic-granular rock in which clusters or megacrysts of phlogopite enclose small rounded crystals of pyroxene and (?) olivine. Interlocking, anhedral clinopyroxene crystals are pale green, commonly twinned but not zoned. Some poikilitically enclose phlogopite and small, rounded crystals of (?) olivine and (?) pyroxene. Most clinopyroxene crystals are fractured and veined with serpentine. Larger columnar apatite crystals are also fractured and contain microscopic opaques parallel to the long axis. Only smaller prismatic crystals are enclosed by phlogopite.

Carbonate occurs in veins within fractured pyroxene and, with opaques, may be replacing some pyroxene. Discrete crystals of carbonate of igneous origin were not recognised.

Conclusion:

Cumulate crystals of pyroxene co-precipitated with apatite and phlogopite. Grains of olivine, pyroxene and apatite, produced at an earlier stage of crystallization were enclosed by cumulate pyroxene and phlogopite. The grains were fractured after precipitation probably by crystal settling. Intercumulus liquid may have penetrated and partly serpentinized the fractured pyroxene.

The rock is a biotite clinopyroxenite.

Exsolution intergrowths of chalcopyrite and pyrrhotite were recognised under binocular microscope. Some apatite grains are fractured, some veined with pyrite.

SAMPLE: MCDDH2 - 53.1

Hand Specimen:

A dark grey medium grained holocrystalline rock, with medium to coarse grained orthopyroxene. Minor serpentine veins. Rare, very fine grained sulphide. Weakly magnetic.

Thin Section:

A visual estimate of the minerals is as follows:

Olivine	2%	
Orthopyroxene (hypersthene)	75%	
Clinopyroxene	10-15%	
Phlogopite	2%	(this section; 5 in hand specimen)
Opaques	8-10%	(probably less in hand specimen)
Minor accessory apatite, carbonate		

This rock is hypidiomorphic - granular consisting largely of interlocking orthopyroxene crystals. Orthopyroxene is medium to coarse grained, strongly pleochroic and commonly fractured. Most orthopyroxene contains opaque dust and many enclose phlogopite and small remnants of strongly birefringent (?) olivine. No crystal is zoned but some smaller, rounded crystals of orthopyroxene appear to be embayed against poikilitic orthopyroxene.

Clinopyroxene is often twinned and contains opaque minerals, occasionally in Widmanstätten structure. No crystals are zoned.

Olivine occurs as small inclusions in orthopyroxene and is only a minor constituent.

Larger opaque crystals are rounded and disseminated; very fine crystals tend to be euhedral. Veinlike aggregates occur in orthopyroxene and in fractured phlogopite. Opaque minerals and serpentine, often associated with carbonate, may be replacing the margins of interlocking orthopyroxene. Some opaques outline pyroxene grains.

Conclusion:

The rock is an orthopyroxenite with an igneous history similar to the previous sample. It has formed by an accumulation of hypersthene and clinopyroxene crystals.

SAMPLE: MCDDH3 - 13.4

Hand Specimen:

A porphyritic rock with large (3 cms) pinkish grey phenocrysts of orthoclase in a greenish brown medium grained mafic groundmass. Under binocular microscope barite was identified and zoning was recognised in some phenocrysts. A shiller effect was also seen in some phenocrysts.

Thin Section:

A visual estimate of the minerals is as follows:

Potash felspar:	phenocrysts	60%	
:	groundmass	5%	
Pyroxene (diopside)		10%	
Biotite		5%	
Opaques		5%	(3 iron oxides, 2 sulphide)
Sericite		5-10%	

Accessory: apatite (3%), carbonate (1-2%), quartz (1-2%), chlorite (1-2%)

This is a hypidiomorphic - granular rock containing euhedral, elongate phenocrysts of orthoclase-microcline in a matrix of orthoclase, diopside, brown biotite and accessory opaques and apatite. The phenocrysts of orthoclase are often twinned and are being replaced by sericite. Microcline is probably perthitic and is also being replaced by sericite. It shows reaction (? replacement) with orthoclase. Some orthoclase enclose small, rounded clinopyroxene grains and apatite crystals.

Small anhedra of pyroxene enclose opaque minerals, apatite and, possibly, biotite. Most pyroxene grains are cloudy.

Biotite is brown, strongly pleochroic, and shows alteration to chlorite. Biotite has inclusions of apatite but no opaque minerals (c.f. early phlogopite). Opaques often occur between adjacent boundaries of potash felspar and between apatite crystals; they also occur in veins cutting felspar and apatite.

Apatite occurs as very fine euhedra in felspar, biotite and pyroxene grains and occurs between the boundaries of adjacent grains.

Some quartz may be a reaction product of (?) replaced microcline; quartz is associated with sericite at corroded margins of microcline.

Conclusion:

The rock is a pyroxene-bearing syenite.

In other thin sections of syenite, minor albite is present in the groundmass and a core of andesine has been recognised in one cloudy orthoclase phenocryst.

APPENDIX 3

Diamond Drill Logs

APPENDIX 3 DIAMOND DRILL LOGS

Diamond Drill Log MCDDHI
Coordinates 20210N 27327E
Inclination -46° Bearing 309° magnetic
Total depth 96.6 metres Started 22/3/1975 Completed 9/4/1975

FROM	TO	INT.	REC.	DESCRIPTION
0	2.2	2.2	0.2	Highly weathered rock: pink calcrete and fragments of porphyritic shonkinite.
2.2	5.1	2.9	0.5	Moderately weathered porphyritic shonkinite: brown-grey magnetic, foliated; orthoclase phenocrysts in a fine chloritic biotite-pyroxene matrix Intersection angle of foliation to core axis is 50° at 5 metres depth.
5.1	7.3	2.2	1.5	Slightly weathered porphyritic shondinite: grey to dark grey, iron-stained, magnetic, foliated; Intersection angle 50° at 7m.
7.3	13.3	6.0	6	Fresh porphyritic shonkinite: dark grey, magnetic, foliated. Minor epidote and chlorite in narrow fractures, some epidotisation of orthoclase phenocrysts. Intersection angle of foliation 50° at 10 m.
13.3	13.4	0.1	0.1	Micro-shonkinite: dark grey, very fine grained, magnetic with dull grey-green pyroxene-felspar veins 1 mm wide.
13.4	28.4	15.0	14.9	Porphyritic shonkinite: dark grey green, magnetic, foliated; orthoclase phenocrysts average 1 cm long (maximum 4 cm) in a fine felspar-magnetite-biotite-clinopyroxene matrix. Minor epidotisation of orthoclase. At 18.0 m a 2 cm shear At 19.7 m a 1 cm vein of epidote cutting core axis at 10° Intersection angle of foliation 50° at 16 m, 55° at 24 m.
28.4	31.0	2.6	2.5	Dyke: fine-grained shonkinite: dark grey-green, weakly magnetic, fine, equigranular rock with no visible foliation. Some calcite filled micro fractures. At 29.3 - 29.5 m, inclusion of porphyritic shonkinite veined with carbonate. Margins of inclusion are brecciated, slickensided; actinolite developed. At 29.8 m, a 2 cm felspar vein parallel to dyke wall chlorite developed at the dyke-vein contact. At 30.5 m, a 2 cm felspar vein cutting dyke. This vein is off-set by a 1 mm carbonate - actinolite - quartz - epidote fracture. Intersection angle of dyke 30° at 30 m.

31.0	36.8	5.8	5.8	Porphyritic shonkinite: dark grey-green, magnetic, foliated felspar phenocrysts in aggregates up to 5 cms long. Narrow (1 - 2 mm) amphibole-carbonate-epidote veins. At 32.5 m, a calcite-quartz vein carrying minor sulphide, altering shonkinite margins to produce fibrous actinolite.
36.8	37.3	0.5	0.5	Fine-grained shonkinite: fine, equigranular, magnetic. Gradational contacts through medium grained shonkinite 10 cms wide. At 37.0 m, a 2 cm felspar-carbonate-quartz vein with irregular, subparallel micro-veins.
37.3	48.0	11.3	11.2	Porphyritic shonkinite: At 43.85 - 44.15 m and at 47.6 - 48.0 is a slight decrease in the number of felspar phenocrysts. At 39.2 m carbonate-quartz veins off-set by calcite-filled micro-fractures. Earlier carbonate is probably dolomitic (HCl test). At 46.0 m, a 1 cm actinolite-epidote vein. Intersection angle of foliation 60° at 48 m.
48.0	74.0	26.0	25.9	Melanocratic syenite: grey, magnetic rock consisting of 50% coarse orthoclase phenocrysts in a fine felspar-biotite-clinopyroxene matrix with minor magnetite calcite and apatite, rare chalcopyrite and pyrite. At 52.2 m a narrow dyke of fine grained shonkinite gradational upper contact; at lower contact is a 2 cm wide vein of actinolite-carbonate-sulphide. At 60.0 m a 2 cm orthoclase-quartz vein with minor epidote and biotite. Intersection angle of foliation 60° at 51 m, 65° at 62 metres.
74.0	80.6	6.6	6.5	Porphyritic shonkinite: At 74.0 to 74.3 m (contact) is a slight decrease in the number of felspar phenocrysts. At 75.1 - 77.8 m is a felspar-quartz vein with minor calcite and apatite cutting foliation at 10 - 15°. Intersection angle of foliation 65° at 78 m.
80.6	96.6	16.0	16.0	Mafic shonkinite: dark grey, medium-grained hydromorphic-granular, magnetic, weakly foliated. At 83.5 to 83.6 m, a vein of pyroxene-felspar cutting core axis at 40 - 47°. At 83.65 m, a 3mm pyrite vein in epidote-carbonate filled fractures. At 83.8 to 83.94 m, a fine-grained (? mafic) shonkinite dyke. At 83.94 m is some serpentinization of dyke and country rock. At 86.0 to 87.95 is a zone of alteration or intrusion by pyroxenite. The enclosing country rock is gradational serpentinized and rock in the zone is medium to coarse grained and hydrothermally altered. The zone or intrusion contains a small fragment of mafic shonkinite. Carbonate veins with minor barite present in the zone. Minor sulphide in small clusters and veinlets. Carbonate veining, bleaching and hydrothermal alteration has a sharp lower contact with the country rock (70° to core axis).

Minor carbonate-filled microfractures to end of section.

SUMMARY

0 - 28.4	Porphyritic shonkinite 25-30% kspar; 30% cpx; 20% bio; 10% Fe.ox; 2% sulphide
28.4 - 31.0	Fine-grained shonkinite 30% kspar; 30% cpx; 30% bio; 3% Fe.ox; 1% sulphide
31.0 - 36.8	Porphyritic shonkinite
36.8 - 37.3	Fine-grained shonkinite 30% kspar; 25-30% cpx; 30% bio; 5% Fe.ox; 2% sulphide
37.3 - 48.0	Porphyritic shonkinite 25-30% kspar; 25-30% cpx; 30% bio; 10% Fe.ox; 2% sulphide
48.0 - 74.0	Melanocratic syenite 50% kspar; 30% cpx; 5-8% bio; 5% Fe.ox; 2% sulphide
74.0 - 80.6	Porphyritic shonkinite 25-30% kspar; 30% cpx; 25% bio; 10-15% Fe.ox; 1% sulphide
80.6 - 96.6	Mafic shonkinite 10-15% kspar; 45-50% cpx; 25% bio; 5-10% Fe.ox; 2% sulphide

Diamond Drill Log MCDDH2
Coordinates 20375N 27028E
Inclination -60° Bearing 129° magnetic
Total depth 91.0 metres Started 10/4/1975 Completed 5/5/1975

FROM	TO	INT.	REC.	DESCRIPTION
0	7.3	7.3	0.3	Highly weathered rock: rock fragments, clay micaceous soil. Pyroxene, biotite, limonite, possible olivine and orthopyroxene identified in fragments.
7.3	16.0	8.7	4.7	Moderately weathered mica dunite: dark grey bands of serpentinized olivine, poikilitic megacrysts of phlogopite, clinopyroxene and possible serpentinized orthopyroxene with olive-grey bands of mica dunite. Becoming less weathered with depth.
16.0	23.0	7.0	6.8	Fresh, strongly serpentinized mica dunite: dark green, weakly magnetic; serpentinite and serpentinized olivine.
23.0	39.9	16.9	16.0	Fresh, serpentinized mica wehrlite: dark grey-green, weakly magnetic bands of wehrlite (serpentinized olivine, clinopyroxene, phlogopite, iron oxides) with subsidiary grey-green bands of serpentinite. At 38.8 - 39.05 m, a weathered vughy vein or breccia cutting core axis at 45-50°. From 39 to 39.8 metres a slight (but definite) increase in the amount of phlogopite from 10% to 15%. Intersection angle of banding to core axis is 65-70° at 22 metres depth and 75° at 25 m.
39.9	41.6	1.7	1.7	Serpentinized mica (?) lherzolite: dark grey, medium grained granular rock with megacrysts of phlogopite. Amount of olivine decreasing and amount of clinopyroxene and biotite increasing with depth in this section. At 39.9 m is a 5-8 mm band of dark rock containing a dense, fine mesh of iron oxide and bleached phlogopite (? hydro-biotite with vermiculite). At 39.9 to 40.7 m are hydrothermally altered and carbonate veined rocks. Intersection angle of band of altered rock 50° at 40 m.
41.6	42.5	0.9	0.9	Serpentinized websterite: grey-green, medium grained rock containing serpentinized orthopyroxene (? bastite), clinopyroxene and biotite. Amount of biotite increases with depth from about 15% to 30%.
42.5	43.2	0.7	0.7	Biotite clinopyroxenite: dark brownish green rock consisting of 60% pyroxene and 30% biotite with accessory apatite, iron oxides and carbonate. Narrow (1 mm max.) veins or fractures filled with carbonate.

43.2	44.4	1.2	1.2	Serpentinized biotite clinopyroxenite: dark grey green, medium grained granular; carbonate veined rock containing 75% pyroxene 15% biotite. From 44.3 to 44.4 65% pyroxene 25% biotite.
44.4	48.6	4.2	4.2	Olivine biotite websterite: dark grey-green fine to medium grained rock containing about 10% olivine and 15% biotite. From 44.4 to 46.0 m, strong carbonate veining, a possible breccia. From 48.5 - 48.6 rock is medium grained.
48.6	52.0	3.4	3.4	Mica lherzolite: dark grey medium grained, weakly serpentinized rock. From 48.9 to 49.1 carbonate veining and serpentinization.
52.0	52.5	0.5	0.5	Serpentinized biotite clinopyroxenite: medium grey-green, partially serpentinized.
52.5	55.7	3.7	3.7	(Biotite) Orthopyroxenite: grey green rock with dark grey bands, fractured, containing at least 75% hypersthene and 10% biotite.
55.7	58.9	3.2	3.2	Serpentinized websterite: dark grey, medium grained rock, containing serpentinized orthopyroxene and about 25% clinopyroxene. Biotite less than 5%. Fractured, sheared and veined with carbonate throughout. At 58.9 a well-defined fault contact cutting core axis at 15-20°.
58.9	68.5	9.6	9.6	Shonkinite - biotite clinopyroxenite: dark grey, gradational, alternating bands of weakly foliated porphyritic shonkinite and clinopyroxenite. Gradational over about 2 cms through mafic shonkinite. Shonkinite 58.9 to 61.4 (2.5 m) Pyroxenite 61.4 to 63.8 (2.4 m) Shonkinite 63.8 to 64.8 (1.0 m) Pyroxenite 64.8 to 68.5 (3.7 m) Intersection angle 45° at 60.4 m, 61.0 m, 68.0 m.
68.5	74.6	5.9	5.9	Porphyritic shonkinite: dark grey green, magnetic, weakly foliated; coarse orthoclase phenocrysts in a fine grained pyroxene-biotite matrix. At 70.4 - 70.6, fine grained shonkinite with pyroxene-felspar veins. Rapidly gradational contacts. At 73.4 - 73.5, orthoclase-biotite vein cutting core axis at 65° country rock walls altered over 2 mms. Intersection angle 40° at 74.0 m.
74.6	91.0	16.4	16.3	Mafic shonkinite: dark grey green, medium grained hypidiomorphic - granular; magnetic, weakly foliated. Rare calcite veins. At 75.1 - 75.2 m, felspar-quartz-chlorite-biotite vein cutting core axis at 75°. Perthitic intergrowths in orthoclase, and polysynthetic twinning in green microcline. Intersection angle 40° at 74.7 m, 10° at 87 m, 35-40° at 90 m.

SUMMARY

0 - 16.0		Mica dunite
	(7.3 m)	80% serpentinized olivine, 10% phlogopite, 5% Fe.ox, 5% access.
	(11.7 m)	65-70% olivine, 10% serpentine, 15% pyroxene, 5% access
	(12.2 m)	75% serpentinized olivine, 10% phlogopite, 10% Fe.ox, 5% hypersthene.
	(15.55m)	85-90% olivine, 10% phlogopite, 1-2% pyroxene.
16.0 - 39.9		Mica wehrlite
	(19.3 m)	50% serpentine, 15% olivine, 20% cpx, 5% Fe.ox, 5% phlogopite.
	(19.6 m)	70-75% serpentine, olivine, 10-15% Fe.ox, 10% phlogopite.
	(37.1 m)	50% serpentine, 2% olivine, 25% cpx, 15% phlogopite, 5% Fe.ox, 3% access.
39.9 - 41.6		Mica lherzolite
	(40.3 m)	50-60% serpentine and olivine, 25% serp. opx., 10% phlog., 10% Fe.ox.
41.6 - 42.5		Websterite
	(42.5 m)	20% serpentine, 50% cpx (+opx), 30% biotite, 5% Fe.ox, 5% apatite.
42.5 - 44.4		Biotite clinopyroxenite
	(43.7 m)	75% cpx, 15% biotite, 5% apatite, 2% Fe.ox, 2% felspar
44.4 - 48.6		Olivine biotite websterite
	(47.7 m)	5-10% olivine, 50% pyroxene, 30% biotite, 5% Fe.ox, 5% felsics.
48.6 - 52.0		Mica lherzolite
	(49.5 m)	35% ol.,serp., 35% cpx., 5% opx., 10-15% Fe.ox, 5-10% bio.
52.0 - 52.5		Biotite clinopyroxenite
52.5 - 55.7		Orthopyroxenite
	(53.1 m)	70-75% opx., 5% serpentine, 5% biotite, 10% Fe.ox, 5-10% cpx.
55.7 - 58.9		Websterite
	(58.2 m)	60% opx., 25% cpx., 5% Fe.ox, 2-3% biotite, 5% felsics
58.9 - 68.5		Interbanded shonkinite and biotite pyroxenite
	(59.1 m)	2% (?) olivine, 60% cpx., 15% bio., 10% Fe.ox, 3% sulph., 5-10% felsics.

68.5 - 74.6 Porphyritic shonkinite

(72.6m) 30-35% orthoclase; 30% cpx; 30% biotite; 5% Fe.ox

74.6 - 91.0 Mafic shonkinite

(91.0m) 15% kspar; 40% cpx; 35% biotite; 5% Fe.ox; access sulph. apatite.

Diamond Drill Log MCDDH3
Coordinates 27481N 26784E
Inclination -60° Bearing 090° magnetic
Total 69.5 metres Started 6/5/1975 Completed 16/5/1975

FROM	TO	INT.	REC.	DESCRIPTION
0	6.2	6.2	1.5	Highly weathered to moderately weathered syenite
6.2	29.0	22.8	22.6	Syenite: greyish pink, hypidiomorphic granular; coarse grained orthoclase phenocrysts in a fine grained matrix of felspar, clinopyroxene, biotite magnetite and accessories. Orthoclase phenocrysts are mainly white to pale orange; some bands with orange-orthoclase phenocrysts. At 18.2 - 18.3m, medium grained syenite At 21.85 - 22.25m, (0.4m) band of orange-orthoclase syenite At 25.85 - 25.9m, (0.05m) orange-orthoclase syenite. At 26.5 - 27.2m, (0.7m) orange-orthoclase syenite At 28.05 - 29m, (0.95m) orange-orthoclase syenite finer grained matrix, some hydrothermal alteration evident.
29.0	29.65	0.65	0.6	Fault zone: dark grey brecciated rock, healed with chalcedony, quartz, calcite. At 29.55 - 29.6 m, soft, black fault-pug At 29.65 the brecciated orthoclase fragments aligned parallel to fault zone. Intersection angle 55° at 29 m, 60° at 29.5 m and 63° at 29.6 m.
29.65	30.25	0.6	0.6	Orange-orthoclase syenite
30.25	30.5	0.25	0.25	Calcite dyke: pale pink coarse grained calcite with minor quartz, biotite and sulphide. Calcite crystals aligned parallel to vein walls, 60° to core axis. Intersection angle 50° at 30.25 m, 70° at 30.5 m.
30.5	35.8	5.3	5.3	Banded syenite: bands of orange to brick-red-orthoclase syenite in grey-orthoclase syenite. At 30.5 - 30.9 (0.4m) orange-orthoclase syenite At 31.95- 32.17(0.22m) " At 32.7 - 33.0 (0.3m) " At 34.4 -34.8 (0.4m) " At 35.5 - 35.8 (o.3m) " At 31.2m, a 3mm carbonate vein (70° to core axis) At 32.3m, a 2mm carbonate vein (53° to core axis) At 33m, a 2mm carbonate vein At 34.0m, a shear filled with calcite and amphibole At 34.45m, carbonate filled fracture At 35.7m, carbonate vein (75° to core axis)
35.8	69.5	33.7	33.6	Syenite: At 37.4m, a 3cm band of fine-grained shonkinite cutting core axis at 65°.

At 42.6 - 42.8m, medium-grained syenite
At 43.8 - 44.0m, medium-grained syenite
At 50.5m, a 2cm quartz vein (10-15° to core axis)
At 53.2 - 53.5m, medium-grained felspar-quartz dyke with epidote in fractures (45° to core axis)
At 60.0 - 60.2m, medium grained syenite with altered margins against country rock syenite, cutting core axis at 45°.

SUMMARY

0 - 21.85		Syenite
21.85 - 29.0		Banded syenite (7.15 metres)
29.0 - 29.65		Fault
29.65 - 35.8		Banded syenite, calcite dyke (6.15 metres)
35.8 - 69.5		Syenite

Syenite

65% kspar; 10% cpx; 5% bio; 5% opaques; 5-10% sericite; 5-10% accessories.

Diamond Drill Log MCDDH4
Coordinates 24568N 30184E
Inclination -45° Bearing 213° magnetic
Total depth 97.5 metres Started 16/5/1975 Completed 22/5/1975

FROM	TO	INT.	REC.	DESCRIPTION
0	3.7	3.7	LOW	Highly weathered rock: calcrete, soil, rubble
3.7	6.7	3.0	2.0	Moderately weathered biotite pyroxenite:
6.7	42.0	35.3	33.0	Fresh mafic shonkinite: dark grey-green fine to medium hypidiomorphic-granular rock containing clinopyroxene, biotite, felspar and iron oxides. Narrow (1-5 cms) felspar veins cutting at various angles to core axis common to 36 metres. Some vein walls are sheared and altered to epidote, actinolite and chlorite. At 19.45 to 19.9 m is a pale green serpentinized band intruded by 3-4 mm wide felspar vein. At 20.5 m is limonite-goethite with a narrow calcite-filled shear. At 22.55 m is a 2 cm felspar vein off-set by hematite-goethite-calcite shear. At 24.0 m, 1 cm actinolite-epidote-calcite vein. At 26.5 m shear. At 30.7 - 30.89 m, sheared, broken core with hematite and calcite. At 36.2 m, a narrow epidote-actinolite-calcite shear. At 37.6 m, (as 36.2) with a calcite-filled micro-fracture off-setting the shear. At 40.4 - 40.7 m, carbonate veining; minor sulphide. At 41.4 - 41.6 m carbonate veining off-set by calcite-filled microfractures. At 41.75 m, a 3 mm vughy carbonate vein. Intersection angle of banding, foliation 30° at 17.5 m, 65° at 35 m.
42.0	42.5	0.5	0.5	Quartz dyke: brecciated quartz healed with chalcedony. Microveins of sulphide. Inclusions of amphibole, felspar. Microfractures filled with calcite.
42.5	43.0	0.5	0.5	Shear: chloritic, brecciated; shearing 60° to core axis.
43.0	45.9	2.9	2.9	Biotite websterite: dark grey green rock with biotite segregated into rosette-like clusters. At 44.1 m, 3 cms shear and brecciation at 60° to core axis.
45.9	48.0	2.1	2.0	Fault: At 45.9 - 46.7 m, shearing, weak brecciation, narrow carbonate veins; some orange-orthoclase felspar developed. At 46.7 - 47.8 m, quartz-carbonate filled breccia At 47.8 - 48.0 m, sheared, brecciated felspathic rock with a truncated felspar vein. Carbonate veining, youngest veins (or fractures) 75° to core axis.

48.0	64.1	16.1	16.1	Biotite websterite: dark grey green, fine grained rock with rosettes of biotite. Carbonate veining, fracture filling throughout with associated actinolite, some quartz. Minor narrow (1 cm) felspar veins, some with hydrothermally altered walls.
64.1	72.2	8.1	8.0	Biotite pyroxenite: dark grey green, medium grained equigranular rock; two periods of carbonate veining or fracturing. Minor narrow (1 cm) felspar veins, some with diffuse contacts. At 66.7 - 67.2 m, a narrow (2 cm) felspar vein off-set by a fine-grained pyroxenite dyke. At 67.2 - 67.65 m, small scale shearing and brecciation with calcite-quartz veins. At 72.2 m, a felspar-amphibole vein.
72.2	76.8	4.6	4.6	Interbanded biotite pyroxenite and shonkinite: dark grey green biotite pyroxenite with subsidiary porphyritic shonkinite. Gradational contacts. Vughs (3-5 mms diameter) throughout, partly lined with quartz and remnant calcite. Vughs tend to interconnect. Rock is carbonated. At 73.0 m, a 2 cm vein of serpentinized pyroxene. At 74.5 m, a 2 cm shear, 35° to core axis. Intersection angle of banding, foliation 45° at 72.8 m.
76.8	80.3	3.5	3.5	Biotite pyroxenite: dark grey green rock with interconnecting cavities throughout. Cavities contain qz and remnant calcite. The rock is carbonate-rich. At 77.65 - 77.9 m, a fine grained shonkinite dyke at 30-40° to core axis. At 79.2 - 80.3 m, carbonate veining and hydrothermal alteration.
80.3	84.2	3.9	3.9	Interbanded shonkinite and pyroxenite: the rocks are gradational series shonkinite - biotite clinopyroxenite - biotite websterite - biotite clinopyroxenite - shonkinite. Felspar veins at 80.5 m, 83.35 m (3 cms). At 82.2 m is a 2-3 mm amphibole-carbonate vein with altered country rock walls. Intersection angle of foliation 30° at 81 m.
84.2	89.5	5.3	5.3	Biotite pyroxenite: dark grey green, fine to medium grained, with rosettes of biotite At 84.2 - 84.7 m, biotite clinopyroxenite At 84.7 - 89.1 m, biotite websterite At 89.1 - 89.5 m, biotite clinopyroxenite At 84.2 - 84.35 m, carbonate veins. At 84.52 m, small scale shearing parallel to lineation. At 86.4 - 86.7 m, fine grained shonkinite slickensides on contact with calcite and amphibole. Cutting core axis at 60-70°. Intersection angle of foliation 45° at 84.2 m, 50° at 84.5 m.

89.5	91.7	2.2	2.2	Porphyritic shonkinite: dark grey rock with coarse orthoclase phenocrysts in a fine grained biotite-pyroxene-felspar matrix. Leach cavities throughout. Felspar veins both cutting foliation and parallel, diffuse into shonkinite forming part of the aggregates of phenocrysts.
91.7	97.5	5.8	5.8	Banded biotite pyroxenite and shonkinite: 91.7 - 92.0 m, mafic shonkinite 92.0 - 92.2 m, fine grained shonkinite 92.2 - 92.4 m, mafic shonkinite, altered 92.4 - 93.7 m, porphyritic shonkinite 93.7 - 95.1 m, biotite websterite 95.1 - 95.5 m, biotite pyroxenite, altered 95.5 - 95.8 m, fine grained shonkinite 95.8 - 96.5 m, biotite pyroxenite 96.5 - 96.6 m, biotite websterite 96.6 - 97.5 m, biotite clinopyroxenite Some bands of chlorite-amphibole pyroxene in the series.

SUMMARY

0 - 42.0	Mafic shonkinite
(13.1 m)	50-55% cpx; 25% biotite; 15% felsic minerals; 2% Fe.ox; 2% sulphide.
(17.4 m)	35% cpx; 20% biotite; 30% felspar; 10% apatite; 3% opaques
(36.4 m)	45-50% cpx; 30-35% bio; 10% felspar; 5% apatite, 4% opaques
(41.5 m)	40-50% cpx; 20% bio; 10% felspar; 10% apatite, carb; 8% Fe.ox.
42.0 - 43.0	Shear and breccia
43.0 - 45.9	Biotite websterite
(43.5 m)	65% cpx (& some opx); 20% bio; 10% felsics; 3% Fe.ox.
45.9 - 48.0	Fault
48.0 - 72.2	Biotite pyroxenite
(62.0 m)	65% pyroxene; 25% bio; 3% chlorite; 2% opaques.
(67.9 m)	50-55% cpx; 35% bio; 5% Fe.ox; 10% felsics (2% felspar)
72.2 - 97.5	Interbanded pyroxenite and shonkinite
(77.3 m)	55% cpx; 25% bio; 10% Fe.ox; 10% felsics fine grained rock: 40% cpx; 40% bio; 10% felsics; 5% Fe.ox
(97.5 m)	35% cpx; 30% opx; 15% bio; 5% Fe.ox; 10% felsics.

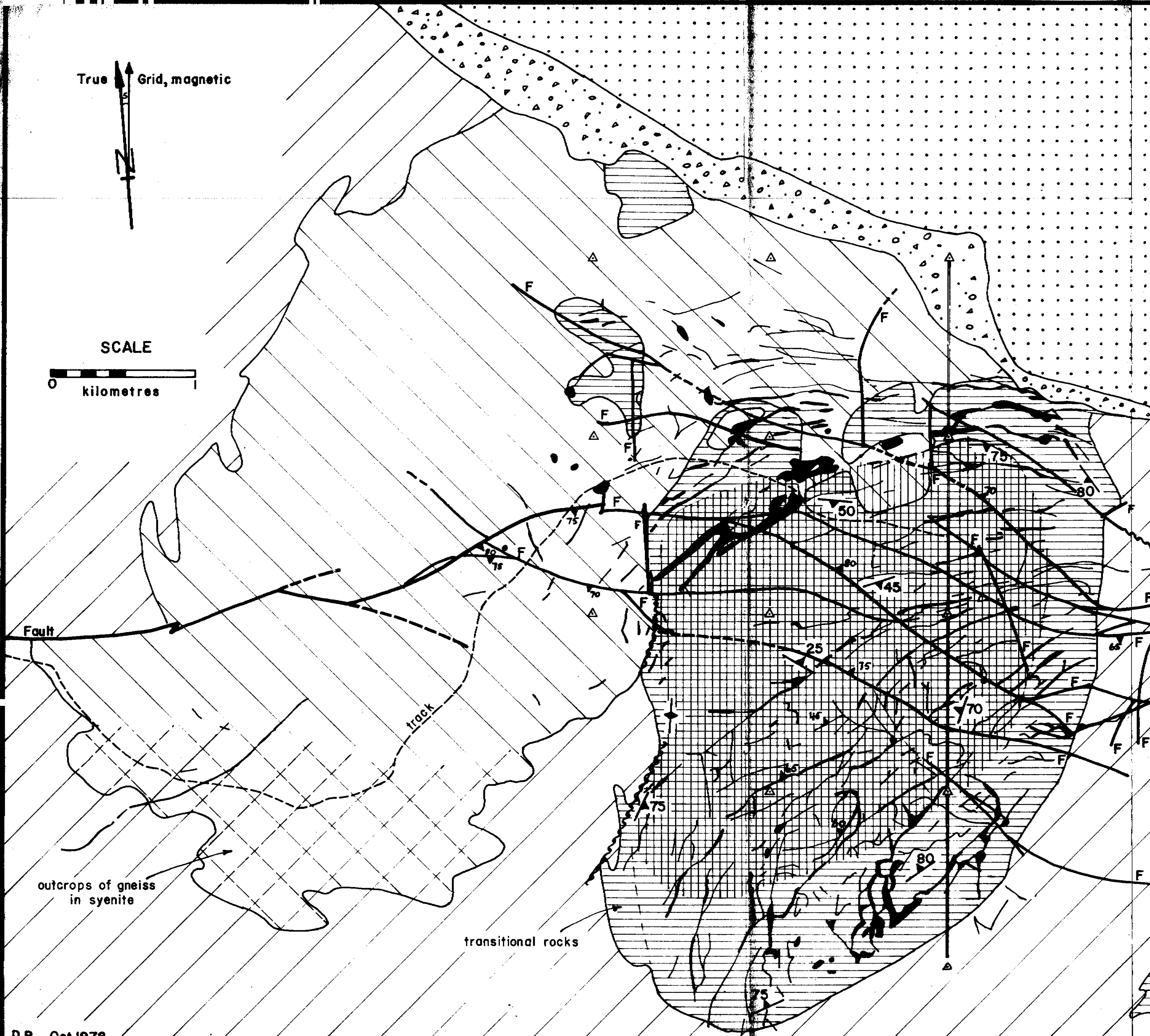

D.B. Oct.1978

THE MORDOR COMPLEX

STATISTICS

Area exposed	28. 8 sq. km.
Felsic rocks	17. 4 sq. km.
Mafic rocks	11. 4 sq. km.
Felsic rocks	
1.) syenite	16.5 sq. km.
2) pegmatite	0.2 sq. km.
3) gneiss (enclosed in syenite)	0.7 sq. km.
Mafic rocks	
1.) peridotite-pyroxenite	0.4 sq. km.
2) shonkinite	10.8 sq. km.
3.) transitional	0.2 sq. km.
Area underlain by ultrabasic rocks (see Kirton & Doe, 1971)	6.5 sq. km.
depth: 6 km volume:	39 cu. km.

SYMBOLS

Cainozoic		Scree
Late Proterozoic		Sediments
Mordor Complex		Felsic rocks
		Mafic rocks
		Area underlain by u.b. rocks.
Proterozoic Arunta Complex		Gneiss, amphibolite

pegmatite
F fault
70 attitude of foliation
base line
surveyed grid point

PLAN 2

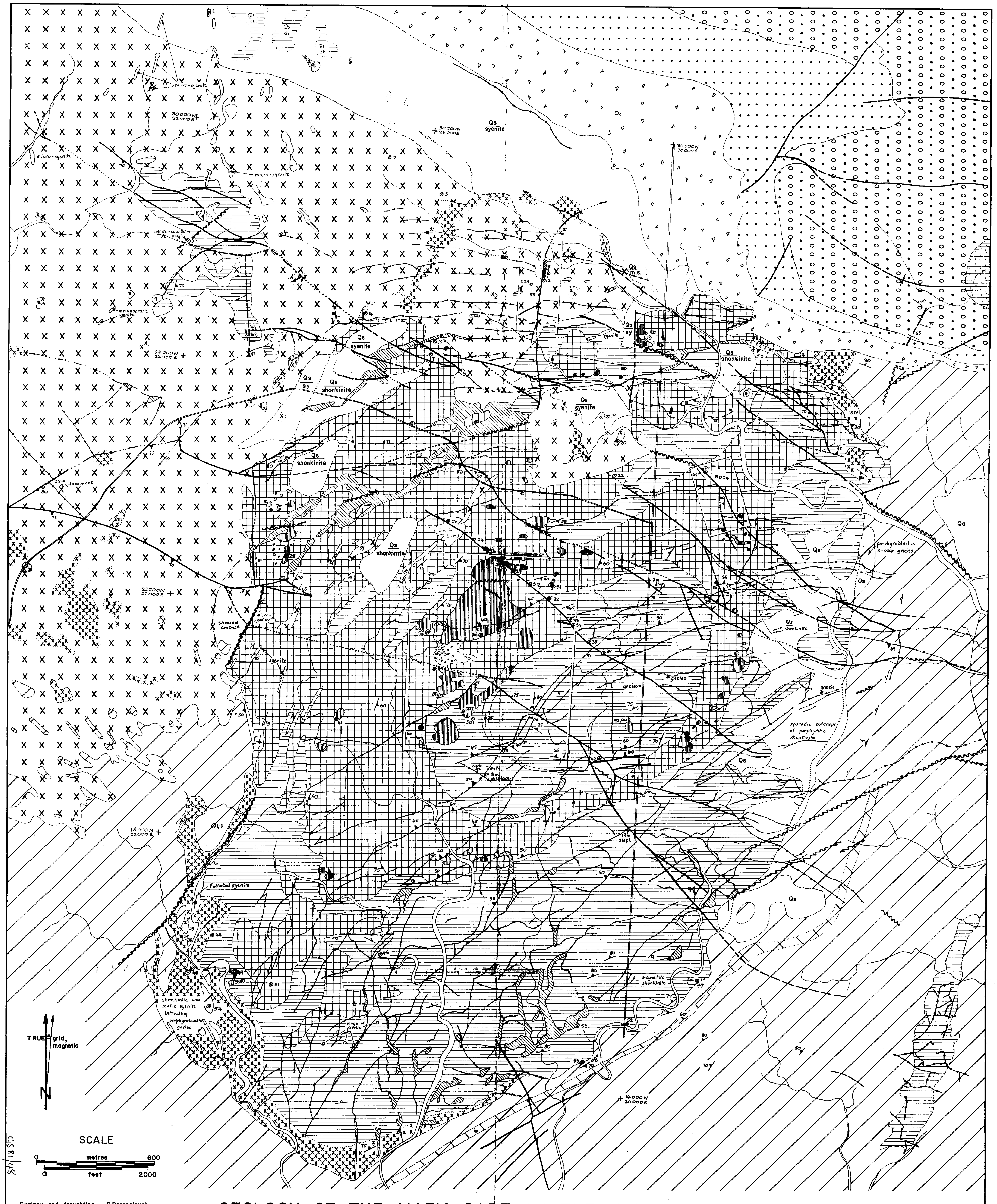

Geology and draughting D.Barraclough
March 1977 Aug. 1981

GEOLOGY OF THE MAFIC PART OF THE MORDOR COMPLEX

For LEGEND see PLAN 5
⊚50 Rock samples, see Appendix 1

PLAN 4

GEOLOGY OF THE CENTRAL PART OF THE MAFIC SECTOR

(over the area of detailed soil-geochemistry)

LEGEND

- Outcrops of : peridotite, pyroxenite
- Area of underlying ultramafic rock, by soil geochemistry
- Mafic shonkinite
- Porphyritic shonkinite
- Melanocratic syenite
- Syenite
- Pegmatite mappable width, dips shown
- Micro-shonkinite dyke
- Fault (carbonate - quartz filled breccia)
- Shear (carbonate - quartz veined)
- 50 Attitude of foliation
- 80 Attitude of magmatic band
- MCDDH Diamond-drill hole

SCALE

0 50 100 metres

Grid and magnetic NORTH

PLAN 5

GS 81/48

DB March 1977 October 1981

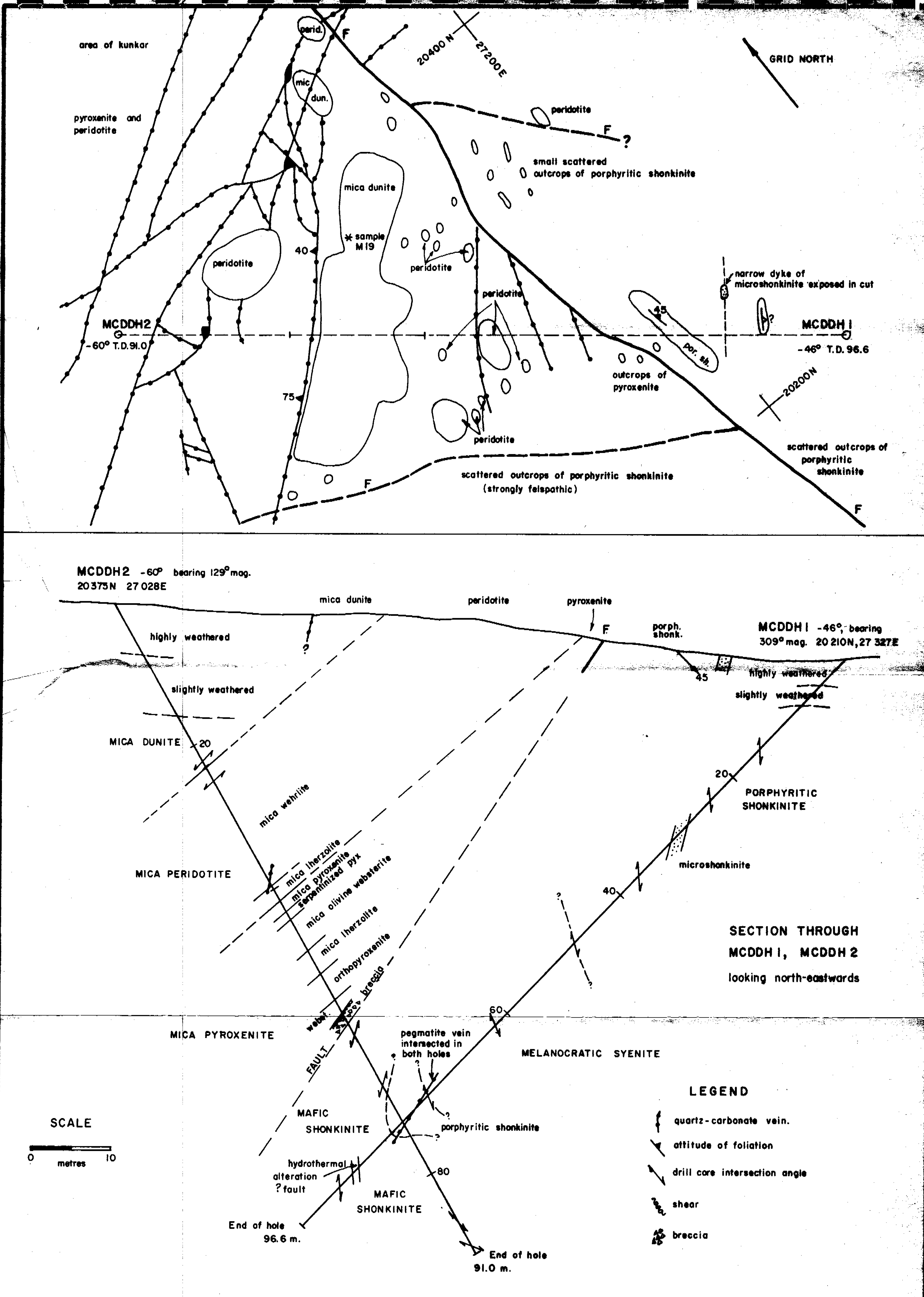

PLAN 6

DB 1975.198

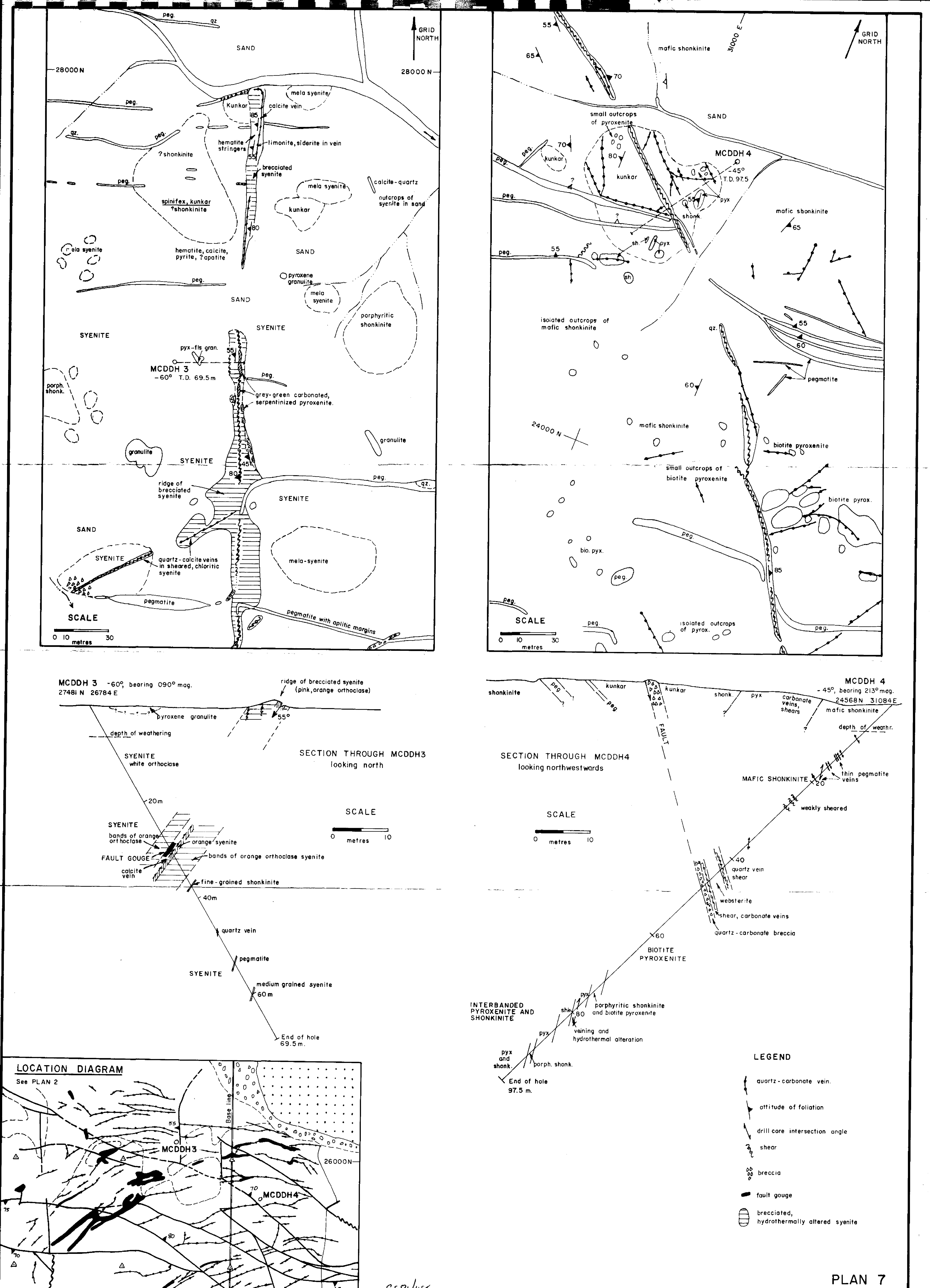

PLAN 7

DB. 1975, 1981.

TABLE 3

Analyses of drill-core samples drill-holes MCDDH 1 to 4, Mordor Complex.

Analyses : East Point Laboratory, Darwin. Certificates of Analysis, (1975)

SAMPLE No.	8101	8100	8098	8099	8096	8113	8116	8095	8117	8102	8094	8097
HOLE No.	2	2	2	2	2	2	2	2	2	2	2	2
DEPTH	20·55-21·55	20·05-20·55	19·05-19·55	19·55-20·05	18·05-18·55	27·1-27·6	28·8-29·3	16·35-18·05	34·0-34·5	21·55-22·1	15·5-16·35	18·55-19·05
ROCK TYPE	serpent. ? dunite	serpent. ? dunite	‡	‡	‡	serp phlogo wehrlite	serp phlogo wehrlite	serp phlogo dunite	serp phlogo wehrlite	‡	mod. weath. dunite	serp dunite
MgO	36·5	36·5	35·7	35·6	35·5	34·7	34·5	34·5	34·4	34·0	34·0	34·0
SiO_2	•	39·0	•	•	34·0	•	31·7	•	•	•	•	•
CaO	2·5	2·7	2·6	2·7	2·4	2·4	2·5	3·1	3·2	2·5	3·0	3·1
Al_2O_3	•	0·8	•	•	0·8	•	0·4	•	•	•	•	•
Fe_2O_3	•	8·8	•	•	8·7	•	8·8	•	•	•	•	•
K_2O	0·3	0·4	0·4	0·4	0·4	0·3	0·3	0·3	0·4	0·3	0·4	0·4
Na_2O	0·2	0·1	0·1	0·1	0·1	0·1	0·1	0·1	0·1	0·2	0·2	0·1
P_2O_5	0·73	0·68	0·73	0·72	0·44	0·71	0·76	0·32	0·91	0·74	0·48	0·68
TiO_2	+	+	+	+	0·2	0·3	0·2	0·2	0·2	+	0·4	+
SrO	+	+	+	+	+	+	+	+	+	+	+	+
BaO	+	+	+	+	+	+	+	+	+	+	+	+
MnO	•	+	•	•	+	•	+	•	•	•	•	•
V_2O_5	+	+	+	+	+	+	+	+	+	+	+	+
Cr_2O_3	0·25	0·26	0·23	0·25	0·23	0·18	0·16	0·21	0·21	0·21	0·23	0·21
L.O.I.	•	•	•	•	9·7	•	9·9	•	•	•	•	•
Ni	750	710	690	700	770	760	780	730	730	770	730	690
Cu	+	+	+	+	+	+	+	20	10	10	20	80
Co	120	130	120	120	120	140	140	130	150	120	140	140
Pb	25	+	40	40	40	35	40	45	30	110	45	170
Zn	60	60	70	50	65	65	75	90	75	55	75	65
Sub.		89·24			82·77		79·42					

SAMPLE No.	8110	8088	8115	8114	8103	8112	8111	8109	8091	8105	8093	8090
HOLE No.	2	2	2	2	2	2	2	2	2	2	2	2
DEPTH	25·6-26·1	7·3-9·3	28·25-28·8	27·6-28·25	22·1-22·6	26·6-27·1	26·1-26·6	25·1-25·6	12·4-13·6	23·1-23·6	14·6-15·5	11·85-12·4
ROCK TYPE	serp phlogo wehrlite	mod weath dunite	serp phlogo wehrlite	‡	‡	‡	‡	‡	mod. weath. dunite	serp wehrlite	mod weath. dunite	‡
MgO	33·9	33·9	33·8	33·8	33·7	33·5	32·8	32·2	31·7	31·5	31·4	31·2
SiO_2	•	37·5	•	•	•	•	•	•	•	•	•	•
CaO	2·9	3·9	2·6	2·9	3·6	2·4	3·0	2·9	3·6	3·5	5·4	3·5
Al_2O_3	•	1·0	•	•	•	•	•	•	•	•	•	•
Fe_2O_3	•	8·8	•	•	•	•	•	•	•	•	•	•
K_2O	0·4	0·4	0·4	0·4	0·4	0·3	0·3	0·4	0·5	0·5	0·6	0·6
Na_2O	0·1	0·2	0·1	0·1	0·1	0·1	•	0·1	0·2	0·1	0·2	0·2
P_2O_5	0·66	0·64	0·75	0·76	0·73	0·71	0·65	0·75	0·44	0·78	0·43	0·55
TiO_2	0·4	0·5	+	0·2	0·3	0·2	0·2	0·2	0·4	0·4	0·3	0·5
SrO	+	+	+	+	+	+	+	+	+	+	+	+
BaO	+	0·2	+	+	+	+	+	+	0·2	+	+	0·3
MnO	•	+	•	•	•	•	•	•	+	•	•	+
V_2O_5	+	+	+	+	+	+	+	+	+	+	+	+
Cr_2O_3	0·20	0·17	0·18	0·17	0·17	0·17	0·18	0·16	0·20	0·17	0·20	0·18
L.O.I.	•	•	•	•	•	•	•	•	•	•	•	•
Ni	740	740	760	750	770	760	740	760	770	790	680	750
Cu	16	10	+	+	+	+	+	55	18	40	35	16
Co	130	130	140	140	140	120	120	150	140	140	120	140
Pb	35	15	45	35	45	35	35	40	15	40	40	25
Zn	75	80	75	65	75	75	75	75	90	75	85	90
Sub.		79·21										

SAMPLE No.	8092	8089	8107	8108	8104	8118	8119	8133	8121	8106	8131	8087
HOLE No.	2	2	2	2	2	2	2	2	2	2	2	2
DEPTH	13·6-14·6	9·3-11·85	24·1-24·6	24·6-25·1	22·6-23·1	34·5-35·0	38·2-38·9	49·6-50·1	39·05-39·9	23·6-24·1	48·6-49·1	6·2-7·3
ROCK TYPE	‡	‡	serp wehrlite	‡	‡	‡	‡	phlogopite lherzolite	‡	phlogo. wehrlite	phlogopite lherzolite	highly weath. rock
MgO	30·5	30·3	30·0	30·0	29·9	28·8	28·8	27·3	26·9	26·4	25·2	23·5
SiO_2	36·5	•	•	33·0	36·5	33·0	•	46·0	35·2	•	37·8	•
CaO	3·7	4·3	3·4	3·4	3·3	6·9	5·1	8·2	5·9	3·4	10·0	3·7
Al_2O_3	1·0	•	•	1·0	0·8	3·6	•	1·5	2·5	•	1·2	•
Fe_2O_3	8·6	•	•	9·6	8·6	10·0	•	12·5	10·1	•	12·5	•
K_2O	0·6	0·5	0·6	0·6	0·5	0·5	0·9	0·4	1·0	0·6	0·3	0·4
Na_2O	0·2	0·2	0·1	0·1	0·1	0·1	0·1	0·2	0·2	0·2	0·2	0·2
P_2O_5	0·48	0·48	0·83	0·84	0·75	1·62	1·02	0·32	0·39	0·71	1·01	0·44
TiO_2	0·4	0·4	0·4	0·4	0·3	0·4	0·9	0·7	1·0	0·3	0·4	0·5
SrO	+	+	+	+	+	+	+	+	+	+	+	+
BaO	0·2	+	+	+	+	+	0·4	+	0·4	+	+	0·2
MnO	+	•	•	+	+	0·3	•	0·1	+	•	+	•
V_2O_5	+	+	+	+	+	+	+	+	+	+	+	+
Cr_2O_3	0·20	0·17	0·15	0·15	0·16	0·17	0·21	0·04	0·21	0·16	0·06	0·15
L.O.I.	•	•	•	3·8	•	•	•	5·2	•	•	•	•
Ni	760	760	790	800	780	620	620	550	580	790	450	750
Cu	50	18	40	40	+	90	130	8	120	10	200	30
Co	130	130	140	150	140	120	120	120	130	140	110	140
Pb	40	20	35	35	40	35	35	35	60	40	+	35
Zn	70	90	80	80	70	120	130	60	85	100	110	80
Sub.	82·38			79·09	80·91	85·33		97·26	83·8		88·6	

SAMPLE No.	8123	8135	8132	8138	8140	8122	8139	8082	8124	8081	8134	8128
HOLE No.	2	2	2	2	2	2	2	1	2	1	2	2
DEPTH	41·0-41·6	52·5-53·0	49·1-49·6	55·7-56·15	58·3-58·9	39·9-41·0	56·15-56·65	86·6-87·4	41·6-42·5	85·7-86·6	52·0-52·5	45·0-46·0
ROCK TYPE	phlogopite lherzolite	phlogopite clinopyx	phlogopite lherzolite	serp. webst.	‡	serp lherzolite	serp websterite	hydro. alt. dyke rocks	serp websterite	altered mafic shonkinite	serp biotite clinopyx	olivine bio websterite
MgO	23·5	23·0	23·0	22·7	22·6	20·5	20·3	18·9	18·3	18·2	17·8	17·5
SiO_2	•	41·1	•	40·0	44·2	35·9	•	•	41·0	•	•	•
CaO	13·3	6·3	12·6	7·8	5·9	14·0	9·7	14·0	16·5	14·5	18·5	14·0
Al_2O_3	•	1·3	•	2·0	1·5	3·0	•	•	3·9	•	•	•
Fe_2O_3	•	15·0	•	17·5	12·0	8·0	•	•	7·5	•	•	•
K_2O	0·7	0·3	0·4	0·2	0·2	0·9	0·2	+	0·8	0·1	0·3	2·2
Na_2O	0·3	0·2	0·2	0·2	0·1	0·3	0·2	0·2	0·4	0·2	0·3	0·3
P_2O_5	0·43	0·33	0·7	0·08	0·17	0·83	0·05	0·23	1·15	0·18	1·09	1·32
TiO_2	0·8	0·5	0·7	0·7	0·6	1·0	0·6	0·4	1·0	0·6	0·6	2·3
SrO	+	+	+	+	+	+	+	+	+	+	+	+
BaO	+	+	+	+	+	0·2	+	0·2	0·2	+	+	2·0
MnO	•	+	•	0·2	+	0·1	•	•	0·1	•	•	•
V_2O_5	+	+	+	+	+	+	+	+	+	+	+	+
Cr_2O_3	0·07	0·06	0·06	0·12	0·07	0·13	0·10	0·04	0·06	0·04	0·03	0·07
L.O.I.	•	•	•	•	4·2	4·7	•	•	2·2	•	•	•
Ni	350	590	360	690	280	330	400	160	160	150	170	230
Cu	65	6	+	+	50	100	5	+	150	+	6	200
Co	80	120	90	110	70	80	60	50	35	50	40	60
Pb	25	30	+	40	50	55	30	15	20	25	20	40
Zn	35	90	55	75	75	75	40	70	55	55	65	50
Sub.		88·09		91·5	87·34	84·86			90·91			

SAMPLE No.	8137	8195	8192	8127	8176	8182	8199	8125	8178	8171	8126	8180
HOLE No.	2	4	4	2	4	4	4	2	4	4	2	4
DEPTH	54·7-55·7	88·5-89·0	81·5-82·0	44·3-45·0	46·0-46·5	64·0-65·5	96·5-97·0	42·5-43·2	47·0-47·5	43·5-44·0	43·2-44·3	48·0-48·5
ROCK TYPE	orthopyx	biotite websterite	‡	olivine phlogopite websterite	sheared altered websterite	biotite clinopyx	bio. webst.	phlogo clinopyx	bio. webst. qz.-carb. vein	biotite websterite	serp bio clinopyx	bio webst carbonate veins
MgO	17·5	17·4	17·1	17·0	16·9	16·8	16·8	16·8	16·5	16·5	16·3	16·3
SiO_2	42·7	•	•	•	•	•	•	38·1	•	•	36·0	40·2
CaO	15·8	9·3	6·8	12·8	12·9	13·9	14·0	15·3	13·5	12·1	17·9	11·9
Al_2O_3	2·9	•	•	•	•	•	•	6·6	•	•	3·1	7·7
Fe_2O_3	8·8	•	•	•	•	•	•	8·6	•	•	8·6	10·0
K_2O	0·2	0·8	0·8	1·9	0·8	1·1	2·7	2·3	1·2	0·6	0·7	2·2
Na_2O	0·3	0·4	0·4	0·2	0·5	0·5	0·5	0·3	0·5	0·3	0·2	0·3
P_2O_5	0·07	1·05	0·97	1·59	0·53	1·00	1·58	1·84	1·56	0·92	1·06	1·80
TiO_2	0·6	2·0	1·6	2·0	1·0	1·3	2·8	2·2	1·2	1·2	0·8	3·4
SrO	+	+	0·3	+	0·2	+	0·1	+	+	+	+	+
BaO	+	+	0·5	1·8	0·2	0·7	2·0	1·7	0·8	+	+	1·9
MnO	0·1	•	•	•	•	•	•	+	•	•	+	0·1
V_2O_5	+	0·1	+	+	+	+	+	+	+	+	+	+
Cr_2O_3	0·04	0·15	0·16	0·04	0·12	0·10	0·04	0·04	0·10	0·15	0·04	0·06
L.O.I.	•	•	•	•	•	•	•	1·6	•	•	•	2·2
Ni	180	180	135	200	210	180	175	230	230	170	110	230
Cu	+	160	85	290	65	70	35	240	80	65	120	160
Co	40	70	55	75	45	50	50	60	45	65	30	75
Pb	20	25	30	40	30	20	50	40	30	40	40	50
Zn	45	50	65	55	40	45	50	55	40	75	90	60
Sub.								98·78			84·7	95·86

SAMPLE No.	8200	8177	8145	8136	8146	8185	8181	8186	8120	8184	8163	8179	8189
HOLE No.	4	4	2	2	2	4	4	4	2	4	4	4	4
DEPTH	97·0-97·5	46·5-47·0	63·8-64·3	54·1-54·7	64·3-64·8	69·7-70·3	63·5-64·0	70·3-70·8	38·9-39·5	68·2-68·7	7·2-7·7	47·5-48·0	73·35-73·85
ROCK TYPE	biotite clinopyx	bio webst. qz vein	porph. shonk	orthopyrox.	phlogopite clinopyx	bio clinopyx	bio webst	bio clinopyx	serp clinopyx carb veins brecciated	bio clinopyx	‡	bio webst. carb. vein	bio clinopyx leach cavities
MgO	16·0	15·9	15·8	15·8	15·5	15·4	15·2	15·1	15·0	14·8	14·7	14·5	14·5
SiO_2	34·5	•	•	•	•	•	•	•	•	•	•	•	•
CaO	14·1	10·7	7·8	18·3	9·1	14·2	14·7	13·3	18·7	12·3	13·3	13·0	14·2
Al_2O_3	7·3	•	•	•	•	•	•	•	•	•	•	•	•
Fe_2O_3	9·9	•	•	•	•	•	•	•	•	•	•	•	•
K_2O	2·7	0·6	1·8	0·2	1·4	1·2	0·8	2·1	0·1	2·5	1·8	2·4	1·6
Na_2O	0·5	0·4	0·1	0·3	0·2	0·7	0·7	0·5	+	0·4	0·5	0·5	0·6
P_2O_5	1·51	0·50	2·83	2·25	2·69	0·61	0·48	1·5	1·04	1·73	1·68	2·36	1·06
TiO_2	3·2	0·9	3·9	0·6	3·2	1·8	1·4	3·2	0·4	3·3	2·5	2·7	2·6
SrO	0·1	+	+	+	+	+	+	0·1	+	0·1	0·1	+	0·2
BaO	2·2	+	1·4	+	0·9	0·4	0·4	1·8	+	1·5	1·4	1·7	1·0
MnO	0·1	•	•	•	•	•	•	•	•	•	•	•	•
V_2O_5	+	+	+	+	+	+	+	+	+	+	+	+	+
Cr_2O_3	0·03	0·12	0·01	0·01	+	0·07	0·09	0·04	0·09	0·04	0·07	0·04	0·06
L.O.I.	1·6	•	•	•	•	•	•	•	•	•	•	•	•
Ni	200	160	75	165	85	170	150	145	260	220	155	175	80
Cu	95	50	85	+	140	70	50	25	+	170	110	140	70
Co	65	40	110	40	100	45	40	55	65	80	60	70	50
Pb	45	30	55	40	50	20	30	40	40	50	45	50	45
Zn	65	30	340	40	250	50	50	55	160	60	65	80	45
Sub.	92·14												

SAMPLE No.	8170	8183	8130	8147	8129	8744	8196	8188	8141	8164	8162
HOLE No.	4	4	2	2	2	2	4	4	2	4	4
DEPTH	43·0-43·5	64·5-65·0	47·3-48·6	64·8-65·3	46·0-47·3	63·3-63·8	89·0-89·5	72·85-73·35	58·9-59·4	36·6-37·1	6·7-7·2
ROCK TYPE	mica websterite	biotite pyroxenite	olivine phlog websterite	phlogo. clinopyx	ol. phlogo. websterite	porphyritic shonkinite	phlogo. clinopyx.	bio clinopy. with leach cavities	porphyritic shonkinite	bio clinopyx	‡
MgO	14·4	14·3	14·2	14·1	14·0	14·0	13·8	13·7	13·7	13·5	13·5
SiO_2	44·1	45·6	30·1	•	•	27·0	•	33·4	28·0	•	•
CaO	11·7	13·7	15·4	11·4	14·7	11·8	14·7	12·6	12·5	12·7	14·7
Al_2O_3	6·0	7·5	5·5	•	•	7·3	•	6·9	6·9	•	•
Fe_2O_3	10·5	10·5	21·0	•	•	23·9	•	15·0	24·0	•	•
K_2O	0·7	2·7	1·6	1·5	1·5	1·5	2·2	1·9	1·8	1·4	2·3
Na_2O	0·3	0·5	0·2	0·2	0·2	0·2	0·5	0·5	0·2	0·4	0·5
P_2O_5	0·95	1·60	2·72	2·62	2·77	2·64	2·06	1·58	2·36	1·74	2·02
TiO_2	0·9	3·2	2·8	3·2	2·8	3·3	3·7	3·5	3·2	2·4	2·7
SrO	+	0·1	0·1	+	+	+	0·1	+	+	0·1	0·2
BaO	+	1·9	2·2	0·9	2·0	1·0	1·9	0·8	2·5	0·9	1·4
MnO	0·2	0·1	0·1	•	•	0·2	•	0·2	0·3	•	•
V_2O_5	+	+	0·1	+	0·1	+	0·1	+	+	+	+
Cr_2O_3	0·13	0·04	+	+	0·01	+	0·03	0·03	+	0·04	0·03
L.O.I.	3·4	2·2	0·5	•	•	•	•	1·9	1·4	•	•
Ni	180	175	100	75	110	60	145	125	75	130	165
Cu	55	130	160	120	140	85	160	110	160	150	180
Co	60	70	85	95	95	75	80	70	95	65	65
Pb	45	50	35	50	40	50	50	50	60	50	40
Zn	85	65	95	170	75	280	70	80	90	90	60
Sub.	89·88	101·74	96·02			92·8		90·1	95·46		

SAMPLE No.	8078	8080	8084	8085	8086	8187	8194	8079	8151	8167	8198
HOLE No.	1	1	1	1	1	4	4	1	2	4	4
DEPTH	81·0-82·0	84·9-85·7	87·95-89·0	89·0-90·0	90·0-91·0	72·3-72·85	82·5-83·0	84·4-84·9	74·6-75·1	41·5-42·0	90·0-90·5
ROCK TYPE	mafic shonk	‡	‡	‡	‡	porphyritic shonk. with cavities	shonkinite	mafic shonk carbonate veins	mafic shonkinite	biotite clinopyx carb veins	porph. shonk with cavities
MgO	13·5	13·5	13·4	13·4	13·0	13·0	12·7	12·5	12·4	12·4	12·4
SiO_2	•	30·0	32·9	•	29·0	38·5	34·8	•	29·5	•	34·0
CaO	15·4	14·3	15·0	14·5	13·9	9·7	13·2	18·1	15·2	14·2	13·8
Al_2O_3	•	5·9	5·8	•	6·0	9·3	7·4	•	5·6	•	7·6
Fe_2O_3	•	17·5	18·4	•	17·8	14·2	11·5	•	17·0	•	14·2
K_2O	1·6	1·4	1·5	1·7	1·7	2·8	2·7	1·0	1·7	1·6	2·6
Na_2O	0·3	0·2	0·2	0·3	0·3	0·7	0·4	0·2	0·4	0·2	0·6
P_2O_5	3·32	3·18	3·22	3·18	3·56	1·70	1·93	2·74	2·30	2·36	2·02
TiO_2	2·8	2·9	2·8	3·0	3·1	3·1	3·5	2·2	3·1	2·1	3·4
SrO	0·1	0·1	0·1	0·2	0·2	0·2	0·1	0·1	0·1	+	0·2
BaO	1·8	1·8	1·8	2·0	0·2	2·0	2·4	1·1	1·8	0·8	2·6
MnO	•	0·3	0·2	•	0·2	0·2	0·1	•	0·2	•	0·1
V_2O_5	+	0·1	0·1	0·1	0·1	+	0·1	0·1	+	+	0·1
Cr_2O_3	0·03	0·01	+	+	0·01	0·03	0·01	+	+	0·04	0·01
L.O.I.	•	0·6	•	•	•	1·6	3·6	•	0·7	•	•
Ni	100	95	80	85	80	115	115	85	85	165	120
Cu	120	140	150	140	130	100	130	110	100	250	130
Co	75	85	85	80	85	75	70	85	80	75	75
Pb	45	45	25	10	80	95	85	100	65	110	85
Zn	90	70	55	80	15	30	50	510	50	65	40
Sub.		91·19	95·42		89·07	95·43	90·84		89·3		93·63

SAMPLE No.	8142	8143	8166	8197	8172	8077	8191	8148	8169	8067	8193
HOLE No.	2	2	4	4	4	1	4	2	4	1	4
DEPTH	59·4-59·9	59·9-60·4	41·0-41·5	89·5-90·0	44·0-44·5	80·0-81·0	81·0-81·5	69·0-69·5	42·5-43·0	28·4-29·4	82·0-82·5
ROCK TYPE	porph. shonk	‡	bio clinopyx carb veins	porph. shonk cavities and pegmatite	bio webst	mafic shonk	porph. shonk	‡	chloritic shear	dyke, fine shonkinite	porph. shonk.
MgO	12·4	12·3	12·1	12·1	12·0	12·0	12·0	12·0	12·0	11·9	11·8
SiO_2	•	•	•	•	33·4	•	•	31·0	•	34·0	•
CaO	12·8	12·8	13·6	10·5	16·3	14·0	14·0	13·5	11·3	10·0	15·0
Al_2O_3	•	•	•	•	5·6	•	•	7·2	•	8·3	•
Fe_2O_3	•	•	•	•	10·8	•	•	23·8	•	8·5	•
K_2O	2·2	2·4	2·1	2·6	0·5	1·9	1·9	2·0	0·6	3·5	2·3
Na_2O	0·3	0·3	0·3	0·6	0·2	0·3	0·5	0·3	0·4	1·1	0·4
P_2O_5	2·24	2·18	2·43	1·93	1·04	2·76	2·29	2·15	0·91	1·21	1·77
TiO_2	3·0	3·4	2·4	3·4	1·3	2·8	3·4	3·2	1·0	1·9	3·3
SrO	+	0·2	+	0·2	+	0·2	0·1	0·2	+	0·3	0·1
BaO	2·6	2·1	0·3	2·6	+	2·3	2·0	1·3	+	1·4	2·0
MnO	•	•	•	•	0·2	•	•	0·2	•	+	•
V_2O_5	+	+	+	0·1	+	+	+	0·1	+	+	+
Cr_2O_3	+	+	0·04	0·01	0·16	+	0·03	+	0·12	0·01	0·04
L.O.I.	•	•	•	•	•	•	•	1·0	•	2·6	•
Ni	85	65	170	115	195	80	100	60	190	210	160
Cu	100	85	100	150	50	65	170	85	50	80	100
Co	85	80	65	70	65	85	85	80	60	50	70
Pb	140	100	110	75	85	100	65	65	100	90	90
Zn	60	50	60	50	70	40	45	45	40	25	65
Sub.					81·5			96·95		82·12	

SAMPLE No.	8165	8149	8068	8150	8076	8075	8073	8190	8070	8072	8064
HOLE No.	4	2	1	2	1	1	1	4	1	1	1
DEPTH	37·1-37·6	69·5-70·0	32·2-32·7	74·1-74·6	79·0-80·0	78·0-79·0	74·0-75·0	80·5-81·0	52·0-53·0	73·0-74·0	5·1-6·1
ROCK TYPE	hydrotherm. altered bio. clinopyx.	porph. shonk.	‡	‡	‡	‡	‡	‡	melanocratic syenite	‡	slightly wth. porph. shonk.
MgO	11·8	11·4	11·1	11·0	10·8	10·8	10·6	9·9	9·7	9·7	9·7
SiO_2	•	•	33·0	32·0	•	•	•	34·5	•	•	33·5
CaO	12·1	12·7	11·2	11·9	13·5	13·1	13·1	12·4	12·5	12·4	11·7
Al_2O_3	•	•	7·3	7·8	•	•	•	8·7	•	•	8·0
Fe_2O_3	•	•	16·0	17·8	•	•	•	15·1	•	•	13·5
K_2O	2·0	2·3	2·7	2·7	2·1	2·1	2·4	3·0	3·0	2·5	2·9
Na_2O	0·4	0·5	0·3	0·4	0·4	0·4	0·6	0·9	0·6	0·5	0·5
P_2O_5	2·24	2·05	2·35	1·77	2·53	2·95	2·94	1·62	2·20	2·43	2·52
TiO_2	2·8	2·9	3·1	2·9	2·8	3·2	3·3	3·3	2·5	3·3	3·1
SrO	0·2	0·2	0·2	0·3	0·2	0·1	0·3	0·3	0·5	0·3	0·5
BaO	1·6	1·4	1·7	2·6	2·3	2·1	2·8	1·5	2·5	2·5	2·4
MnO	•	•	+	0·2	•	•	•	0·1	•	•	0·1
V_2O_5	+	0·1	+	+	+	+	+	0·2	+	+	+
Cr_2O_3	0·03	+	0·01	+	+	+	+	+	0·01	+	0·01
L.O.I.	•	•	•	•	•	•	•	•	•	•	•
Ni	120	55	95	75	60	55	55	80	90	60	85
Cu	160	85	90	70	160	110	110	100	120	80	90
Co	75	80	75	85	75	55	65	65	55	80	65
Pb	80	65	110	70	100	95	270	85	80	25	80
Zn	40	45	40	40	25	25	40	50	50	80	35
Sub.			88·96	91·07				91·52			88·43

SAMPLE No.	8069	8066	8065	8071	8083	8063	8173	8157	8153	8175	8161
HOLE No.	1	1	1	1	1	1	4	3	3	4	3
DEPTH	51·0-52·0	7·1-8·1	6·1-7·1	53·0-54·0	87·4-87·95	2·2-5·1	44·5-45·0	29·0-29·55	23·8-24·3	45·5-46·0	30·9-31·4
ROCK TYPE	mela syenite	porph. shonk	sl. weath porph shonk	melasyenite	serp mafic shonkinite	mod. weath. porph. shonk	sheared biotite websterite	fault brecc. in syenite	syenite white fels.	sheared bio webst.	syenite, white fels
MgO	9·5	9·4	9·3	8·8	8·7	8·1	6·1	5·6	5·5	5·3	4·7
SiO_2	30·0	33·5	•	•	•	•	54·0	•	•	•	48·0
CaO	12·0	11·0	11·2	10·9	23·8	10·5	4·9	3·1	4·4	5·4	6·9
Al_2O_3	7·8	8·0	•	•	•	•	4·5	•	•	•	13·4
Fe_2O_3	11·8	12·0	•	•	•	•	7·4	•	•	•	9·9
K_2O	3·2	3·2	3·1	3·7	+	3·8	+	2·0	5·8	0·6	4·6
Na_2O	0·5	0·5	0·5	0·6	+	0·7	+	0·1	0·4	0·1	1·3
P_2O_5	2·22	1·97	2·13	2·08	0·11	1·81	0·92	0·98	1·27	0·31	1·45
TiO_2	3·0	3·0	3·0	2·9	+	2·6	1·4	1·2	1·7	0·4	1·8
SrO	0·5	0·6	0·6	0·5	0·6	0·6	+	+	0·1	+	0·6
BaO	2·5	2·6	2·6	3·0	+	3·4	+	+	1·2	+	2·4
MnO	+	+	•	•	•	•	+	•	•	•	+
V_2O_5	+	+	+	+	+	+	+	+	+	+	+
Cr_2O_3	0·01	0·01	0·01	+	0·06	0·01	0·08	0·11	+	0·07	+
L.O.I.	•	•	•	•	•	•	•	•	•	•	3·1
Ni	75	75	75	70	85	70	175	160	20	135	35
Cu	110	100	90	85	+	75	60	20	12	150	30
Co	65	60	60	50	35	55	40	45	40	25	40
Pb	100	60	75	70	25	65	80	85	95	50	85
Zn	25	40	40	25	40	40	40	30	50	30	65
Sub.	83·03	85·76					79·28				95·08

SAMPLE No.	8158	8074	8152	8154	8168	8174	8160	8155	8156	8159
HOLE No.	3	1	3	3	4	4	3	3	3	3
DEPTH	29·55-30·2	75·0-76·0	23·3-23·8	24·3-24·8	42·0-42·5	45·0-45·5	30·5-30·9	28·0-28·5	28·5-29·0	30·2-30·5
ROCK TYPE	syenite, orange fels.	porph. shonk. pegmatite vein	syenite white fels	‡	quartz vein	altered clinopyx	syenite orange fels	‡	hydrotherm alt. syenite orange fels	calcite vein
MgO	4·0	3·9	3·7	3·6	2·9	2·7	2·6	1·9	1·9	0·1
SiO_2	•	•	45·5	45·0	•	76·0	•	•	65·0	•
CaO	5·7	5·0	5·3	4·2	1·4	4·9	7·8	2·7	1·6	62·0
Al_2O_3	•	•	14·7	14·5	•	2·1	•	•	10·4	•
Fe_2O_3	•	•	8·7	7·9	•	3·3	•	•	5·5	•
K_2O	4·5	2·8	5·1	5·1	0·3	+	4·8	5·8	4·8	+
Na_2O	0·4	2·1	1·5	1·6	0·4	+	0·9	1·2	0·6	+
P_2O_5	1·46	1·05	1·10	1·00	0·56	0·36	1·29	1·06	0·71	+
TiO_2	1·7	1·1	1·4	1·3	0·2	0·2	1·8	1·2	0·7	+
SrO	0·2	0·1	0·6	0·5	+	+	0·4	+	+	+
BaO	1·8	1·2	2·7	2·8	+	+	2·1	0·9	0·3	+
MnO	•	•	+	+	•	+	•	•	+	•
V_2O_5	+	+	+	+	+	+	+	+	+	+
Cr_2O_3	+	+	+	+	+	0·04	+	+	+	+
L.O.I.	•	•	•	•	•	•	•	•	•	•
Ni	45	25	20	12	55	75	40	25	45	30
Cu	8	20	25	14	260	140	30	10	12	+
Co	45	18	30	35	15	20	45	40	20	20
Pb	65	190	80	75	30	30	65	30	30	10
Zn	30	20	150	30	15	40	80	20	10	80
Sub.			90·31	92·0		89·6			91·51	

• Assay not determined

+ Result below level of detection

Detection Level

K_2O	0.1%
Na_2O	0.1%
P_2O_5	0.01%
TiO_2	0.2%
SrO	0.1%
BaO	0.2%
MnO	0.1%
V_2O_5	0.1%
Cr	0.1%
Cu	5ppm
Pb	10ppm